Supporting Information for

Distinct insight into the use of difunctional double-decker silsesquioxanes as building blocks for alternating A-B type macromolecular frameworks

Julia Duszczak[a,b], Aleksandra Mrzygłód[a,b], Katarzyna Mituła[a,b], Michał Dutkiewicz[c], Rafał Januszewski[a,b], Monika Rzonsowska[a,b], Beata Dudziec*[a,b], Marek Nowicki[b,d], Maciej Kubicki[a]

[a]*Faculty of Chemistry, Adam Mickiewicz University in Poznan, Uniwersytetu Poznańskiego 8, 61-614 Poznan, Poland.*
E-mail: beata.dudziec@gmail.com
[b]*Centre for Advanced Technologies, Adam Mickiewicz University in Poznan, Uniwersytetu Poznańskiego 10, 61-614 Poznan, Poland*
[c]*Adam Mickiewicz University Foundation, Poznań Science and Technology Park, Rubież 46, 61-612 Poznań, Poland*
[d]*Institute of Physics, Poznan University of Technology, Piotrowo 3, 60-965 Poznan, Poland*

Table of contents:

1. General Considerations:

The chemicals were purchased from the following sources: Hybrid Plastics for DDSQ tetrasilanol form ($C_{48}H_{44}O_{14}Si_8$) (DDSQ-4OH); Sigma-Aldrich for dichloromethane (DCM), tetrahydrofuran (THF), toluene, methanol, acetonitrile, *n*-hexane, chloroform-*d*, Karstedt's catalyst – 2% xylene solution, chlorosilanes (dichloromethylsilane, dichloromethylvinylsilane and chloro(dimethyl)vinylsilane), dimethylphenylsilane, dimethylphenylvinylsilane, 1,1,3,3-tetramethyldisiloxane, 1,3-divinyltetramethyldisiloxane, 1,4-bis(dimethylsilyl)benzene, magnesium, vinylmagnesium bromide solution 1M in THF, 4Å molecular sieves, triethylamine and silica gel 60; Deutero for dichloromethane-d_2; Fluorochem for 1,2-bis(chlorodimethylsilil)ethane and 1,1,3,3,5,5-hexamethyltrisiloxane; ABCR for 1,1,3,3-tetramethyldisilazane; TCI for 1,4-dibromobenzene; Alfa Aesar for platinum(IV) oxide. Following double-decker silsesquioxanes: DDSQ-2SiH (**1a**), DDSQ-2SiVi (**1b**), DDSQ-2OSiVi (**1c**) were prepared according to the literature procedures[1–3] so as the DDSQ-2SiOH,[3] 1,4-bis(vinyldimethylsilyl)benzene,[4] 1,2-bis(dimethylvinylsilyl)ethane[5] and 1,2-bis(dimethylsilyl)-ethane.[6] All solvents were dried over CaH_2 prior to use and stored under argon over 4Å molecular sieves. All liquid substrates were also dried and degassed by bulb-to-bulb distillation. All syntheses were conducted under argon atmosphere using standard Schlenk-line and vacuum techniques.

1.1 Measurements

Nuclear Magnetic Resonance (NMR)
^1H, ^{13}C, and ^{29}Si Nuclear Magnetic Resonance (NMR) were performed on Brucker Ultra Shield 400 and 300 spectrometers using $CDCl_3$ and CD_2Cl_2 as a solvents. Chemical shifts are reported in ppm with reference to the residual solvents peaks for ^1H and ^{13}C and to TMS for ^{29}Si NMR.

FT-IR spectroscopy
Fourier Transform-Infrared (FT-IR) spectra were recorded on a Nicolet iS5 (Thermo Scientific) spectrophotometer equipped with a single reflection diamond ATR unit. In all cases, 16 scans at a resolution of 2 cm^{-1} were collected, to record the spectra in a range of 4000-650cm^{-1}.

Real-time *in situ* FT-IR analyses were performed on a Mettler Toledo ReactIR 15 equipped with a DS 6.3mm AgX Di Comp Fiber Probe with a diamond window along with a Mercury Cadmium Telluride detector. In each case, 256 scans were recorded at a resolution of 1 cm^{-1} in 1, 2, 5, and 10 min intervals.

Thermogravimetric Analysis (TGA)
The analyses were performed using a TGA/DSC 1 Mettler-Toledo thermal gravimetric apparatus. The analyses were performed in an air atmosphere (flow of 60 mL/min), from ambient temperature to 1000 °C at the heating rate of 10 °C/min. The temperature of initial degradation ($T^{5\%}$) was taken as the onset temperature at which 5 wt% of mass loss occurs.

Elemental Analysis.
Elemental analyses were performed using a Vario EL III instrument.

Gel Permeation Chromatography (GPC)
Gel permeation chromatography analyses were performed using a Waters Alliance 2695 system equipped with a Waters 2412 RI detector and a set of three serially connected 7.8x300 mm columns (Water Styragel HR1, HR2, and HR4). THF was used as a mobile phase at a flow rate of 0.6 mL/min; column oven temperature was 35 ˚C and detector temperature 40 ˚C. Molecular weight (M_n, M_w) and

polydispersity index ($Đ$) values were calculated based on a polynomial calibration curve using polystyrene standards (Shodex) in a range from 1.31×10^3 to 3.64×10^6 Da.

Gas Chromatography coupled with Mass Spectrometry (GCMS)

Mass spectra of compounds were acquired by gas chromatograph mass spectrometer (GCMS) analysis on a Brucker Scion 436-GC with a 30 m Varian DB-5 0.25 mm capillary column and a Scion SQ-MS mass spectrometry detector.

X-ray crystallography

Diffraction data were collected by the ω-scan technique at 100(1) K on Rigaku XCalibur four-circle diffractometer with EOS CCD detector and graphite-monochromated MoK$_\alpha$ radiation (λ=0.71073 Å). The data were corrected for Lorentz-polarization as well as for absorption effects.[7] Precise unit-cell parameters were determined by a least-squares fit of 14314 (**1b**) and 5949 (**1c**) reflections of the highest intensity, chosen from the whole experiment. The structures were solved with SHELXT-2013[8] and refined with the full-matrix least-squares procedure on F^2 by SHELXL-2013.[9] All non-hydrogen atoms were refined anisotropically, hydrogen atoms were placed in idealized positions and refined as 'riding model' with isotropic displacement parameters set at 1.2 (1.5 for CH$_3$) times U$_{eq}$ of appropriate carrier atoms. In the structure **1b** a disorder has been found: the methyl and vinyl groups interchange each other with site occupation factors of 0.670(6) and 0.330(6). In **1c** in turn, one of the C=C distances (C123-C124) was constrained to the typical value.

Crystal data: **1b**: $C_{54}H_{52}O_{14}Si_{10}$, M$_r$ = 1205.85, monoclinic, P2$_1$/c, a = 10.58660(10) Å, b = 18.1559(3) Å, c = 15.2045(2) Å, β = 93.6360(10)°, V = 2916.56(7) Å^3, Z = 2, F(000) = 1256, d$_x$ = 1.373 g·cm^{-3}, μ = 0.289 mm^{-1}. 27755 reflections collected up to 2Θ = 26.8°, of which 5847 independent (R$_{int}$ = 0.016), 5529 with I>2σ(I). Final R(F) [I>2σ(I)] = 0.0345, wR(F^2) [I>2σ(I)] = 0.0916, R(F) [all data] = 0.0365, wR(F^2) [all data] = 0.0933, S = 1.03, max/min $\Delta\rho$ = 0.43/−0.53 e·Å^{-3}.

1c: $C_{58}H_{64}O_{16}Si_{12}$, M$_r$ = 1354.17, triclinic, P-1, a = 13.5310(9) Å, b = 14.1236(9) Å, c = 19.7262(12) Å, α = 91.086(5)°, β = 101.240(6)°, γ = 113.236(6)°, V = 3378.3(4) Å^3, Z = 2, F(000) = 5949, d$_x$ = 1.331 g·cm^{-3}, μ = 0.293 mm^{-1}. 22904 reflections collected up to 2Θ = 25.0°, of which 11804 independent (R$_{int}$ = 0.037), 8560 with I>2σ(I). Final R(F) [I>2σ(I)] = 0.0807, wR(F^2) [I>2σ(I)] = 0.1815, R(F) [all data] = 0.1098, wR(F^2) [all data] = 0.1951, S = 1.03, max/min $\Delta\rho$ = 1.25/−1.19 e·Å^{-3}.

Crystallographic data for the structural analysis has been deposited with the Cambridge Crystallographic Data Centre, Nos. CCDC-1972875 (**1b**) and 1891035 (**1c**). Copies of this information may be obtained free of charge from: The Director, CCDC, 12 Union Road, Cambridge, CB2 1EZ, UK; e-mail: deposit@ccdc.cam.ac.uk, or www: www.ccdc.cam.ac.uk.

Water contact angles (WCAs)

Water contact angles of polymer-coated stainless steel or glass plates were measured using a Krüss GmbH DSA 100E Drop Shape Analyzer equipped with a software-controlled (DAS4 2.0): x, y, z-axis table, quadruple dosing unit with zoom, and focus adjustment, illumination, and a camera with 780 × 580 pix resolution. All presented data are arithmetic means of values measured for 3 drops (5 μL) per sample.

Nanoindentation technique

Mechanical parameters were determined using the nanoindentation technique. This technique allows to calculate them also for thin layers and small volumes of polymer materials.[10,11] The measurements were taken with Berkovich tip geometry and an Agilent G200 indenter. The device was calibrated by standard method before measurements.[12] The elasticity modulus and hardness of layers made of synthesized polymers were determined. The indentation depth was up to 1000 nm. Measurements were carried out in CSM mode with a DCMII indenter head. Tests were performed at a temperature of 19 ˚C and at a humidity of 50%. The apparatus simultaneously records the force applied to the probe pressed into the surface and the indentation depth. Applied loading curves contain a segment retaining the maximum force for 10 seconds. For each sample, at least 10 tests were performed, and the results were averaged.

Scanning electron microscopy

Scanning electron microscopy (SEM) images were taken using an FEI Quanta 250 FEG microscope equipped with an EDAX EDS detector. Images were taken in high vacuum mode, and accelerating voltage (5 kV). Thin films of selected samples were fabricated on glass plates using the spin-coating technique. Thin films in one layer were prepared by a spin-coating technique using 5-10 wt% solution of compounds in DCM that was deposited on the glass plates (spin speed of 100 rpm for 40 sec.) to form a homogeneous surface. The film thickness was in the range of ca. 400-700 nm.

1.2 Synthetic procedures

1.2.1 General synthetic procedure for DDSQ-2OSiVi (1c) obtained *via* condensation reaction

(**1c**)
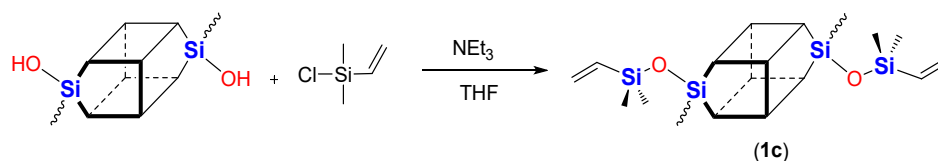
The synthesis was based on the hydrolytic condensation of DDSQ-2SiOH with chloro(dimethyl)vinylsilane carried out in the presence of triethylamine under argon atmosphere. A Schlenk flask, placed on ice bath, was charged with dry THF (11 mL), DDSQ-2SiOH (0.478 g, 0.40 mmol), triethylamine (0.22 mL, 1.60 mmol), followed chloro(dimethyl)vinylsilane (0.134 mL, 0.96 mmol) introduced by dropping to the obtained solution. The reaction mixture became cloudy as a result of hydrochloride formation and consequently [HNEt$_3$]Cl was observed as a white solid. After one hour, the mixture was warmed to room temperature and kept at stirring for 23 hours. Then the post-reaction mixture was subjected to filtration to remove the formed triethylamine hydrochloride and the filtrate was evaporated under reduced pressure. The crude product was dissolved in DCM and precipitated in MeOH. After decantation, the remains of MeOH were evaporated and DDSQ-2OSiVi (**1c**) was isolated as a white solid in 34% yield. The methanol decant was left again at 4 °C (in the refrigerator) for 1 week. After this time, there was additional precipitation of **1c** observed. This gradual precipitation was repeated 3 times and finally, **1c** was isolated as white solid, with a total yield of 94%. While this procedure, fine crystals were also obtained and subjected to XRD analysis, and also its structure was confirmed *via* spectroscopic analysis (see p. S-8-).

1.2.2 General synthetic procedure for difunctional DDSQ molecular compounds obtained *via* hydrosilylation reaction

The procedure for the synthesis of **3a-Vi** is described as an example. To a two-neck round-bottom flask equipped with a condenser and magnetic stirrer, **1a** (0.100 g, 0.08 mmol) was placed in argon atmosphere along with anhydrous toluene (3.0 mL), dimethylphenylvinylsilane (**2-Vi**) (0.027 mL, 0.18 mmol) and [Pt$_2$(dvds)$_3$] (0.826 µL, 1.6×10^{-8} mol). The reaction mixture was kept at 95 °C to obtain complete Si-H consumption that was verified *via* FT-IR technique based on changes in the surface areas of bands at $\bar{\upsilon} = 895$ cm^{-1} and $\bar{\upsilon} = 2130$ cm^{-1} characteristic for stretching vibrations of Si-H bond (usually 20 hours). After cooling it to room temperature, the silane excess and solvent were evaporated under a vacuum and the crude product was transferred onto a chromatographic column (silica gel 60) using chloroform as eluent. Evaporation of eluent gave an analytically pure sample of **3a-Vi** in a 95% yield.

## 1.2.3 General synthetic procedure for linear DDSQ-based co-oligomers (type 6 and 7) obtained *via* hydrosilylation reaction – exemplary reaction for the synthesis of 7b-d

The procedure for the synthesis of **7b-d** is described as an example. To a two-neck round-bottom flask equipped with a condenser and magnetic stirrer, **1b** (0.101 g, 0.08 mmol) was placed in argon atmosphere along with anhydrous toluene (3.0 mL), 1,1,3,3-tetramethyldisiloxane (**5d**) (0.015 mL, 0.08 mmol) and [Pt$_2$(dvds)$_3$] (1.914 µL, 1.6×10^{-8} mol). The reaction mixture was kept at 95 °C for 24 hours. After cooling it to room temperature, the disiloxane excess and solvent were evaporated under a vacuum. Washing the crude product with MeOH, MeCN, or *n*-hexane.

2. Additional information on the hydrosilylation reaction

2.1 General synthetic procedure for checking the reactivity of the catalyst

(1a) + **(4d)** → **(6a-d)**

i) - excess of [Pt$_2$(dvds)$_3$]
ii) - excess of [Pt$_2$(dvds)$_3$] + Styrene + H-SiMe$_2$Ph
iii) - additional Styrene + H-SiMe$_2$Ph
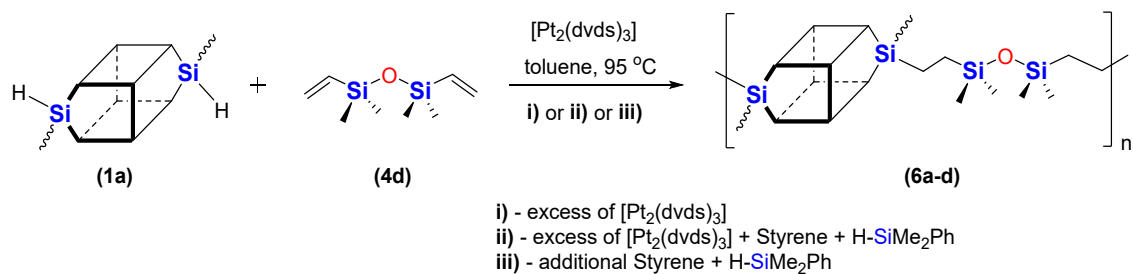
To a two-neck round-bottom flask equipped with a condenser and magnetic stirrer, **1a** (0.081 g, 0.07 mmol) was placed in an argon atmosphere along with anhydrous toluene (3.0 mL), 1,3-divinyltetramethyldisiloxane (**4d**) (0.017 mL, 0.07 mmol) and [Pt$_2$(dvds)$_3$] (1.605 µL, 1.4×10^{-7} mol). The reaction mixture was kept at 95°C for 72 hours.

i)   The excess of [Pt$_2$(dvds)$_3$] (1.6 µL, 1.4×10^{-7} mol) was added and the reaction mixture was kept at the same temperature next 24 hours. After cooling it to room temperature, the excess disiloxane and solvent were evaporated under a vacuum. Next GPC analysis was performed.

ii) The excess of [Pt$_2$(dvds)$_3$] (9.8 µL, 8.6×10^{-7} mol) was added and mixed for 15 minutes. Styrene (100 µL, 0.86 mmol) and dimethylphenylsilane (142 µL, 0.91 mmol) was added and the reaction mixture was kept at the same temperature next 24 hours. After cooling it to room temperature, cold hexane (12 mL) was added to precipitate oligomers. The precipitate was filtered off on a syringe filter (0.2 µm). Next GC-MS analysis of the solution was performed. The styrene conversion was estimated at 92%.

iii) Styrene (100 µL, 0.86 mmol) and dimethylphenylsilane (142 µL, 0.91 mmol) was added and the reaction mixture was kept at the same temperature next 24 hours. After cooling it to room temperature, cold hexane (12 mL) was added to precipitate oligomers. The precipitate was filtered off on a syringe filter (0.2 µm). Next GCMS analysis of the solution was performed that revealed 68% conversion of styrene.
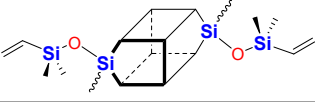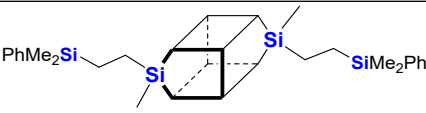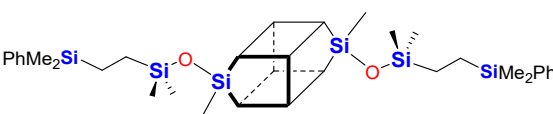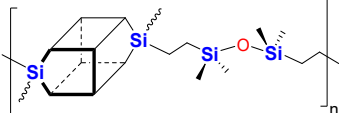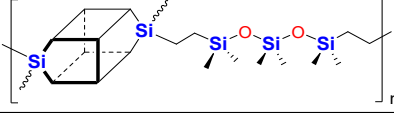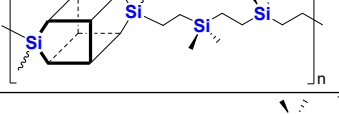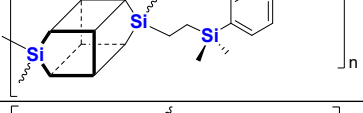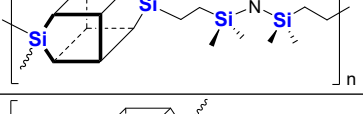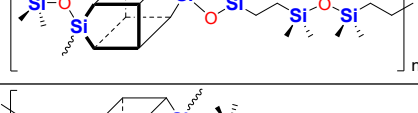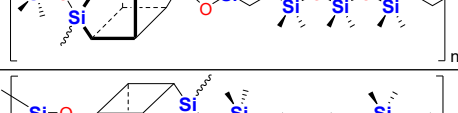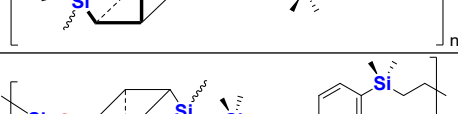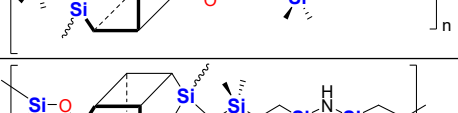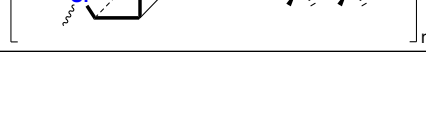
2.2 Synthetic procedure for dimethylphenyl(2-phenylethyl)silane obtained *via* hydrosilylation reaction- checking the reaction time
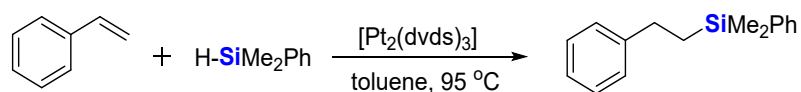
To a two-neck round-bottom flask equipped with a condenser and magnetic stirrer, styrene (100 µL, 0.86 mmol) was placed in an argon atmosphere along with anhydrous toluene (3.0 mL), dimethylphenylsilane (142 µL, 0.91 mmol) and [Pt$_2$(dvds)$_3$] (9.852 µL 8.6×10^{-7} mol). The reaction mixture was kept at 95 °C to obtain complete Si-H consumption that was verified *via* the real-time *in situ* FT-IR technique based on changes in the surface areas of bands at $\bar{\upsilon} = 895$ cm^{-1} and $\bar{\upsilon} = 2130$ cm^{-1} characteristic for stretching vibrations of Si-H bond (8 hours).

3. List of isolated compounds:

Table S1. The list of obtained compounds with structures and respective autogravitation.

Structure	Compound Abbrev.	NMR spectra page:
	1c	8-9
	3a-Vi **3b-H**	10-11
	3c-H	12-13
	7b-d	14-15
	7b-e	16-17
	7b-f	18-19
	6a-g	20-21
	7b-h	22-23
	7c-d	24-25
	7c-e	26-27
	7c-f	28-29
	7c-g	30-31
	7c-h	32-33

4. Analytical data of obtained products incl. ^{1}H, ^{13}C, ^{29}Si NMR spectra

1c
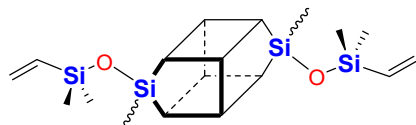
White solid. Isolated Yield 94%.

^{1}H NMR (300 MHz, CDCl$_3$, ppm): δ = 0.11 (s, 12H, SiCH$_3$), 0.28 (s, 6H, SiCH$_3$), 5.66 (dd, J_{H-H} = 20.1, 3.9 Hz, 2H), 5.75 (dd, J_{H-H} = 15.0, 3.9 Hz, 2H), 6.06 (dd, J_{H-H} = 20.1, 15.0 Hz, 2H), 7.17-7.59 (m, 40H, Ph).

^{13}C NMR (101 MHz, CDCl$_3$, ppm): δ = -2.67 (Si(CH$_3$)$_2$), 0.19 (SiCH$_3$), 127.70-127.86 (Ph), 130.43-130.47 (Ph), 131.15 (H$_2$C=CH-), 132.05-132.23 (Ph), 134.16-134.31 (Ph), 138.67 (H$_2$C=CH-).

^{29}Si NMR (79.5 MHz, CDCl$_3$, ppm): δ = -1.81 (Si(CH$_3$)$_2$Vi), -64.10 (Si(CH$_3$)), -79.29, -79.36, -79.54, -79.74 (-Si-Ph).

IR (ATR, cm^{-1}): 3072.99, 3050.41 (C-H phenyl), 2962.61 (C-H), 1594.32, 1430.09 (C=C phenyl), 1258.67 (Si-C), 1092.13, 1025.54 (Si-O-Si), 997.20 (C-H phenyl).

EA: Anal. calcd for C$_{58}$H$_{64}$O$_{16}$Si$_{12}$ (%): C, 51.44, H, 4.76; found: C, 51.45, H, 4.77.
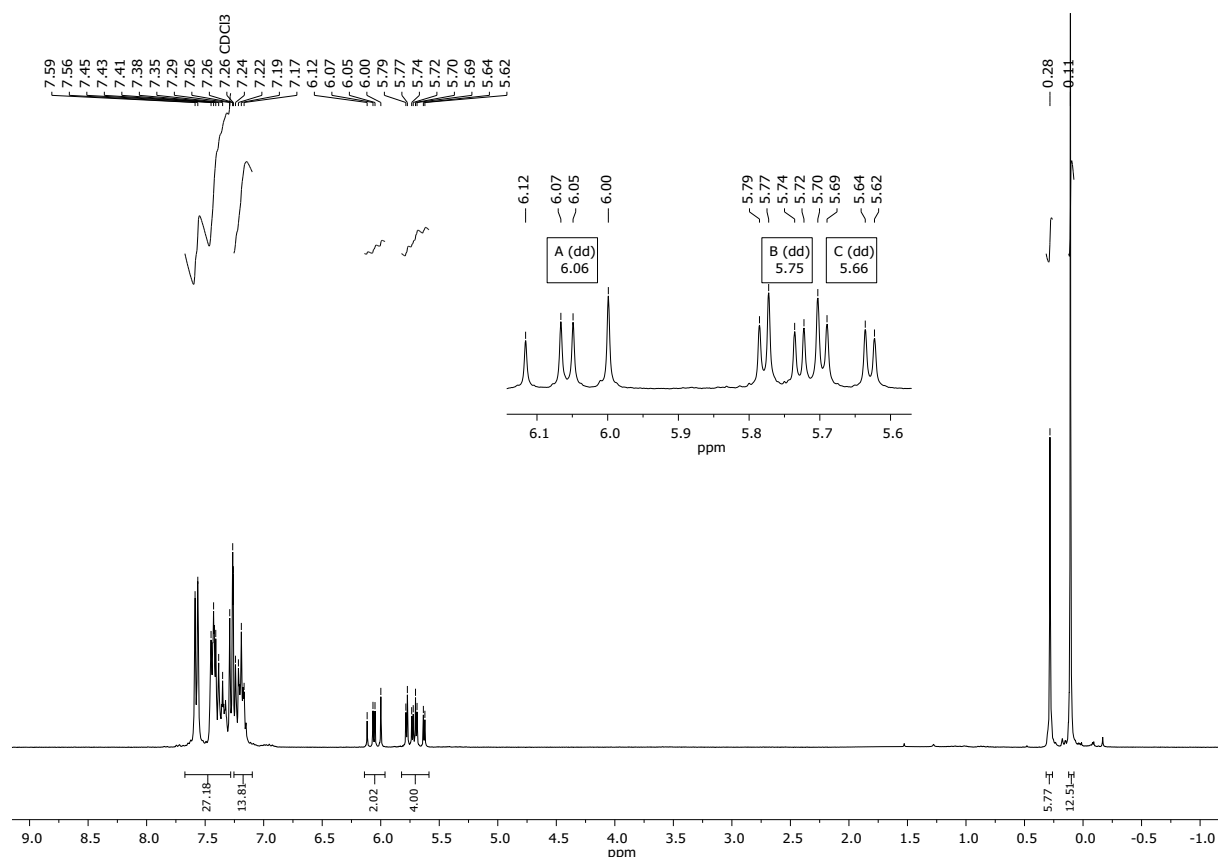
Figure S1 ^{1}H NMR (300 MHz, CDCl$_3$) spectrum of **1c**.
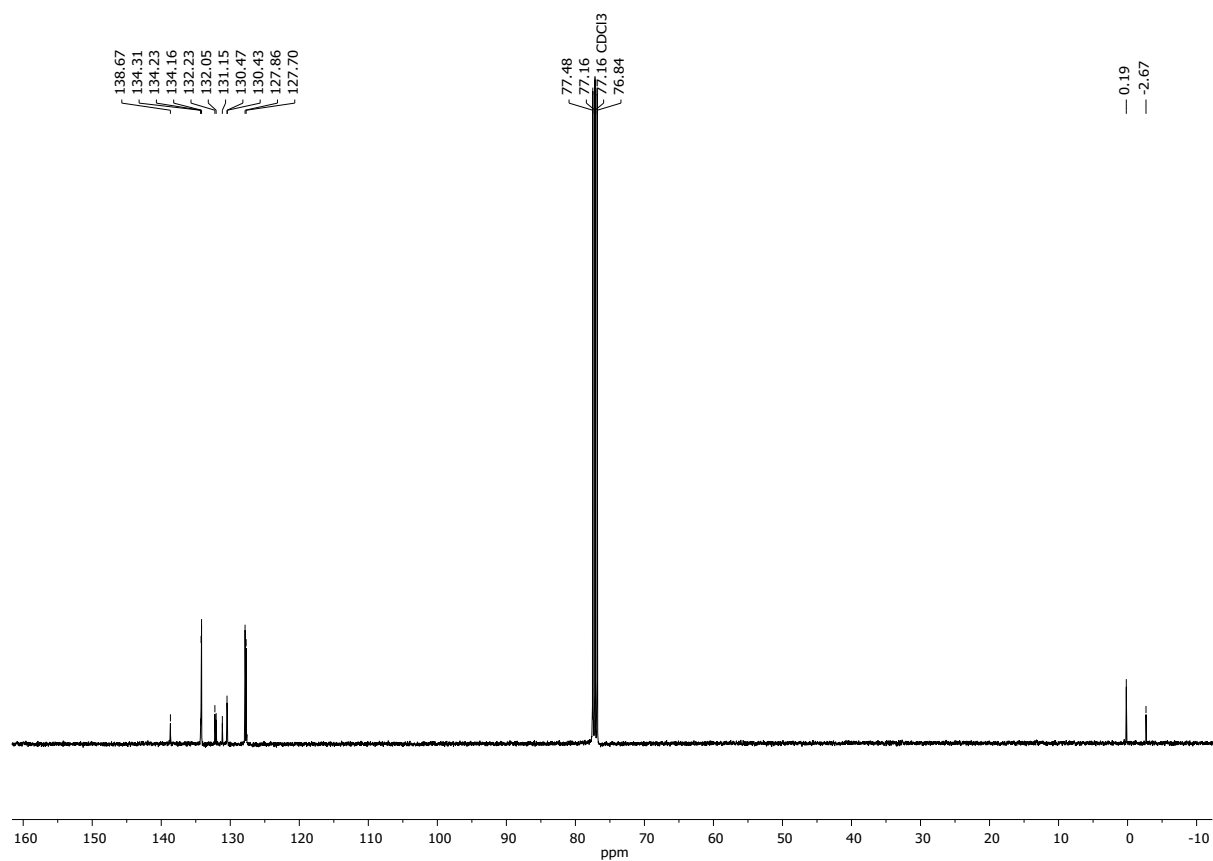
Figure S2 ^{13}C NMR (101 MHz, CDCl$_3$) spectrum of **1c**.
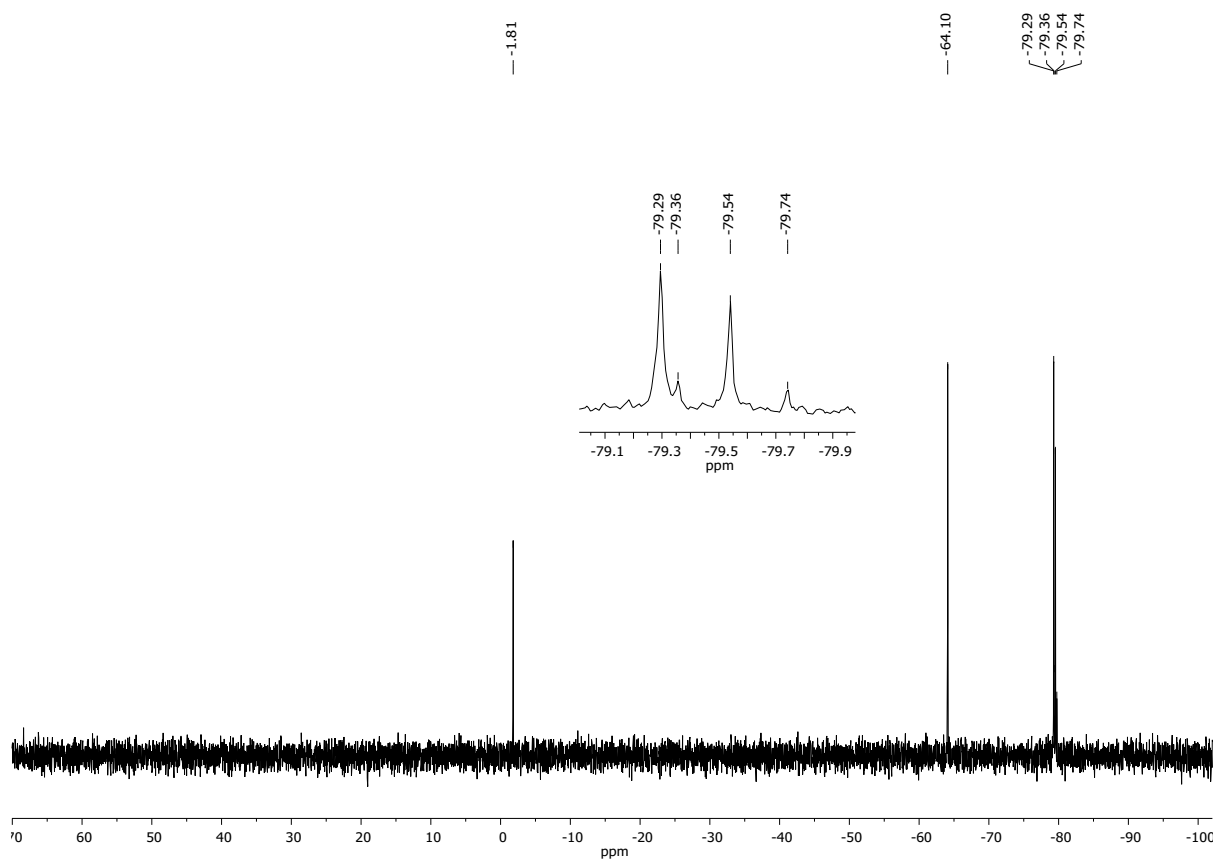
Figure S3 ^{29}Si NMR (79.5 MHz, CDCl$_3$) spectrum of **1c**.

3a-Vi / 3b-H
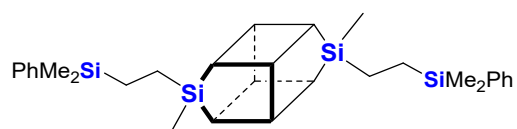
White solid. Isolated Yield 94% for **3b-H** and 92% for **3a-Vi** .

^{1}H NMR (300 MHz, CDCl$_3$, ppm): δ = 0.12 (s, 12H, SiCH$_3$), 0.28 (s, 6H, SiCH$_3$), 0.59-0.68 (m, 4H, -Si-CH$_2$-), 0.75-0.81 (m, 4H, -Si-CH$_2$-), 7.15-7.47 (m, 40H, Ph), 7.55 (d, J_{H-H} = 7.3 Hz, 10H).
^{13}C NMR (101 MHz, CDCl$_3$, ppm): δ = -3.58 (Si(CH$_3$)$_2$), -1.40 (SiCH$_3$), 6.52 (Si-CH$_2$-), 9.03 (Si-CH$_2$), 127.77-127.90 (Ph), 128.80 (Ph), 130.43 (Ph), 131.23 (Ph), 132.26 (Ph), 133.70 (Ph), 134.07 (Ph), 134.19 (Ph), 139.26 (Ph).
^{29}Si NMR (79.5 MHz, CDCl$_3$, ppm): δ = -1.22 (Si(CH$_3$)$_2$), -17.39 (Si(CH$_3$)),-78.69, -79.65 (-Si-Ph).
IR (ATR, cm^{-1}): 3071.16, 3007.30 (C-H phenyl), 2954.96, 2912.39 (C-H), 1593.93, 1429.29 (C=C phenyl), 1258.15 (Si-C), 1077.25, 1028.51 (Si-O-Si), 997.91 (C-H phenyl).
EA: Anal. calcd for C$_{70}$H$_{76}$O$_{14}$Si$_{12}$ (%): C, 56.87, H, 5.18; found: C, 56.89, H, 5.19.

The analytical data of **3a-Vi** and **3b-H** are consistent.
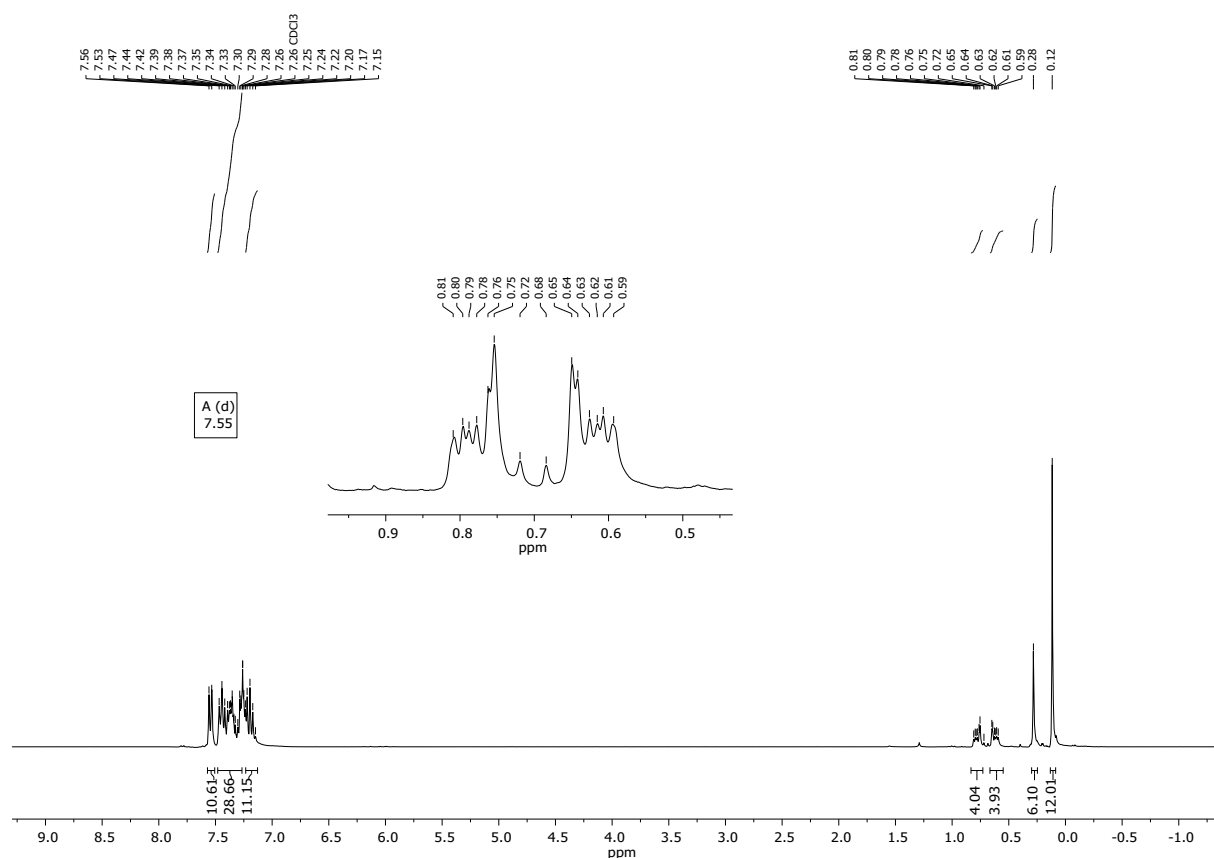
Figure S4 ^{1}H NMR (300 MHz, CDCl$_3$) spectrum of **3a-Vi** / **3b-H**.
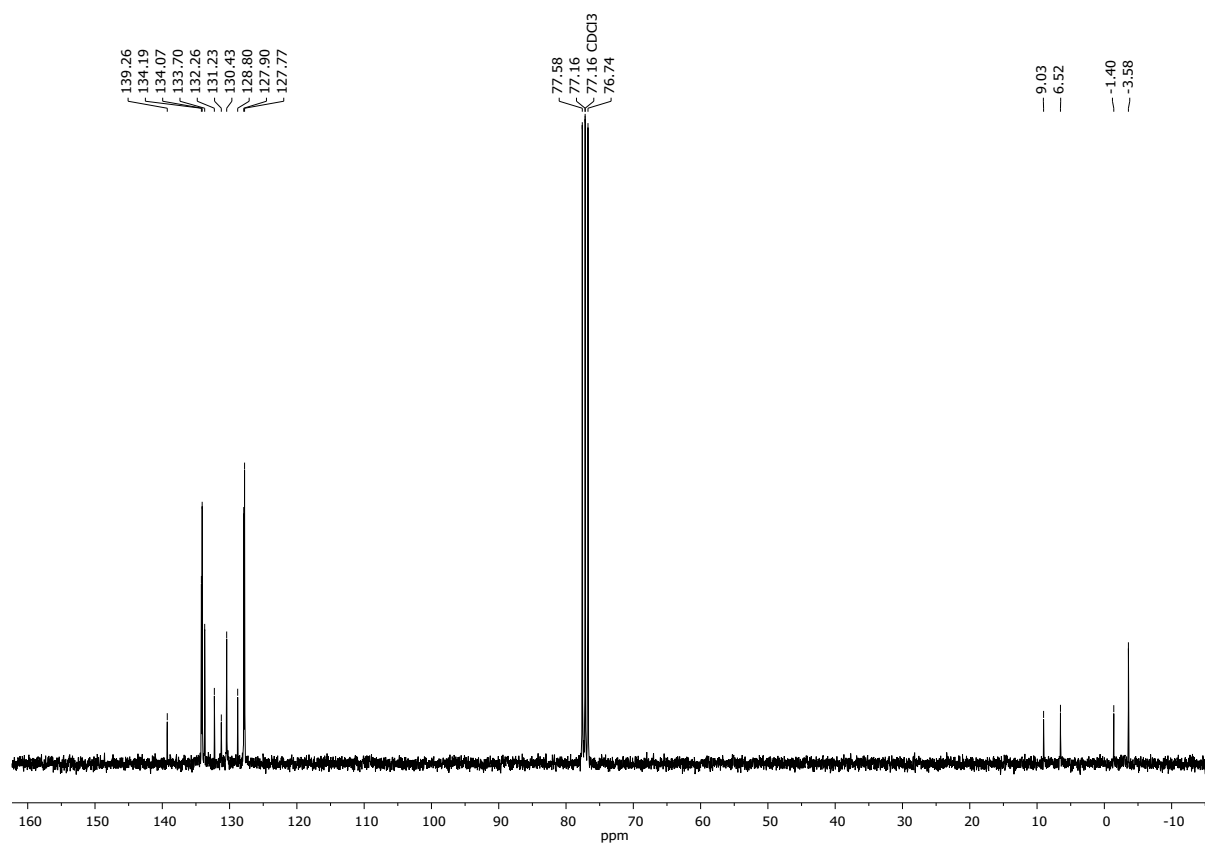
Figure S5 ^{13}C NMR (101 MHz, CDCl$_3$) spectrum of **3a-Vi / 3b-H**.
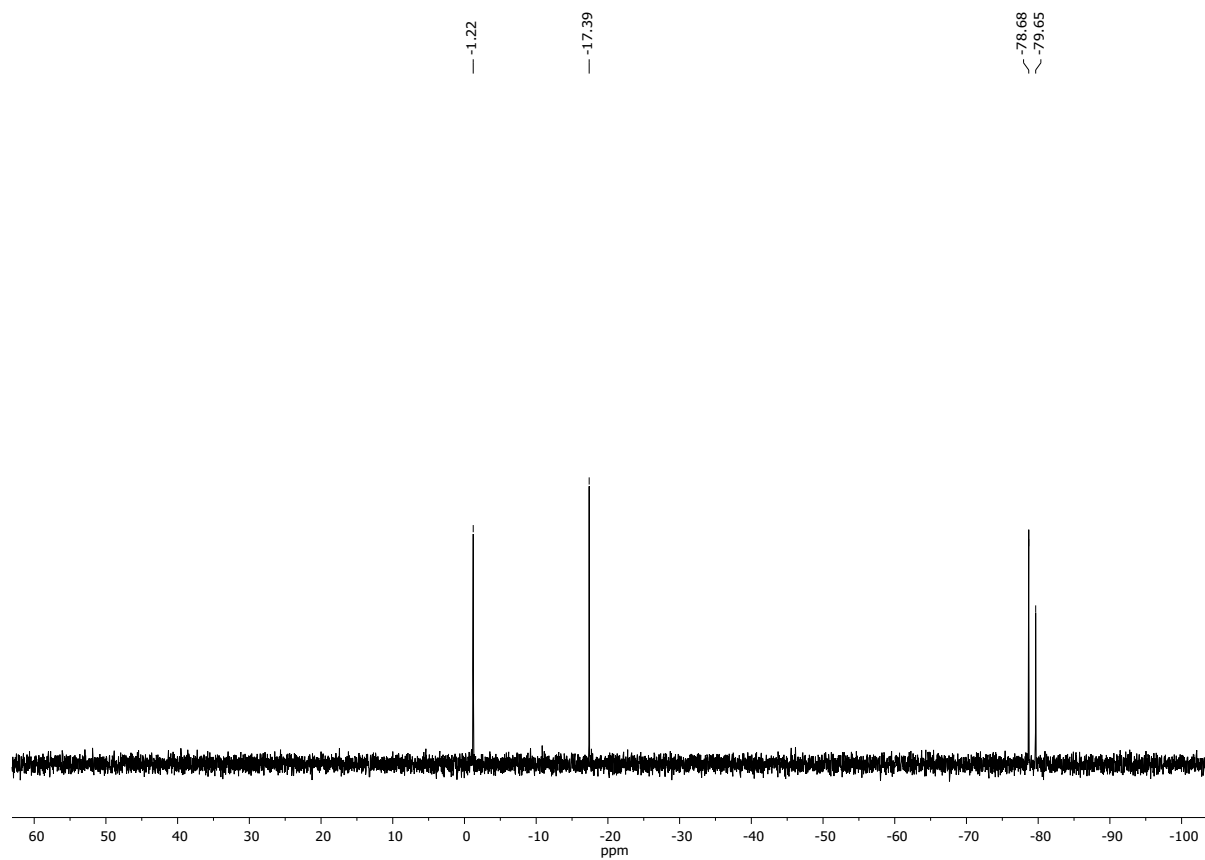
Figure S6 ^{29}Si NMR (79.5 MHz, CDCl$_3$) spectrum of **3a-Vi / 3b-H**.

3c-H
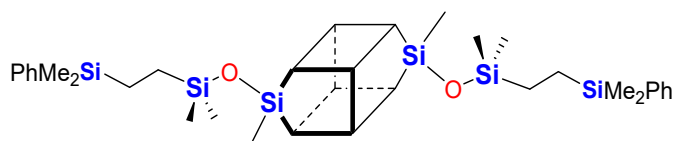
White solid. Isolated Yield 96%.

^{1}H NMR (300 MHz, CDCl$_3$, ppm): δ = 0.08 (s, 12H, Si(CH$_3$)$_2$), 0.11 (s, 12H, Si(CH$_3$)$_2$) 0.25 (s, 6H, SiCH$_3$), 0.37-0.43 (m, 4H, -Si-CH$_2$-), 0.55-0.61 (m, 4H, -Si-CH$_2$-), 7.16-7.43 (m, 40H, Ph), 7.55 (d, J_{H-H} = 7.3 Hz, 10H).

^{13}C NMR (101 MHz, CDCl$_3$, ppm): δ = -3.57 (Si(CH$_3$)$_2$), -2.59 (Si(CH$_3$)$_2$), -0.57 (SiCH$_3$), 6.96 (Si-CH$_2$-), 10.05 (Si-CH$_2$-), 127.72-128.80 (Ph), 130.42-130.47 (Ph), 131.17 (Ph), 132.08 (Ph), 132.72 (Ph), 134.12-134.36 (Ph), 139.58 (Ph).

^{29}Si NMR (79.5 MHz, CDCl$_3$, ppm): δ = 10.66 (Si(CH$_3$)$_2$), -1.40 (Si(CH$_3$)$_2$), -64.25 (Si(CH$_3$)), -79.29, -79.58 (-Si-Ph).

IR (ATR, cm^{-1}): 3072.39, 3052.94, 3019.08 (C-H phenyl), 2957.45, 2905.83 (C-H), 1594.04, 1429.68 (C=C phenyl), 1257.76 (Si-C), 1097.76, 1057.46 (Si-O-Si), 997.60 (C-H phenyl).

EA: Anal. calcd for C$_{74}$H$_{88}$O$_{16}$Si$_{12}$ (%):C, 54.64, H, 5.45; found: C, 54.72, H, 5.53.
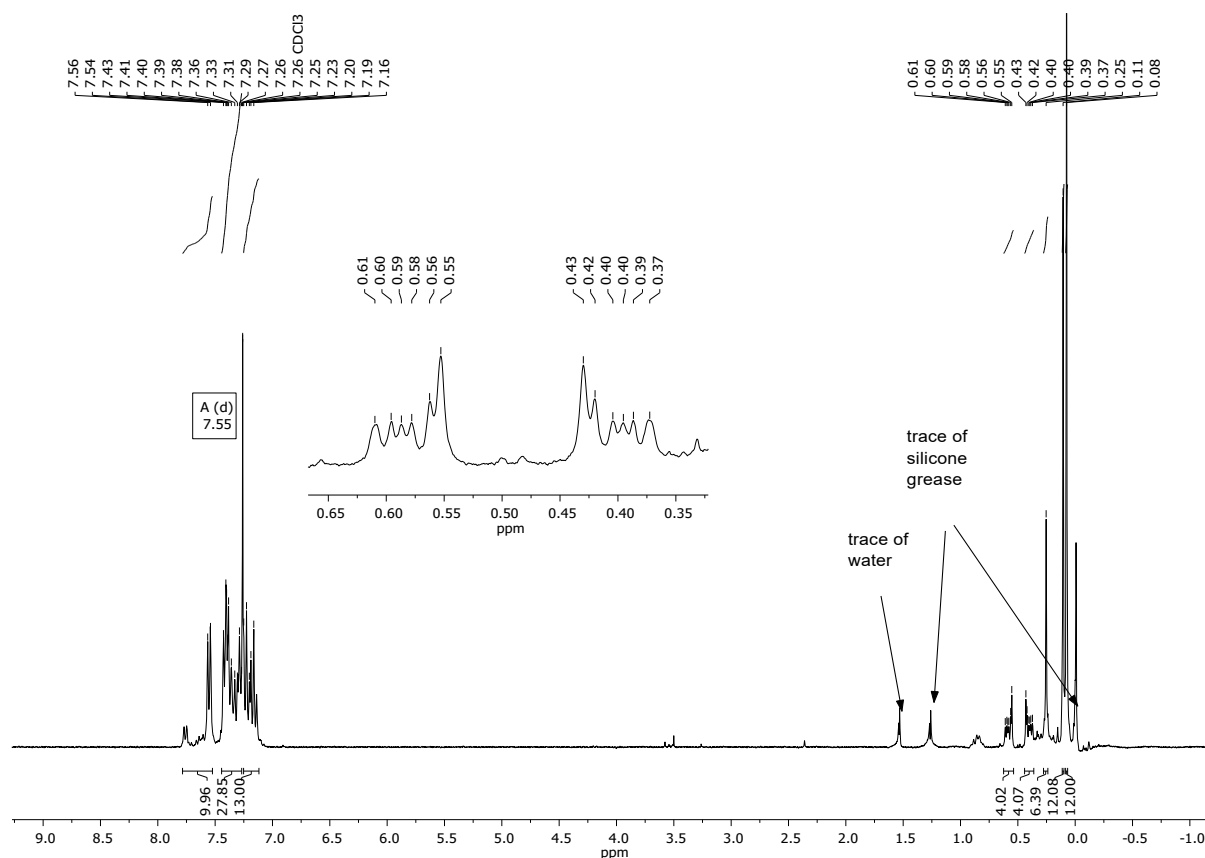
Figure S7 ^{1}H NMR (300 MHz, CDCl$_3$) spectrum of **3c-H**.
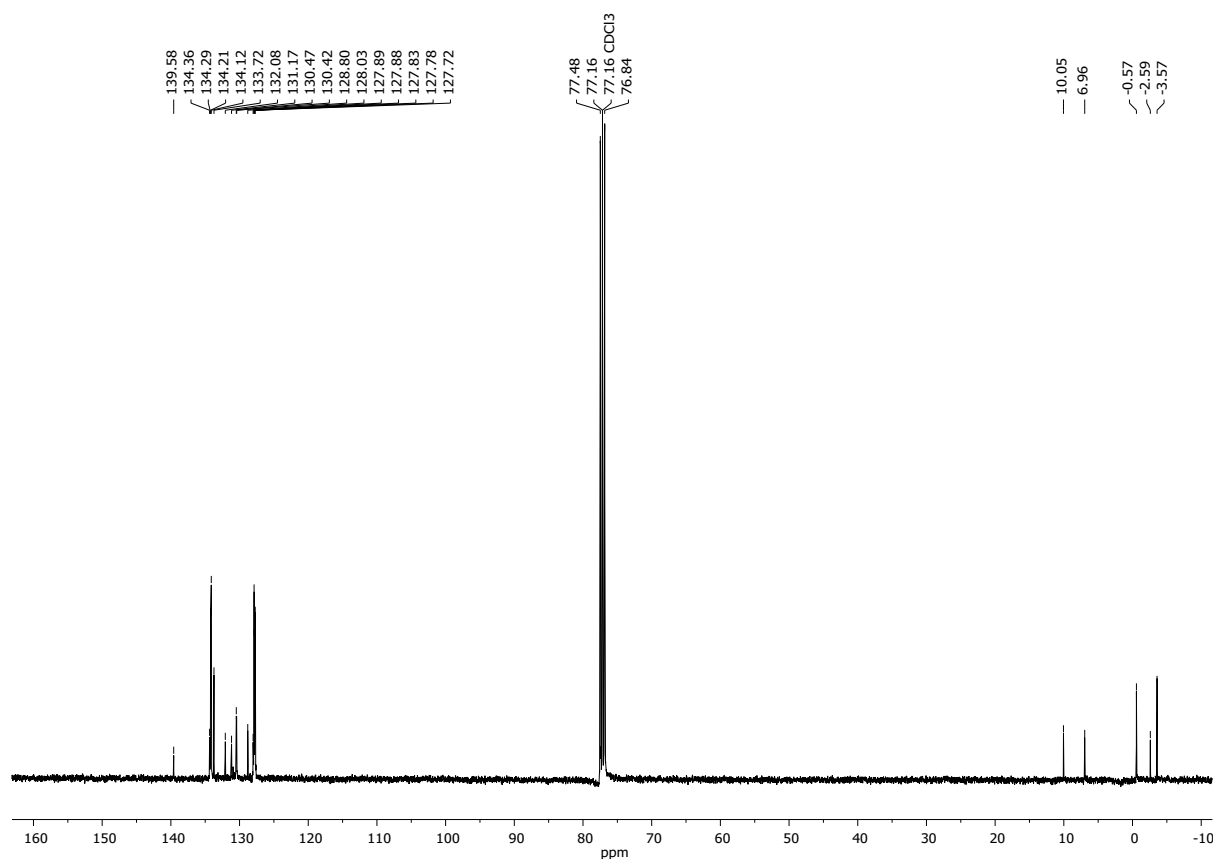
Figure S8 ^{13}C NMR (101 MHz, CDCl$_3$) spectrum of **3c-H**.
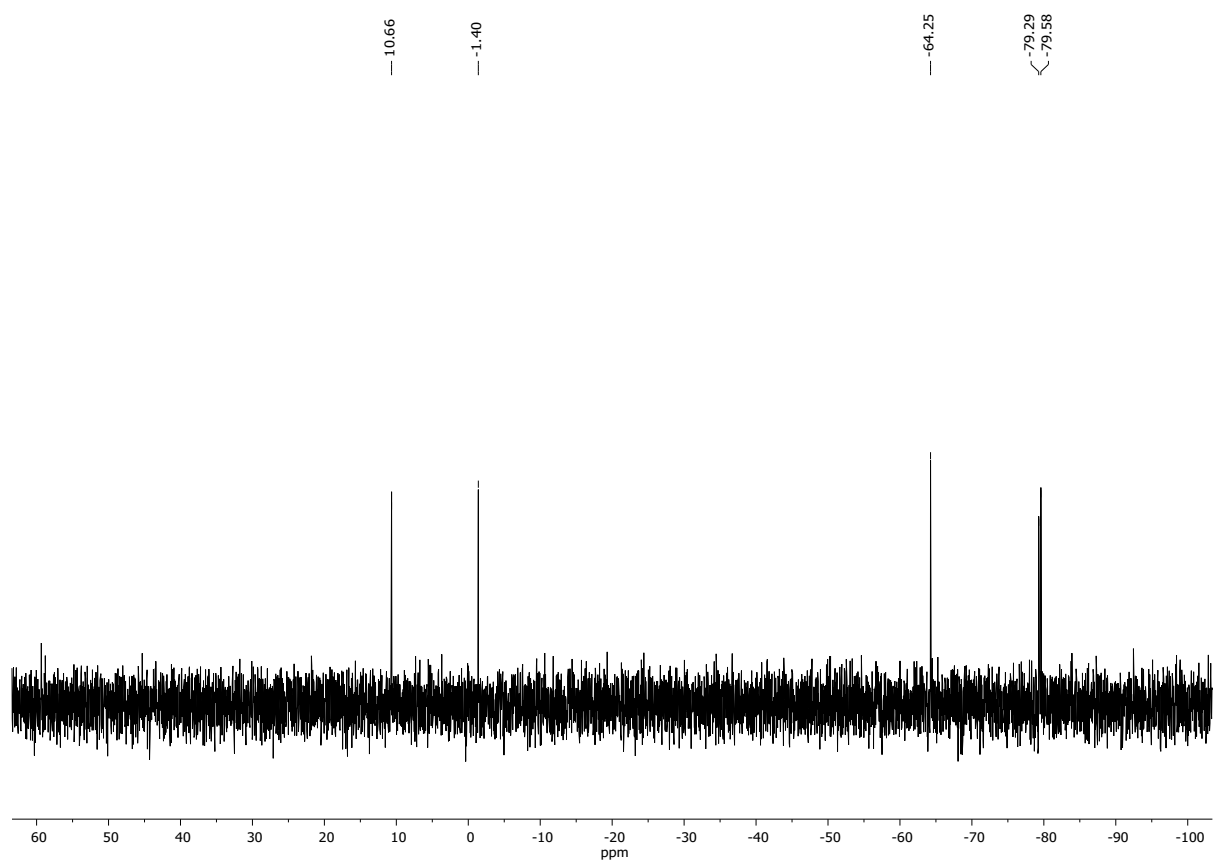
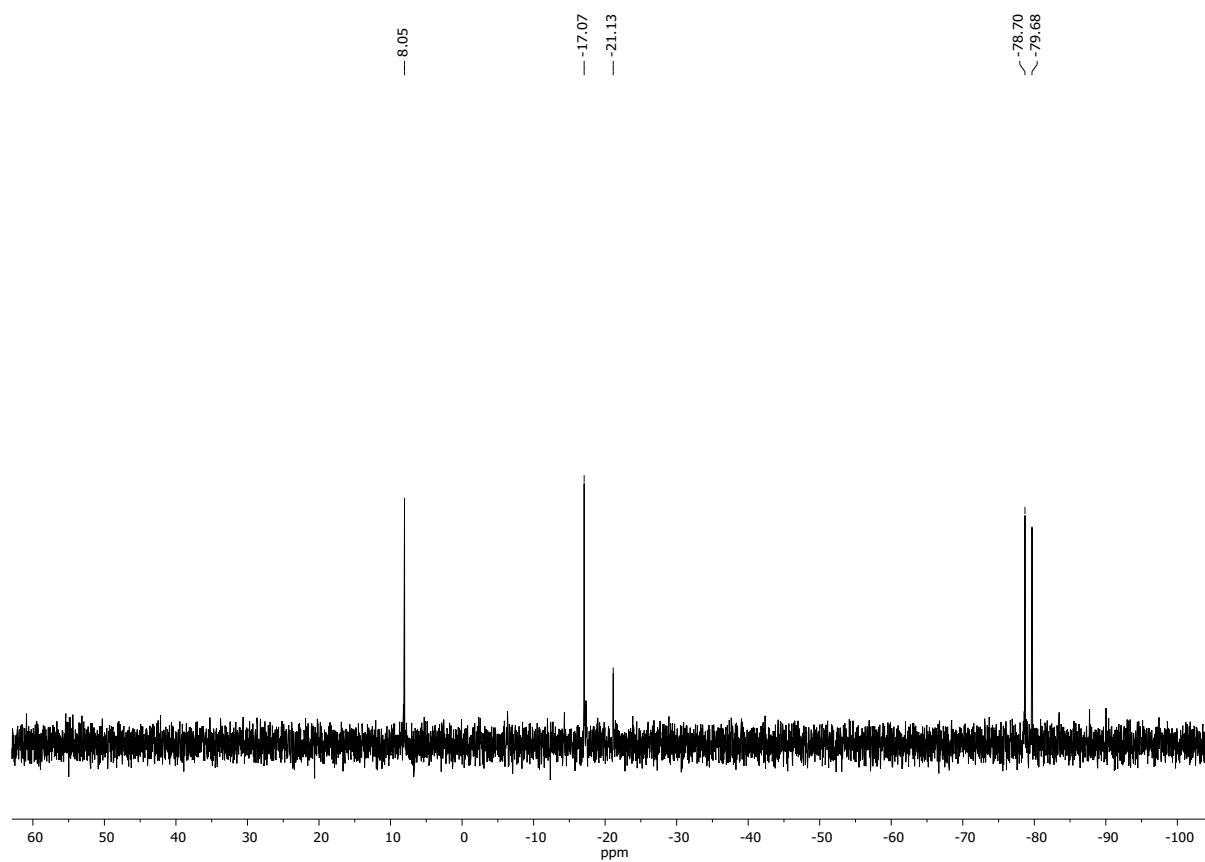**Figure S9** ^{29}Si NMR (79.5 MHz, CDCl$_3$) spectrum of **3c-H**.

7b-d
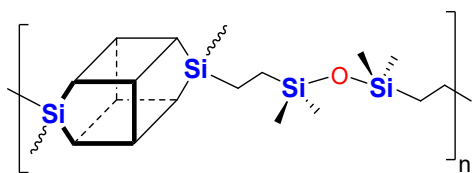
White viscous solid.

¹H NMR (300 MHz, CDCl₃, ppm): δ = -0.19 (s, SiCH₃), -0.13 (s, SiCH₃), -0.10 (s, SiCH₃), 0.25-0.28 (d, J_{H-H} = 6.5, -Si-CH₂-), 0.38-0.56 (m, -Si-CH₂-), 5.90-6.23 (m, terminal bond), 7.15-7.54 (m, Ph).
¹³C NMR (101 MHz, CD₂Cl₂, ppm): δ = -1.44 (SiCH₃), -0.21 (SiCH₃), 1.37 (SiCH₃), 8.76 (-Si-CH₂-), 9.59 (-Si-CH₂-), 128.24-128.41 (Ph), 131.00-13.45 (Ph), 132.59 (Ph), 134.46-134.62 (Ph).
²⁹Si NMR (79.5 MHz, CDCl₃, ppm): δ = 8.28, (Si(CH₃)), -16.77 (Si(CH₃)), -78.62, -79.66 (-Si-Ph).
IR (ATR, cm⁻¹): 3072.62, 3051.14 (C-H phenyl), 2956.29, 2912.16 (C-H), 1594.06, 1430.06 (C=C phenyl), 1256.11 (Si-C), 1077.17 (Si-O-Si), 997.82 (C-H phenyl).
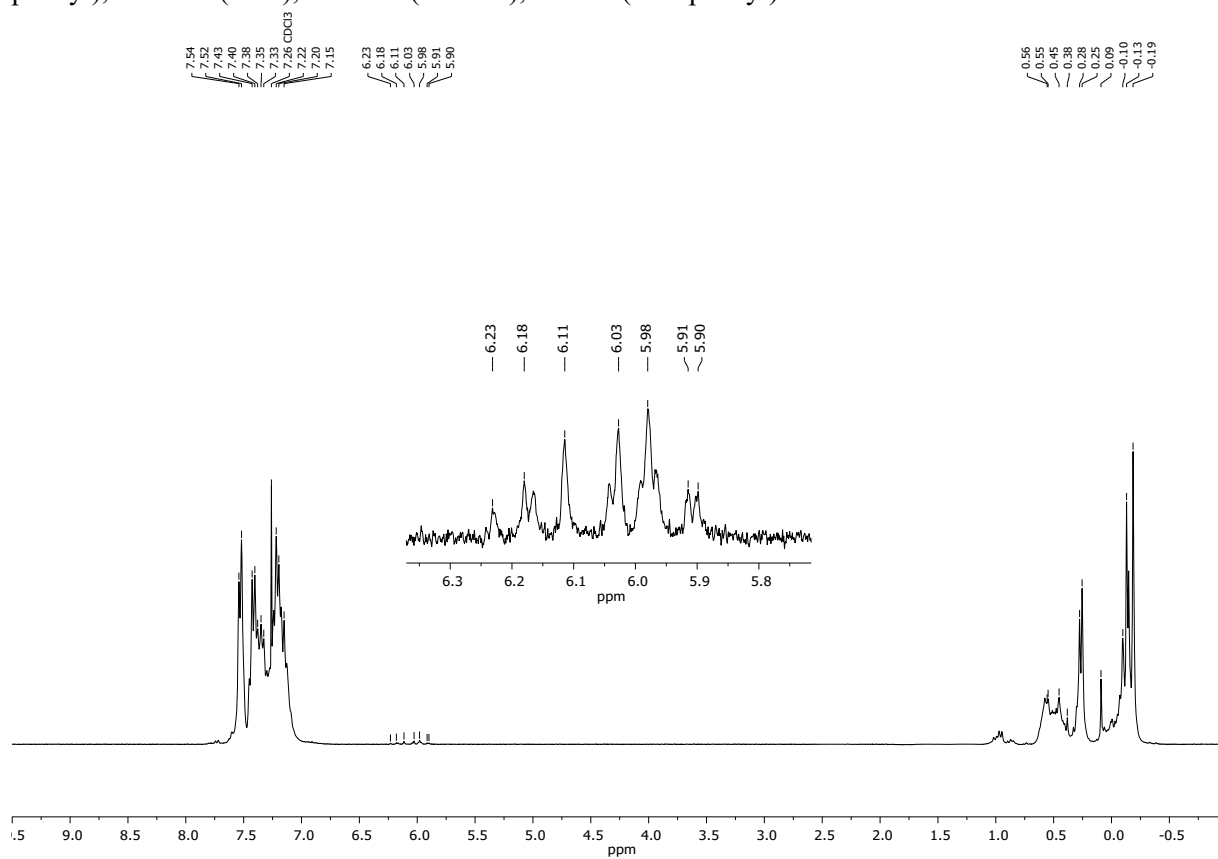
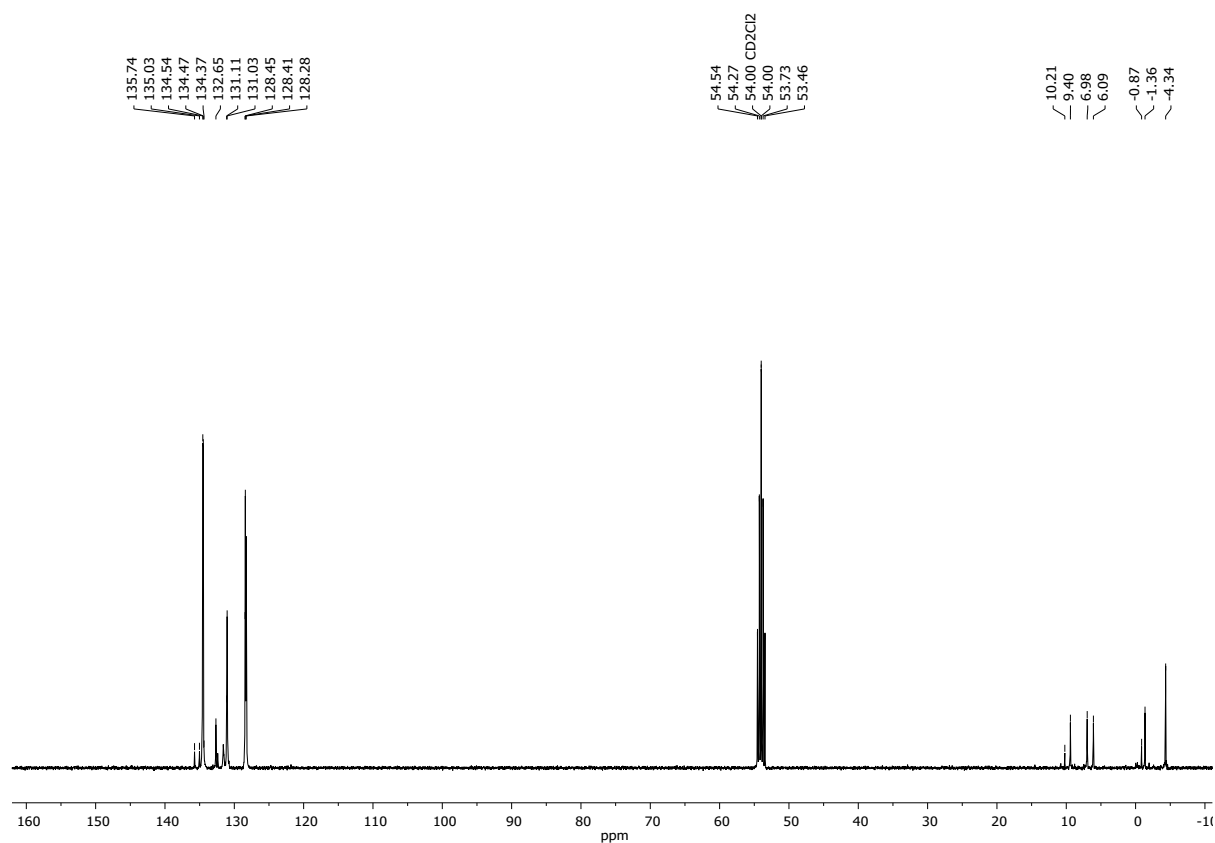**Figure S10** ¹H NMR (300 MHz, CDCl₃) spectrum of **7b-d**.
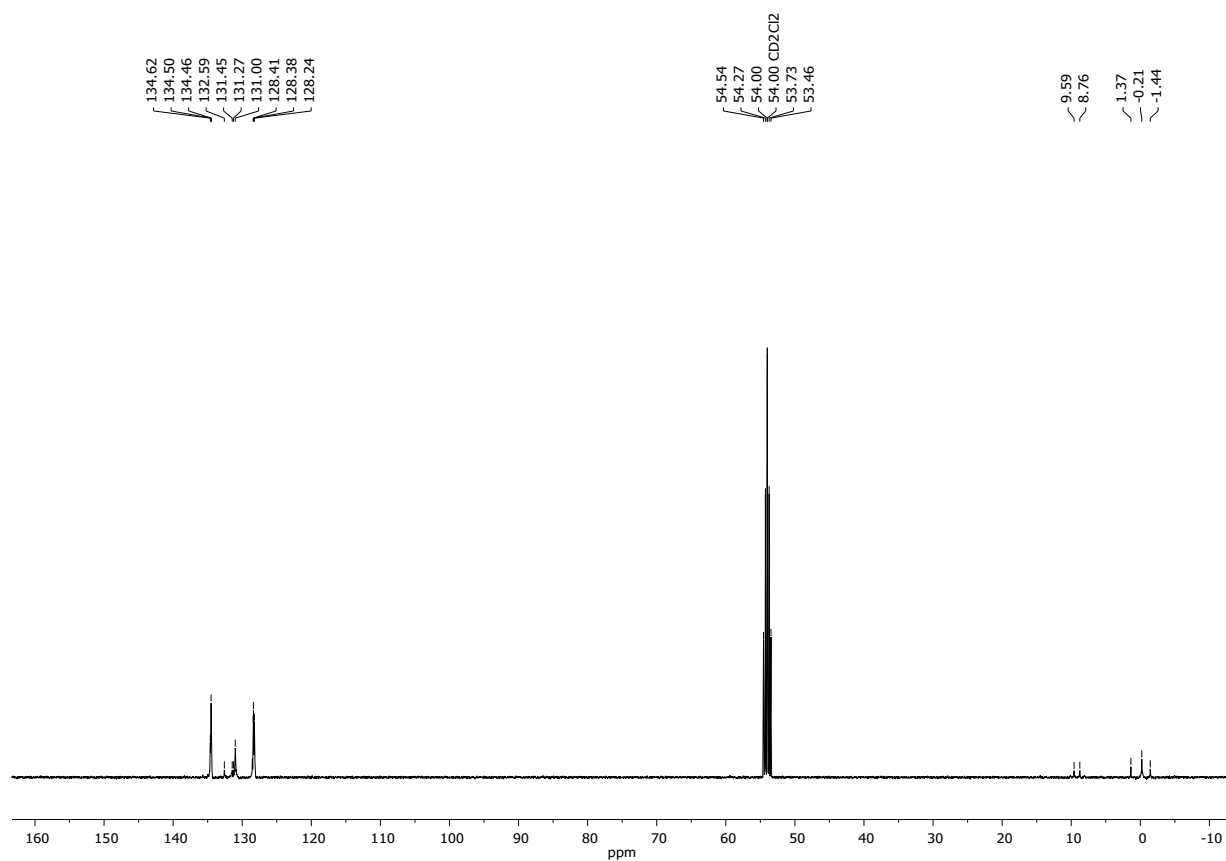
Figure S11 ^{13}C NMR (101 MHz, CD$_2$Cl$_2$) spectrum of **7b-d**.
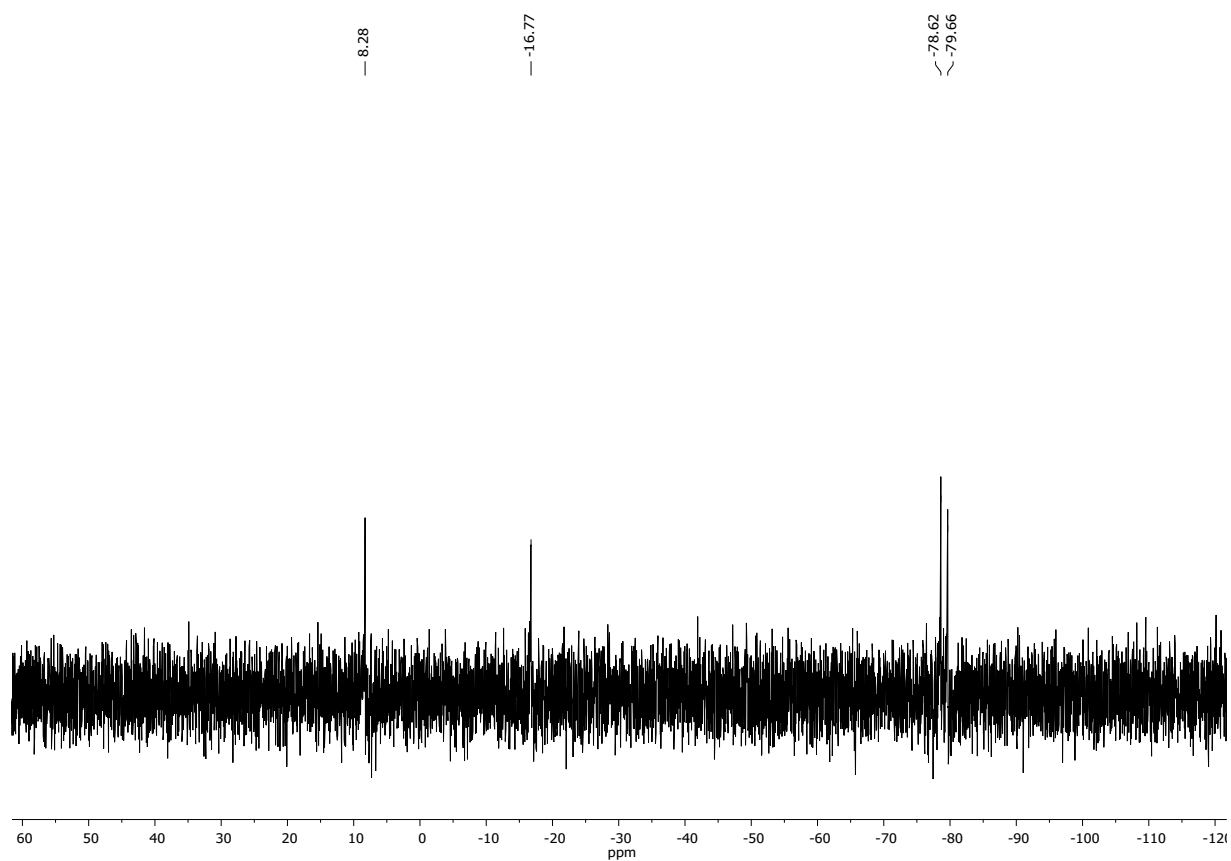
Figure S12 ^{29}Si NMR (79.5 MHz, CDCl$_3$) spectrum of **7b-d**.

7b-e
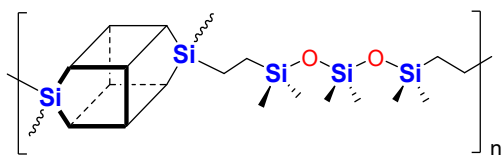
White viscous solid.

¹H NMR (300 MHz, CDCl₃, ppm): δ = -0.16 (s, SiCH₃), -0.14 (s, SiCH₃), 0.26 (s, SiCH₃), 0.45-0.50 (m, -Si-CH₂-), 0.55-0.61 (m, -Si-CH₂-), 7.12-7.53 (m, Ph).

¹³C NMR (101 MHz, CDCl₃, ppm): δ = -1.58 (SiCH₃), -0.54 (SiCH₃), 1.35 (SiCH₃), 8.28 (-Si-CH₂-), 9.03 (-Si-CH₂-), 127.73-127.86 (Ph), 130.40 (Ph), 131.21-132.27 (Ph), 134.05-134.15 (Ph).

²⁹Si NMR (79.5 MHz, CDCl₃, ppm): δ = 8.05 (Si(CH₃)), -17.07 (Si(CH₃)), -21.13 (Si(CH₃)), -78.70, -79.68 (-Si-Ph).

IR (ATR, cm⁻¹): 3072.49, 3051.11, 3027.39 (C-H phenyl), 2957.11, 2914.51 (C-H), 1593.87, 1429.97 (C=C phenyl), 1257.17 (Si-C), 1076.96 (Si-O-Si), 997.51 (C-H phenyl).
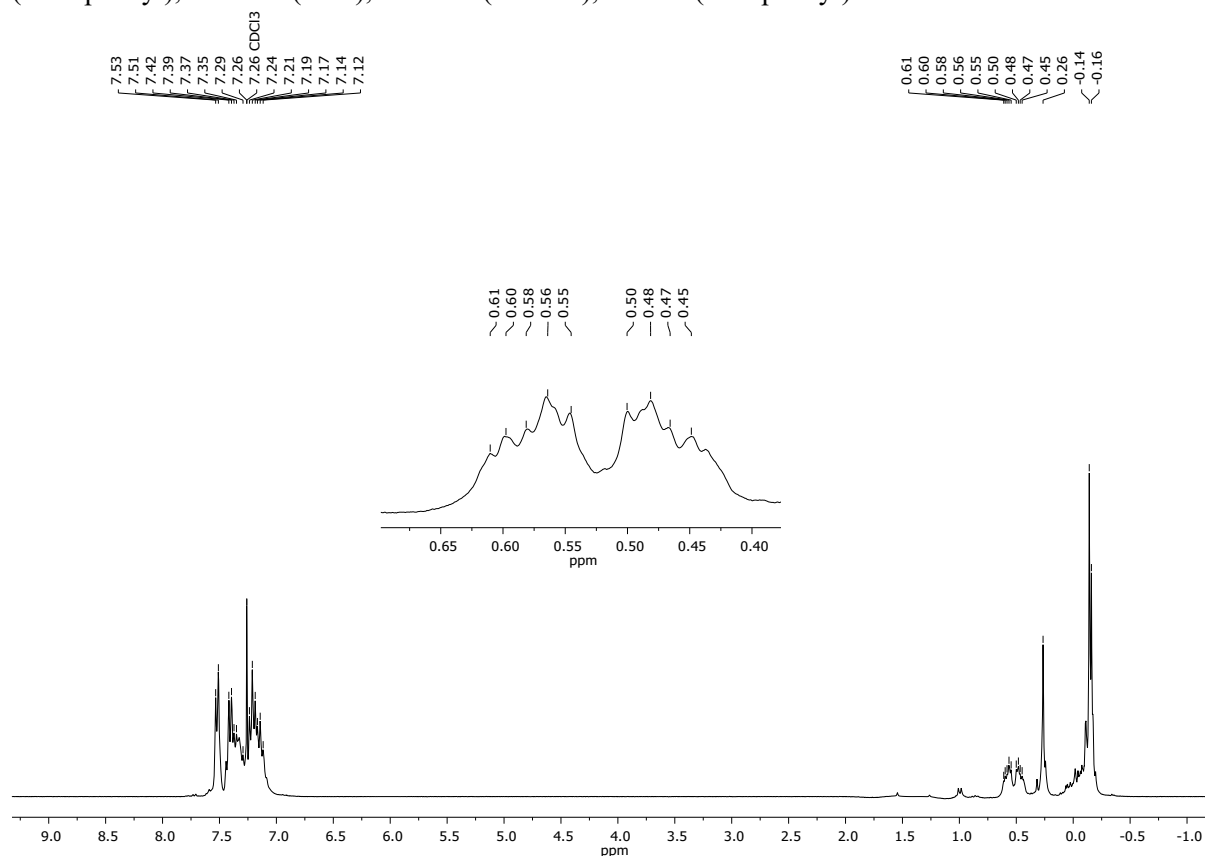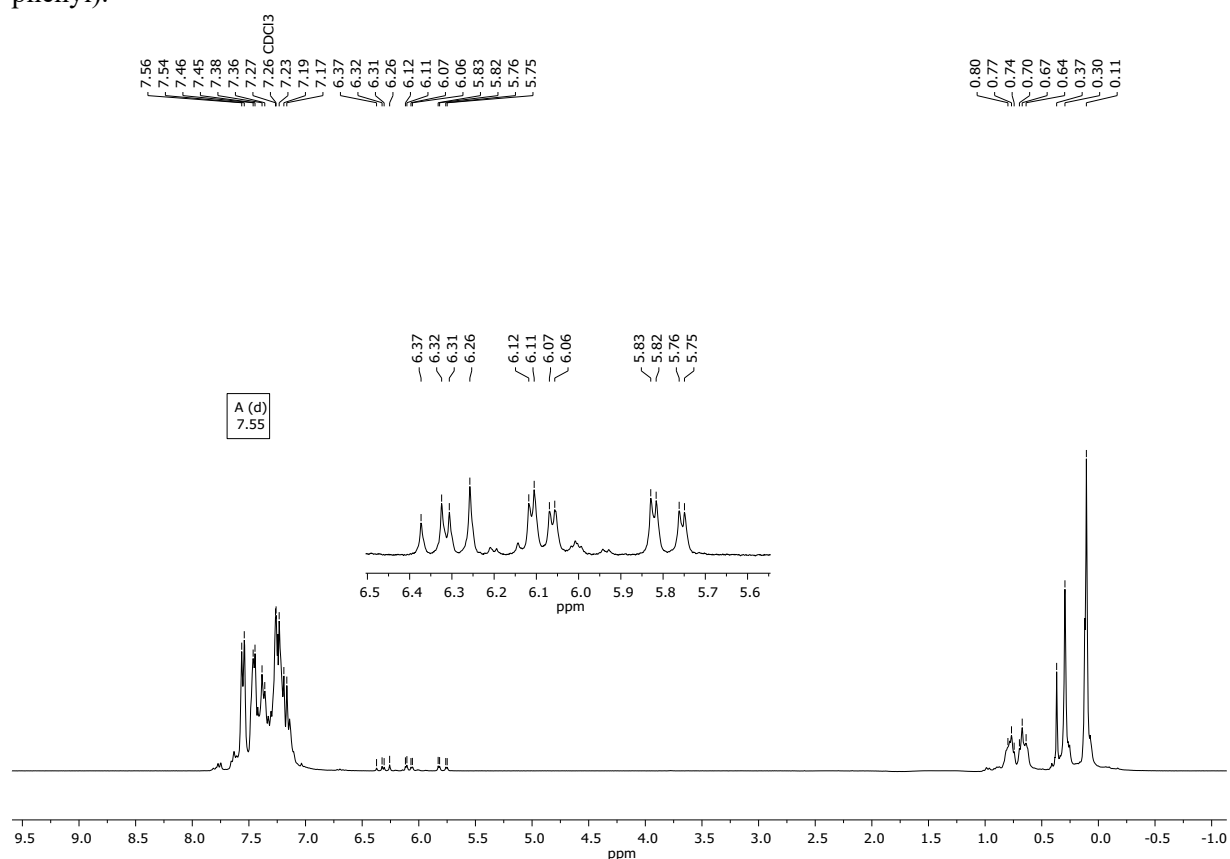

Figure S13 ¹H NMR (300 MHz, CDCl₃) spectrum of **7b-e**.
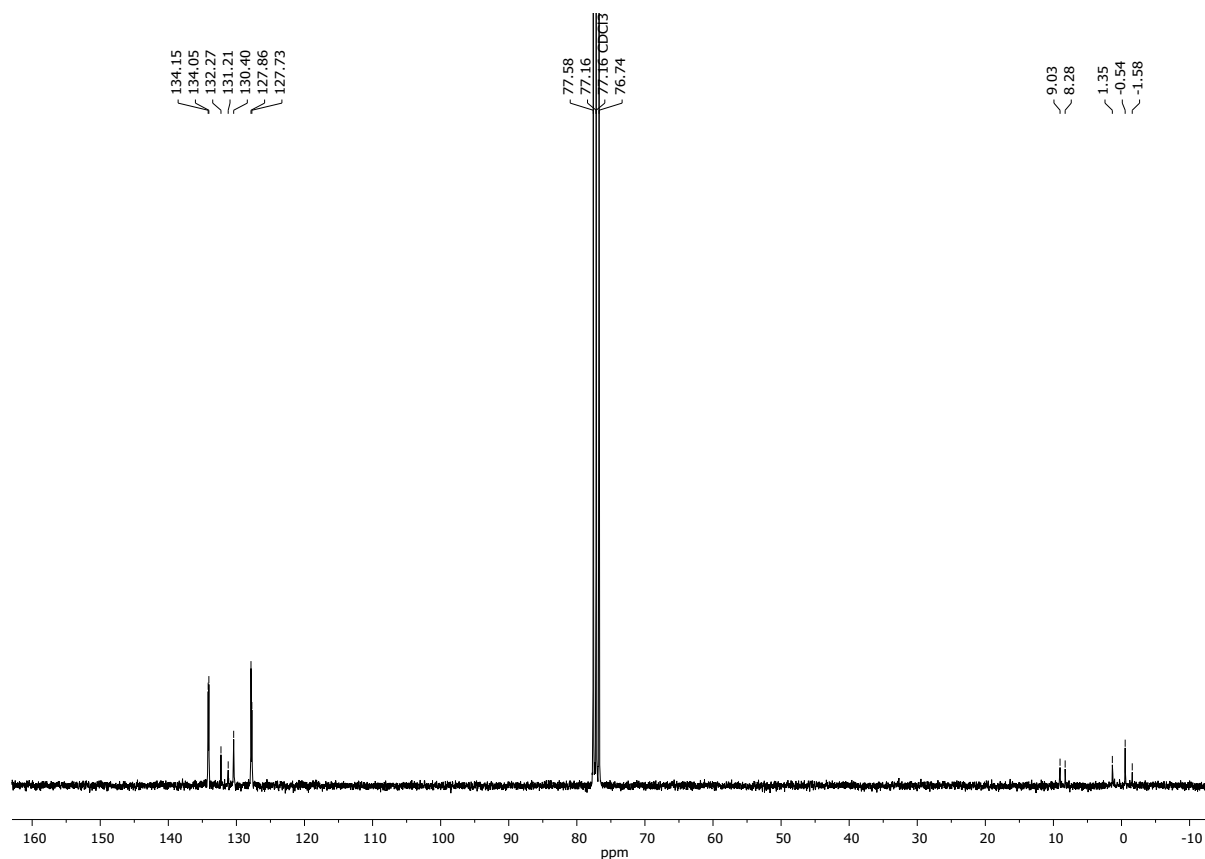
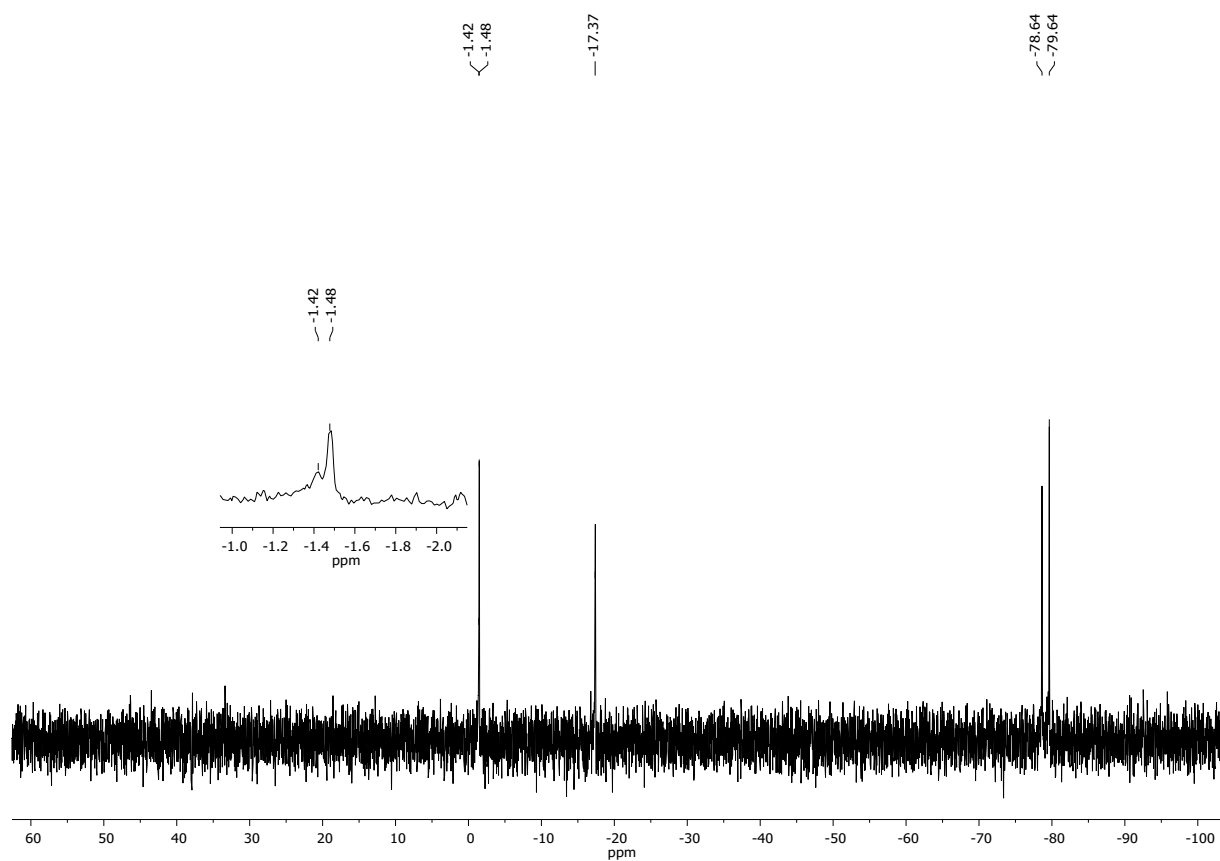**Figure S14** ^{13}C NMR (101 MHz, CDCl$_3$) spectrum of **7b-e**.

Figure S15 ^{29}Si NMR (79.5 MHz, CDCl$_3$) spectrum of **7b-e**

7b-f
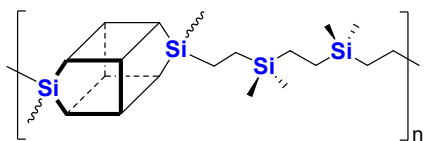
White viscous solid.

¹H NMR (300 MHz, CD$_2$Cl$_2$, ppm): δ = -0.24 (s, SiCH$_3$), -0.08- -0.06 (d, -Si-CH$_2$-CH$_2$-), 0.30 (s, SiCH$_3$), 0.41 (s, SiCH$_3$), 0.55-0.62 (m, -Si-CH$_2$-), 5.93-5.95 (m, terminal bond), 6.04 (dd, J_{H-H} = 14.9, 4.3 Hz terminal bond), 6.21 (dd, J_{H-H} = 19.6, 15.1 Hz, terminal bond), 7.16-7.56 (m, Ph).

¹³C NMR (101 MHz, CD$_2$Cl$_2$, ppm): δ = -4.92 (SiCH$_3$), -1.94 (SiCH$_3$), -1.45 (SiCH$_3$), 5.51 (-Si-CH$_2$-), 6.40 (-Si-CH$_2$-), 8.82 (-Si-CH$_2$-), 9.63 (-Si-CH$_2$-), 127.70-127.87 (Ph), 130.45-13.53 (Ph), 132.07 (Ph), 133.79-134.45 (Ph), 135.16 (Ph).

²⁹Si NMR (79.5 MHz, CDCl$_3$, ppm): δ = 16.14 (Si(CH$_3$), 5.91 (Si(CH$_3$)), -17.12 (Si(CH$_3$)), -78.68, -79.67 (-Si-Ph).

IR (ATR, cm^{-1}): 3073.47, 3050.70 (C-H phenyl), 2954.07, 2900.05 (C-H), 1594.00, 1430.02 (C=C phenyl), 1259.21 (Si-C), 1074.39, 1028.42 (Si-O-Si), 997.49 (C-H phenyl).
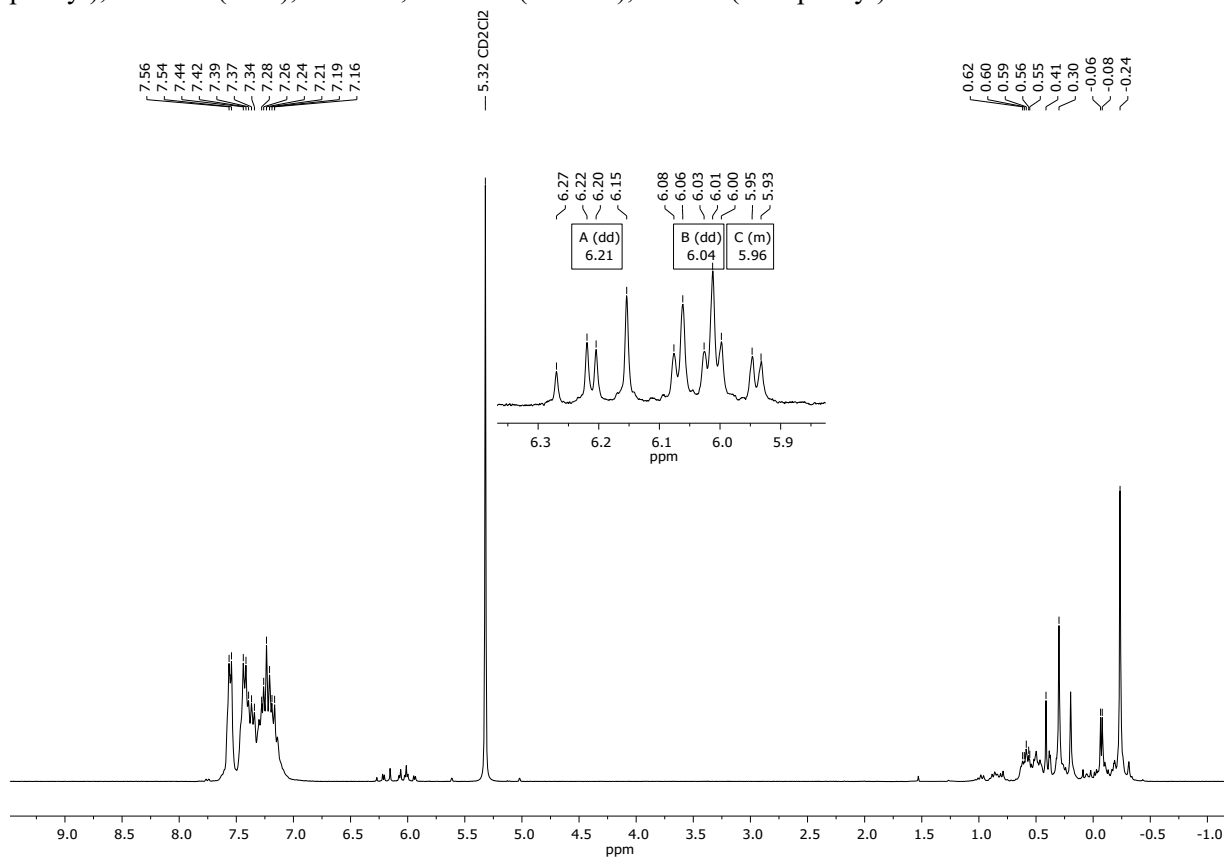
Figure   S16   ¹H   NMR   (300   MHz,   CD$_2$Cl$_2$)   spectrum   of   **7b-f**.

135.74
135.03
134.54
134.47
134.37
132.65
131.11
131.03
128.45
128.41
128.28

54.54
54.27
54.00 CD2Cl2
54.00
53.73
53.46

10.21
9.40
6.98
6.09

-0.87
-1.36
-4.34

160 150 140 130 120 110 100 90 80 70 60 50 40 30 20 10 0 -10

ppm

Figure S17 ^{13}C NMR (101 MHz, CD$_2$Cl$_2$) spectrum of **7b-f**.

16.14

5.91

-17.12

-78.68
-79.67

60 50 40 30 20 10 0 -10 -20 -30 -40 -50 -60 -70 -80 -90 -100

ppm
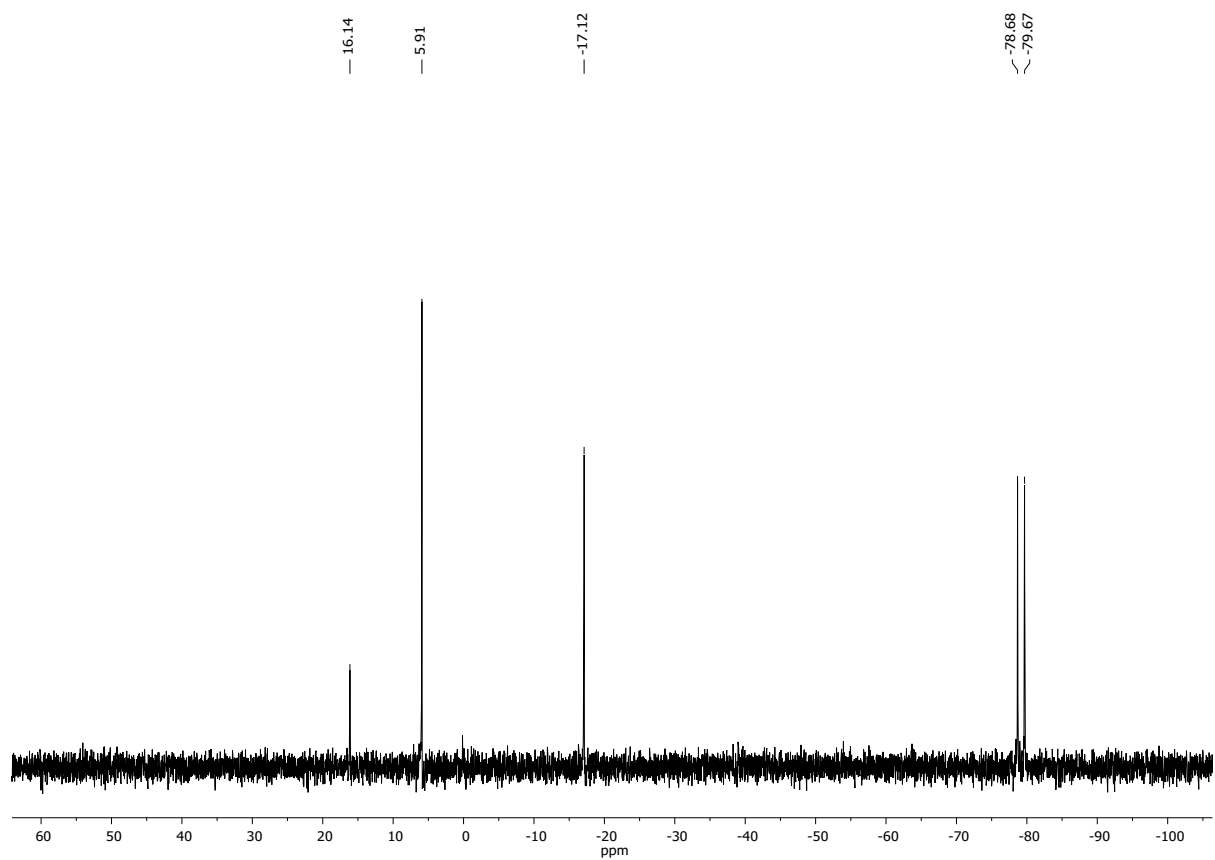
Figure **S18** ^{29}Si NMR (79.5 MHz, CDCl$_3$) spectrum of **7b-f**.

6a-g
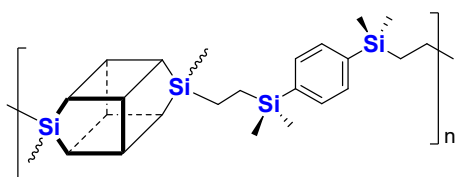
White viscous solid.

^{1}H NMR (300 MHz, CDCl$_3$, ppm): δ = 0.11 (s, Si(CH$_3$)$_2$), 0.30 (s, SiCH$_3$), 0.37 (s, SiCH$_3$), 0.64-0.70 (m, -Si-CH$_2$-), 0.74-0.80 (m, -Si-CH$_2$-), 5.75-6.37 (m, terminal bonds), 7.17-7.46 (m, Ph), 7.51 (d, J_{H-H} = 6.7 Hz).

^{13}C NMR (101 MHz, CDCl$_3$, ppm): δ = -3.58 (Si(CH$_3$)$_2$), -1.39 (SiCH$_3$), 6.44 (-Si-CH$_2$-), 9.08 (-Si-CH$_2$-), 127.77-127.89 (Ph), 130.42 (Ph), 131.21 (Ph), 132.26 (Ph), 132.93 (Ph), 134.07-134.18 (Ph), 139.66 (Ph).

^{29}Si NMR (79.5 MHz, CDCl$_3$, ppm): δ = -1.42, -1.48 (Si(CH$_3$)$_2$), -17.37 (Si(CH$_3$)), -78.64, -79.64 (-Si-Ph).

IR (ATR, cm^{-1}): 3072.25, 3026.24 (C-H phenyl), 2954.45, 2916.67 (C-H), 1594.19, 1494.91, 1430.17 (C=C phenyl), 1378.65 (C-H), 1259.11 (Si-C), 1129.00, 1091.14, 1029.30 (Si-O-Si), 998.36 (C-H phenyl).

Figure S19 ^{1}H NMR (300 MHz, CDCl$_3$) spectrum of **6a-g**.
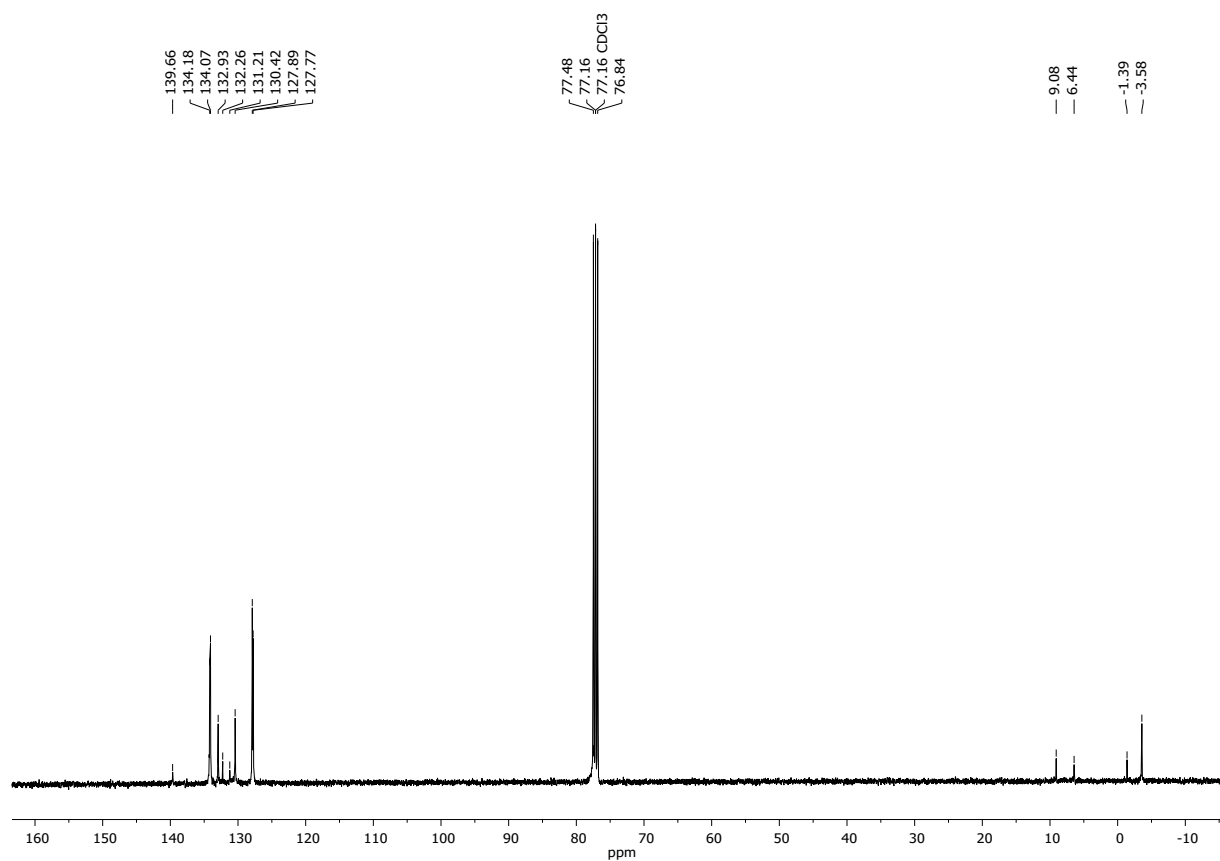
**Figure S20** ^{13}C NMR (101 MHz, CDCl$_3$) spectrum of **6a-g**.

Figure S21 ^{29}Si NMR (79.5 MHz, CDCl₃) spectrum of **6a-g**.

7b-h
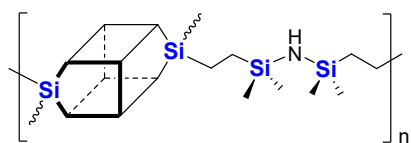
White viscous solid.

¹H NMR (300 MHz, CDCl₃, ppm): δ = -0.19 (s, SiCH₃), -0.03 (s, SiCH₃), 0.30 (s, SiCH₃), 0.39-0.53 (m, -Si-CH₂-), 0.93-1.04 (m, -CH₂-, terminal bond), 1.65 (s, N-H- terminal bonds), 7.16-7.54 (m, Ph).
¹³C NMR (101 MHz, CDCl₃, ppm): δ = -1.51 (SiCH₃), 0.01 (SiCH₃), 1.02 (SiCH₃), 8.82 (-Si-CH₂-), 9.76 (-Si-CH₂-), 127.76-127.99 (Ph), 130.42-130.50 (Ph), 131.28 (Ph), 132.35 (Ph), 134.08-134.35 (Ph).
²⁹Si NMR (79.5 MHz, CDCl₃, ppm): δ = 4.67, (Si(CH₃)), 4.43 (Si(CH₃)), -16.54 (Si(CH₃)- terminal bond), -16.89 (Si(CH₃)), -78.67, -79.58, -79.66 (-Si-Ph).
IR (ATR, cm⁻¹): 3636.43, 3366.73 (N-H), 3072.79, 3050.46, 3027.52 (C-H phenyl), 2955.94, 2910.78 (C-H), 1594.22, 1430.03 (C=C phenyl), 1256.39 (Si-C), 1073.02, 1027.73 (Si-O-Si), 997.47 (C-H phenyl).
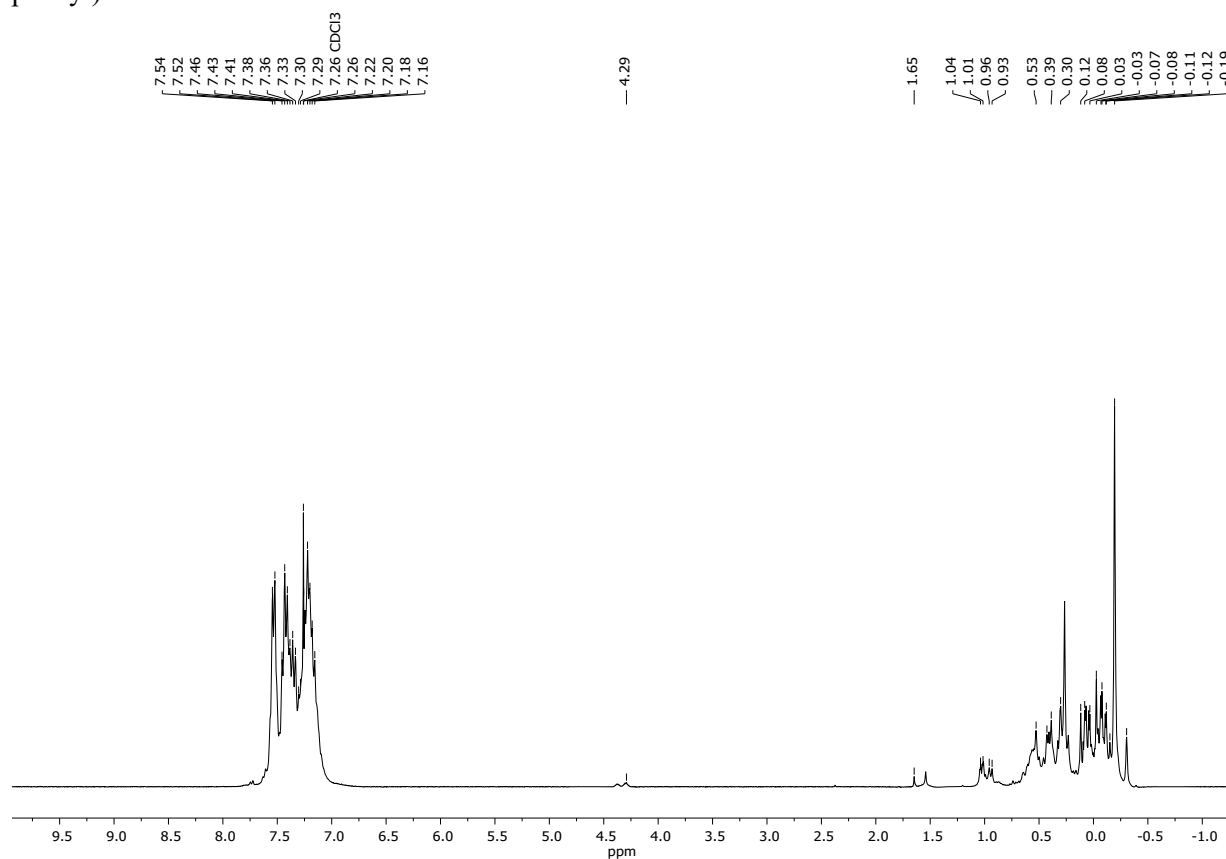
Figure S22 ¹H NMR (300 MHz, CDCl₃) spectrum of **7b-h**.
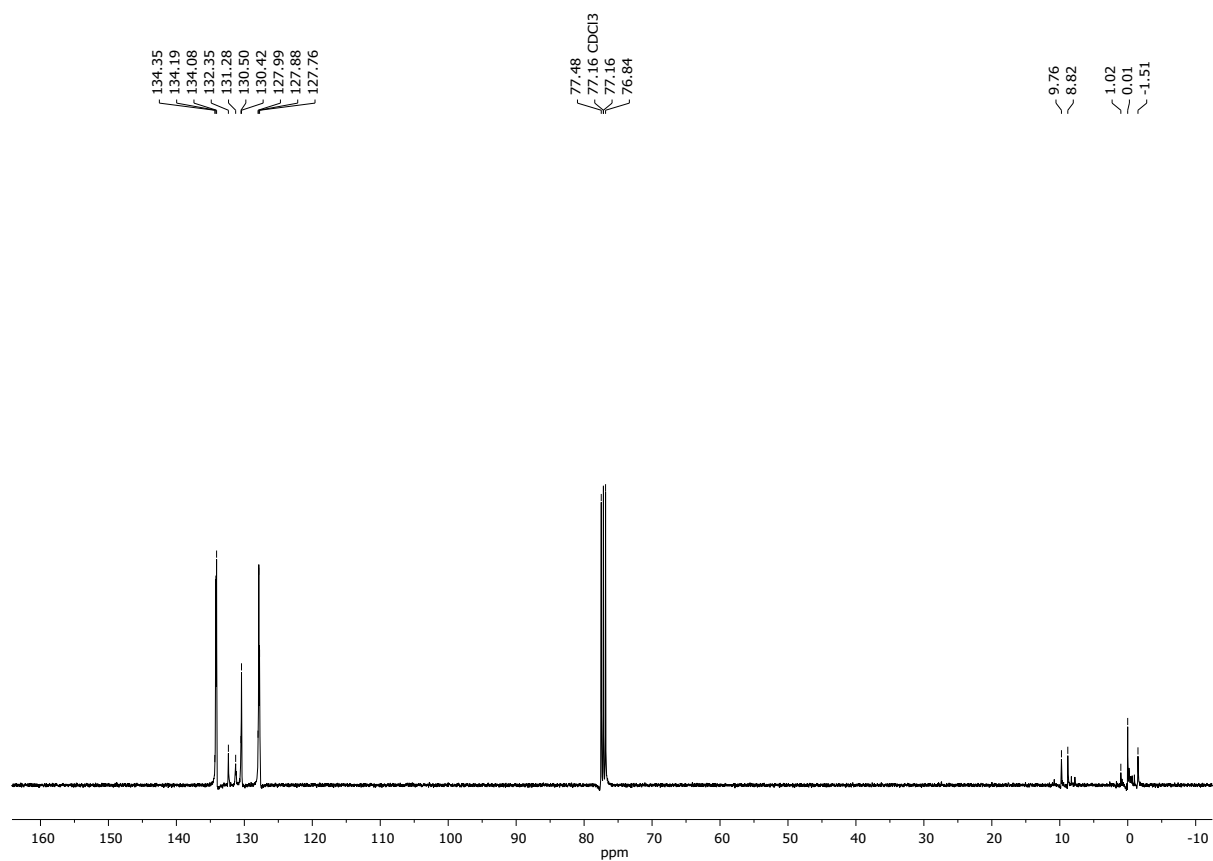
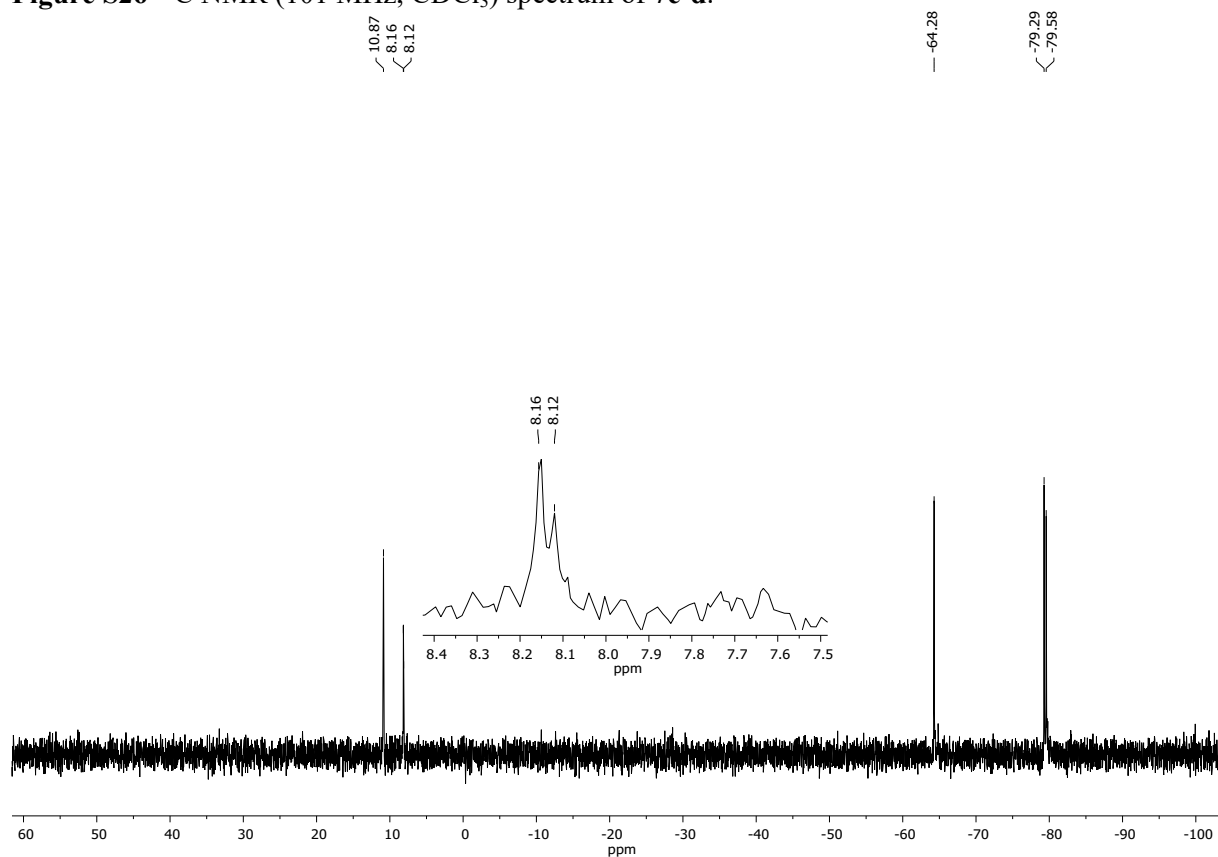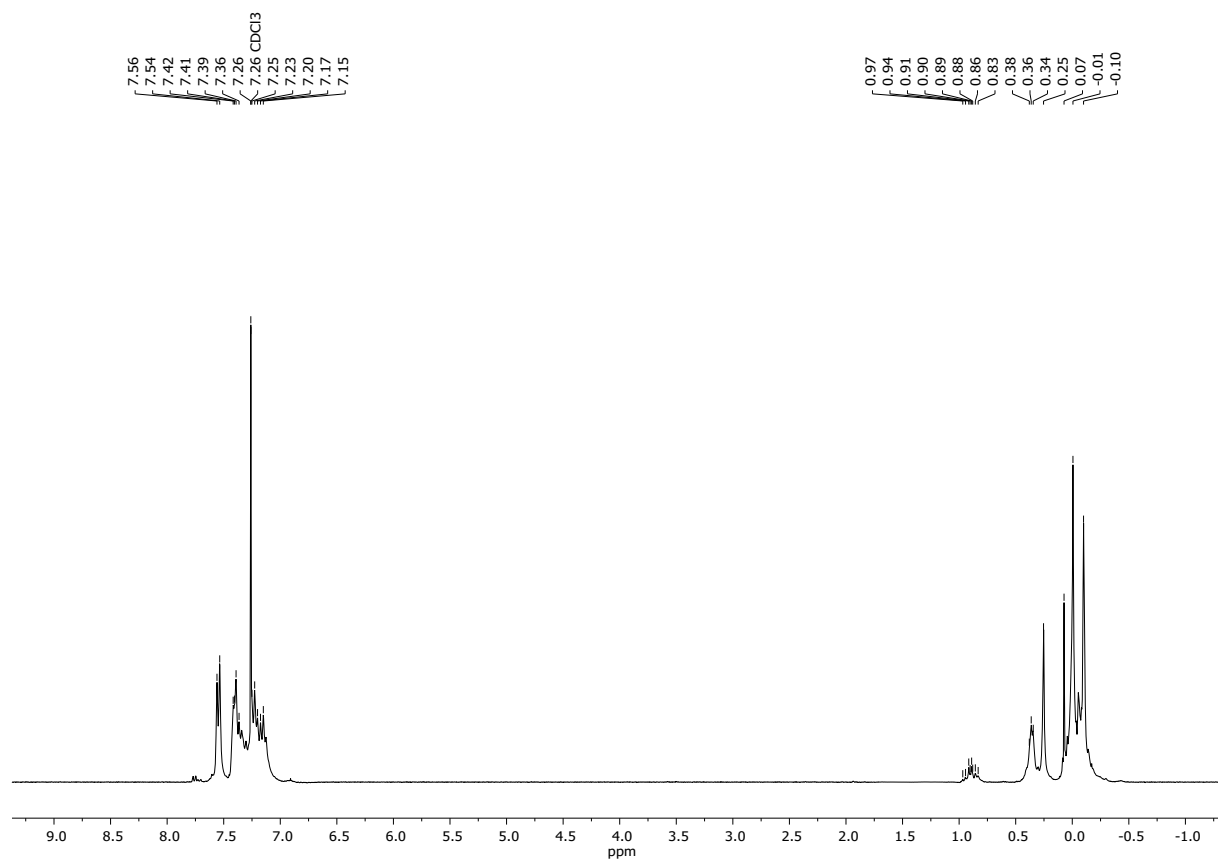**Figure S23** ^{13}C NMR (101 MHz, CDCl$_3$) spectrum of **7b-h**.
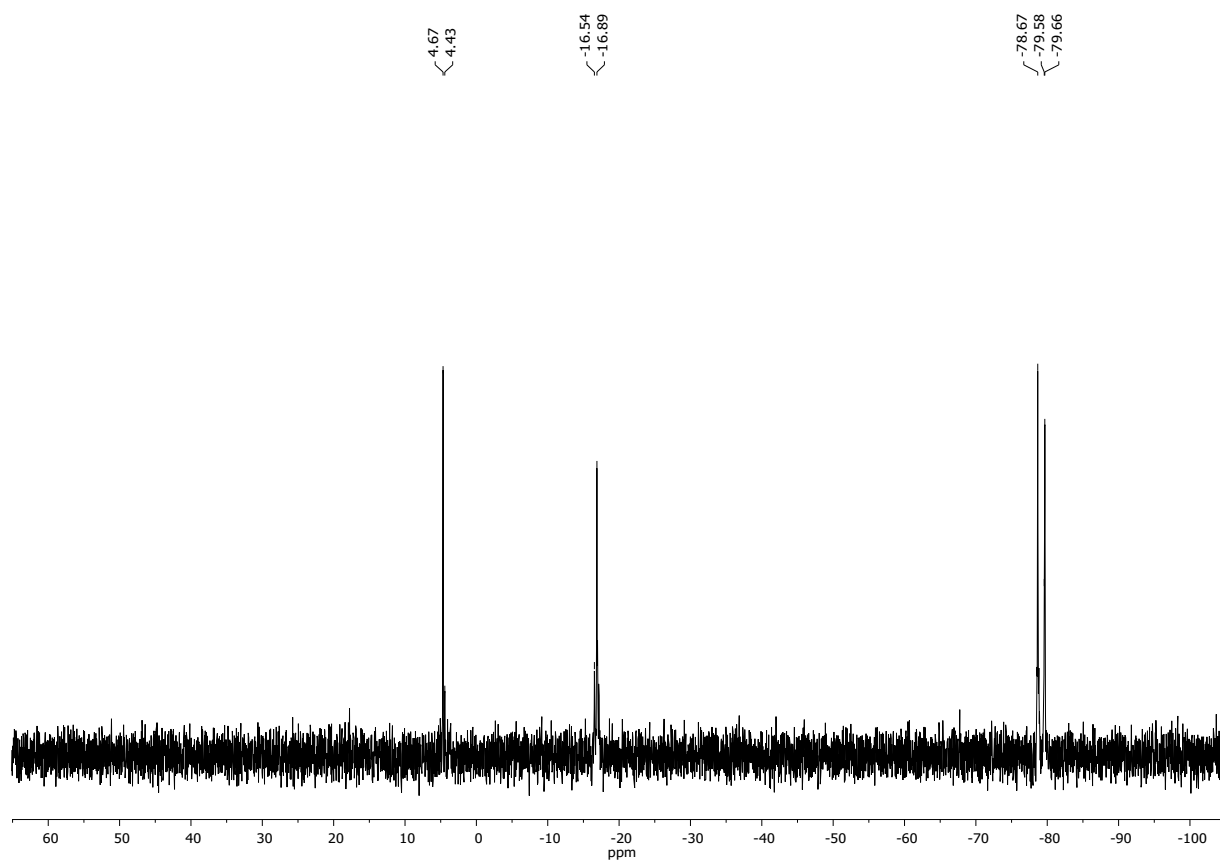
Figure S24 ^{29}Si NMR (79.5 MHz, CDCl$_3$) spectrum of **7b-h**.

7c-d
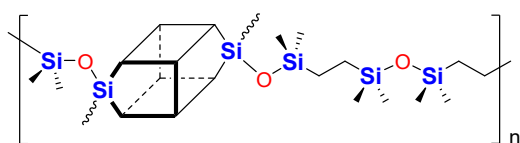
White viscous solid.

¹H NMR (300 MHz, CDCl₃, ppm): δ = -0.13 (s, SiCH₃), -0.09 (s, SiCH₃) -0.00 (s, SiCH₃), 0.26 (s, SiCH₃), 0.32-0.39 (m, -Si-CH₂-), 0.78-0.98 (m, -Si-CH₂-), 5.66 (dd, J_{H-H} = 20.2, 3.9 Hz, terminal bond), 5.75 (dd, J_{H-H} = 15.0, 3.9 Hz, terminal bond), 6.06 (dd, J_{H-H} = 20.2, 14.9 Hz, terminal bond), 7.16-7.57 (m, Ph).

¹³C NMR (101 MHz, CDCl₃, ppm): δ = -2.60 (SiCH₃), -0.60 (SiCH₃), -0.33 (SiCH₃), 1.19 (SiCH₃), 9.37 (Si-CH₂-), 9.49 (Si-CH₂-), 127.69-128.86 (Ph), 130.41-130.46 (Ph), 131.13 (Ph), 132.05 (Ph), 134.10-134.18(Ph).

²⁹Si NMR (79.5 MHz, CDCl₃, ppm): δ = 10.87 (Si(CH₃)₂), 8.16 (Si(CH₃)₂), 8.12 (Si(CH₃)₂), -64.28 (SiCH₃), -79.29, -79.58 (-Si-Ph).

IR (ATR, cm⁻¹): 3073.01, 3051.71 (C-H phenyl), 2957.50, 2907.67 (C-H), 1594.29, 1430.14 (C=C phenyl), 1254.44 (Si-C), 1100.10, 1027.08 (Si-O-Si), 997.64 (C-H phenyl).
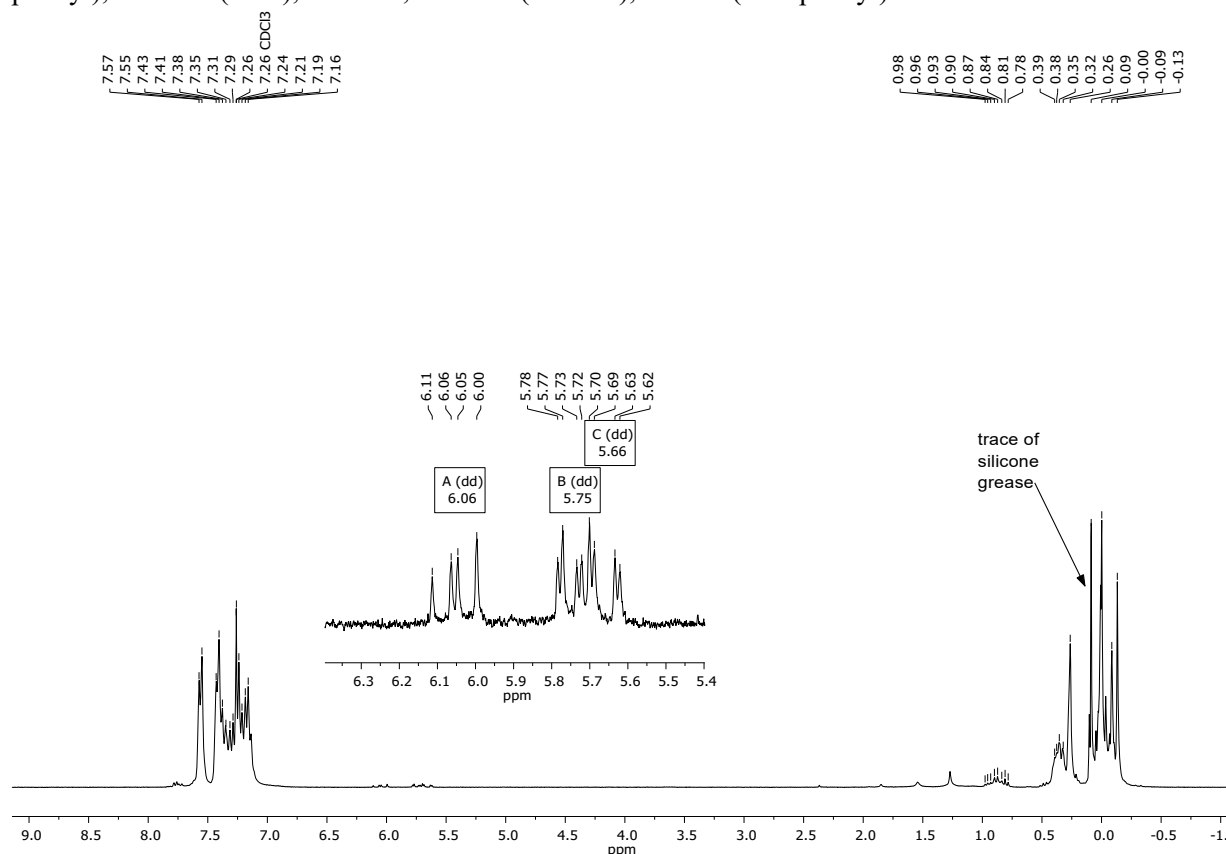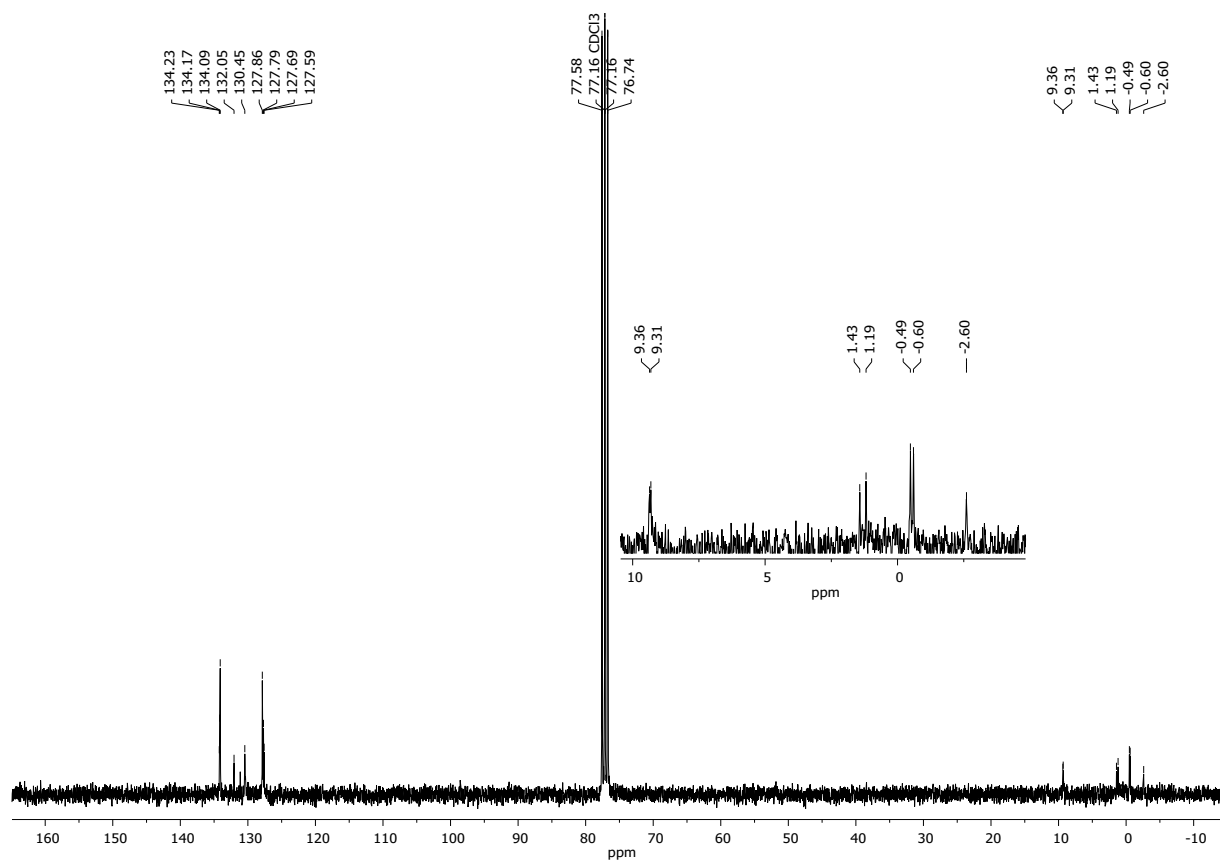

Figure S25 ¹H NMR (300 MHz, CDCl₃) spectrum of **7c-d**.
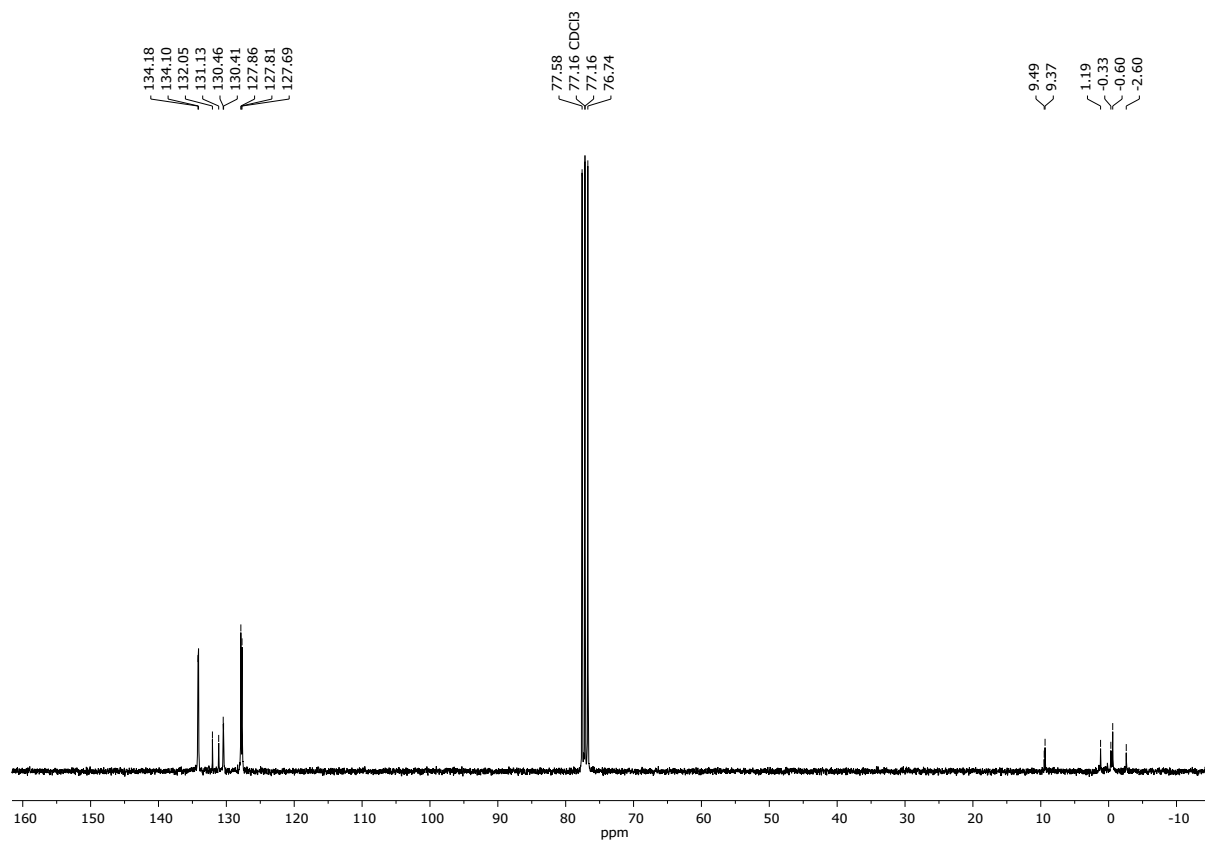
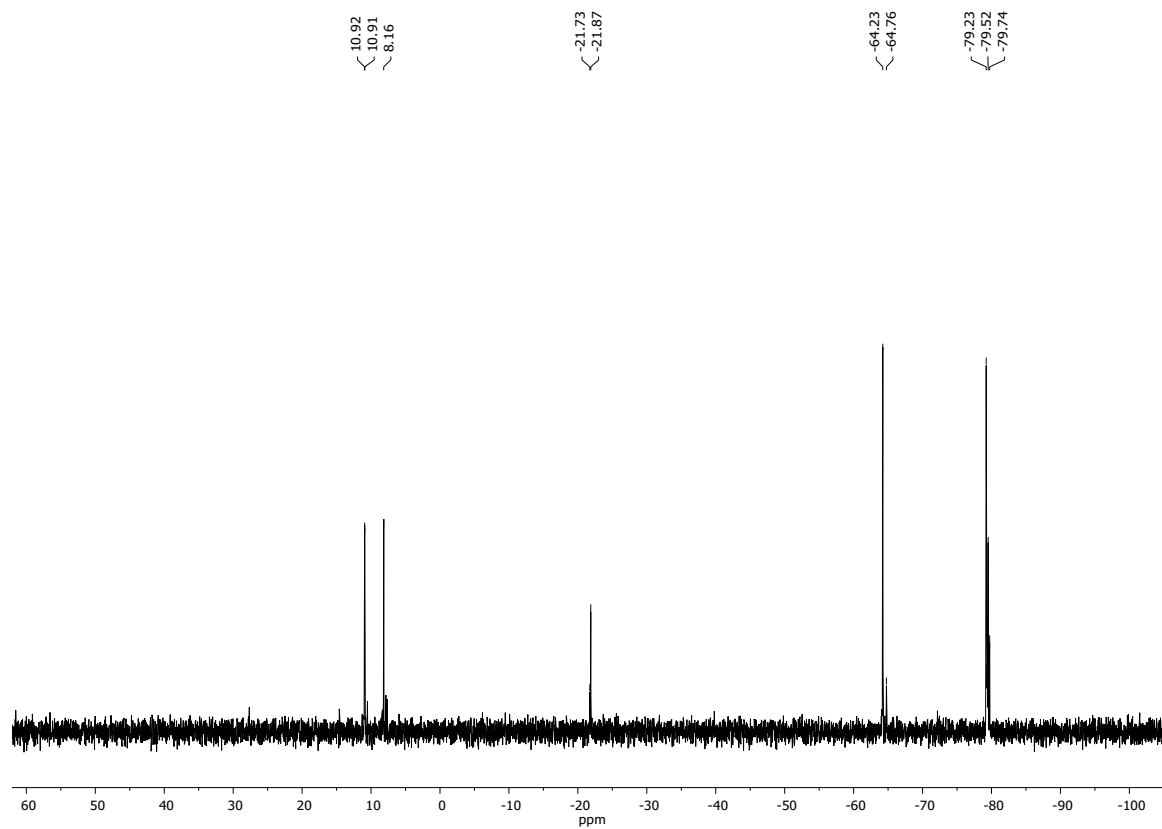**Figure S26** ^{13}C NMR (101 MHz, CDCl$_3$) spectrum of **7c-d**.

**Figure S27** ^{29}Si NMR (79.5 MHz, CDCl$_3$) spectrum of **7c-d**.

7c-e
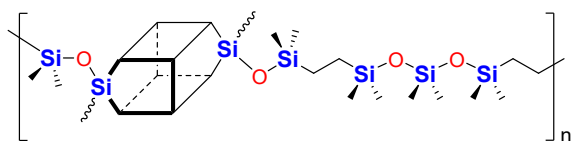
White viscous solid.

^{1}**H NMR** (300 MHz, CDCl$_3$, ppm): δ = -0.10 (s, SiCH$_3$), -0.01 (s, SiCH$_3$), 0.02 (s, SiCH$_3$), 0.25 (s, SiCH$_3$), 0.34-0.38 (m, -Si-CH$_2$-), 0.83-0.97 (m, -Si-CH$_2$-), 7.15-7.56 (m, Ph).

^{13}**C NMR** (101 MHz, CDCl$_3$, ppm): δ = -2.60 (SiCH$_3$), -0.60 (SiCH$_3$), -0.49 (SiCH$_3$), 1.19 (SiCH$_3$), 1.43 (SiCH$_3$), 9.31 (Si-CH$_2$-), 9.36 (Si-CH$_2$-), 127.59-128.86 (Ph), 130.45 (Ph), 132.05 (Ph), 134.09- 134.23 (Ph).

^{29}**Si NMR** (79.5 MHz, CDCl$_3$, ppm): δ = 10.91 (Si(CH$_3$)), 10.92 (Si(CH$_3$)), 8.16 (Si(CH$_3$)), -21.87 (Si(CH$_3$)), -21.73 (Si(CH$_3$)), -64.76 ((SiCH$_3$)), -64.23 (Si(CH$_3$)), -79.74, -79.52, -79.23 (-Si-Ph).

IR (ATR, cm^{-1}): 3072.97, 3051.66 (C-H phenyl), 2959.37, 2907.32 (C-H), 1594.36, 1430.23 (C=C phenyl), 1257.25 (Si-C), 1108.67, 1028.65 (Si-O-Si), 997.23 (C-H phenyl).
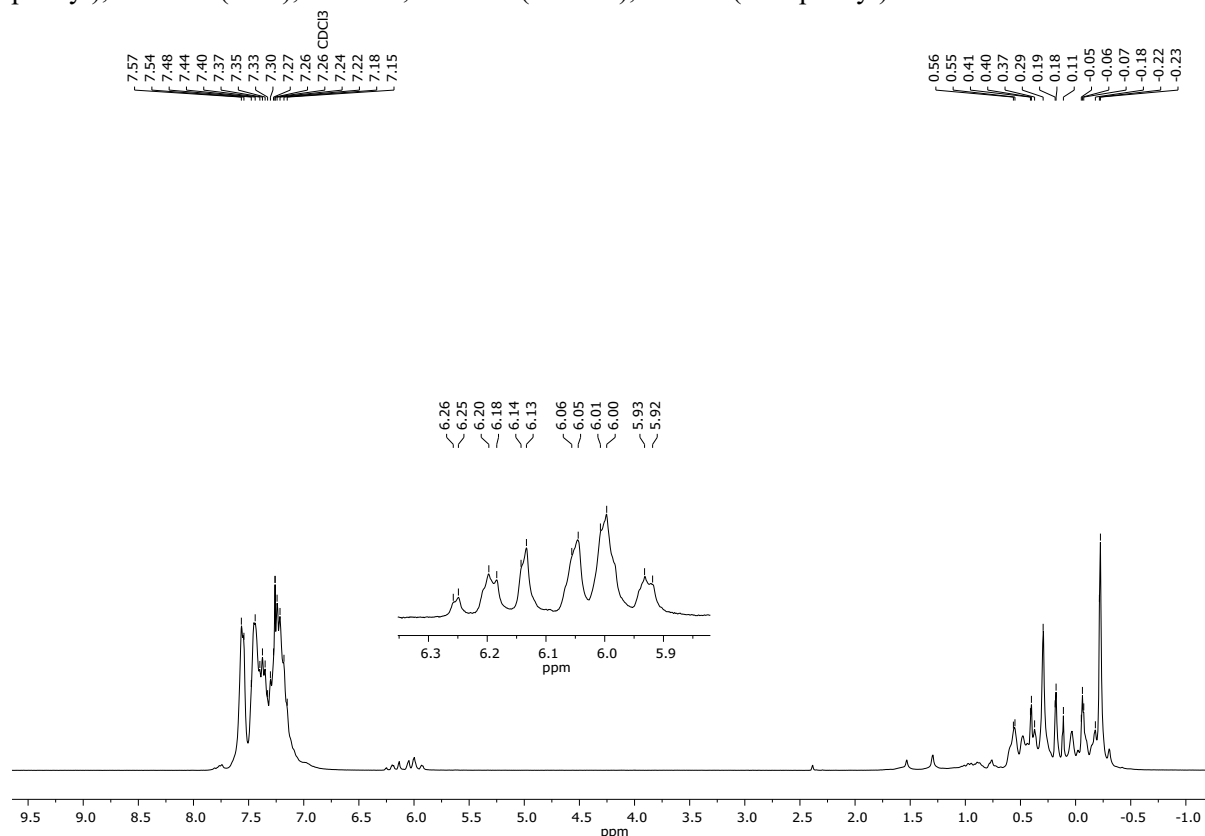

Figure S28 ^{1}H NMR (300 MHz, CDCl$_3$) spectrum of **7c-e**.
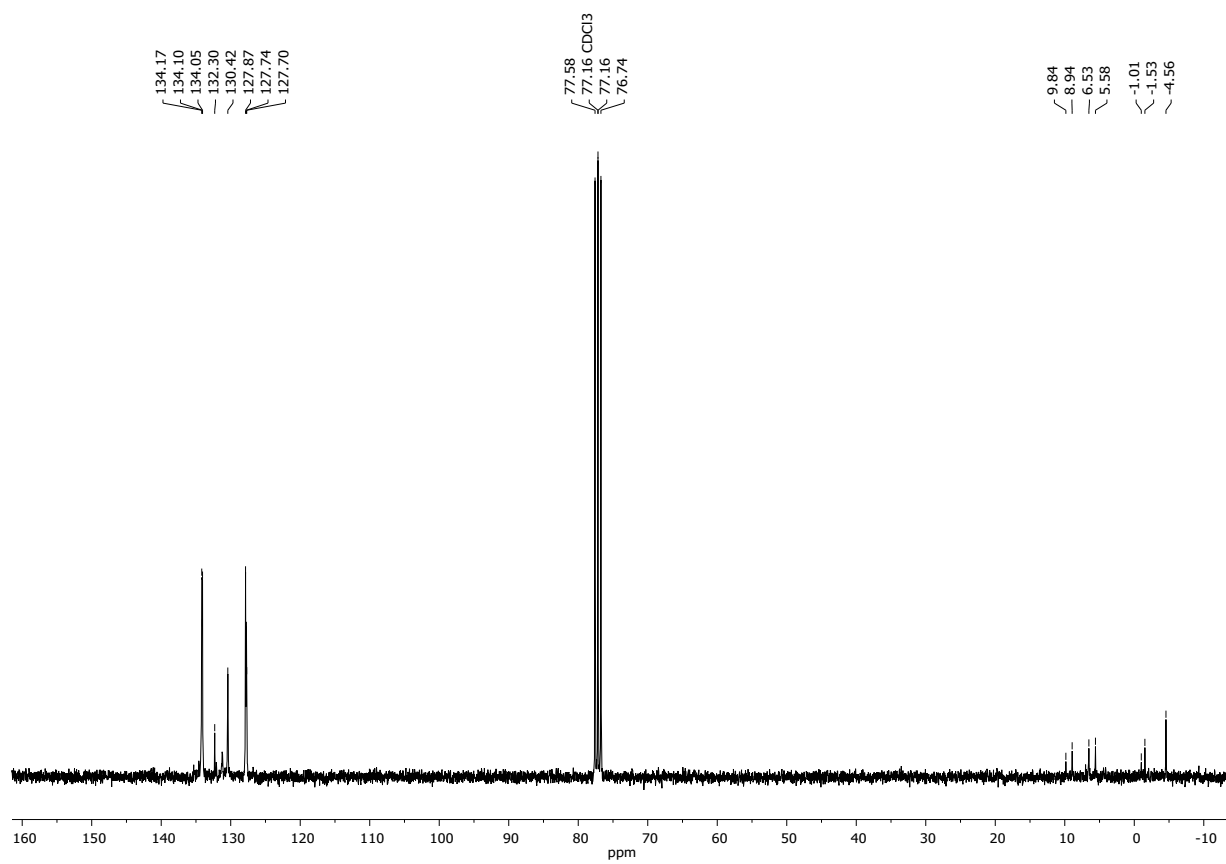
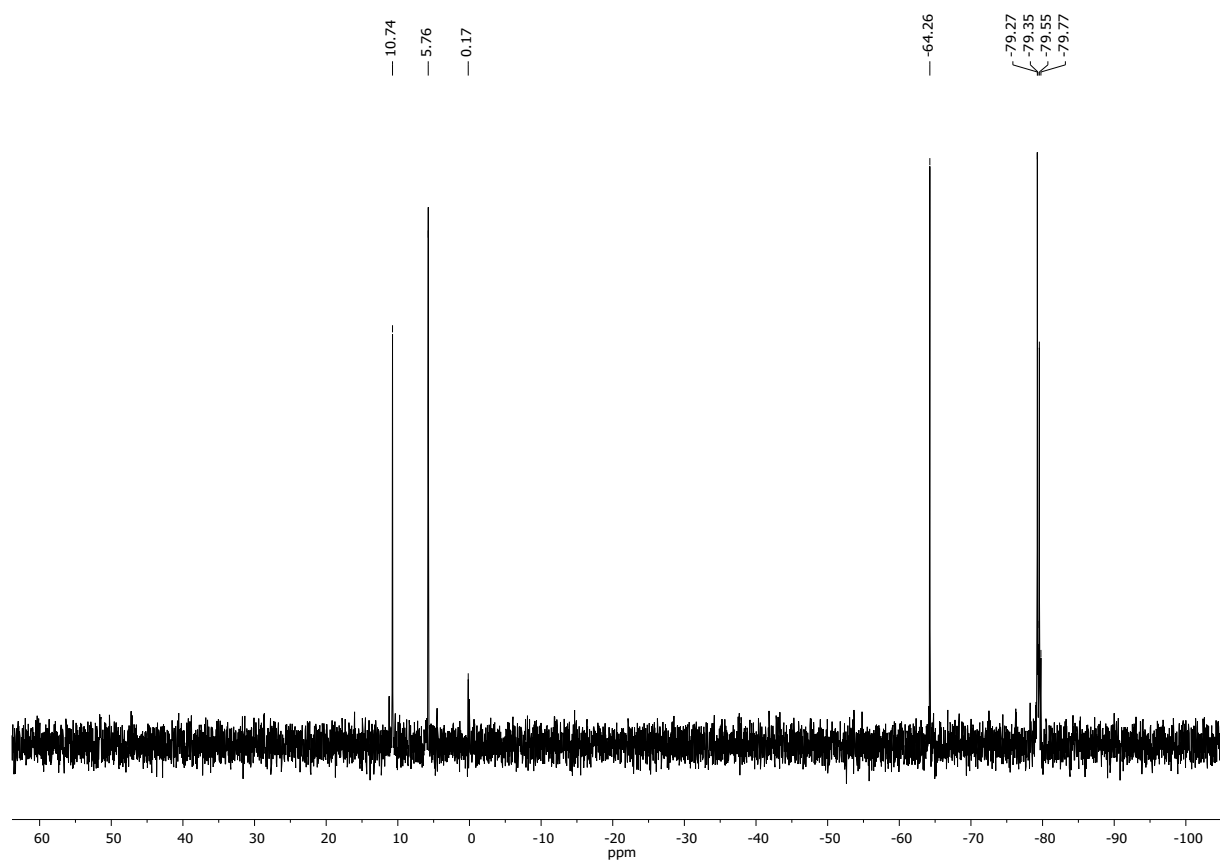**Figure S29** ^{13}C NMR (101 MHz, CDCl$_3$) spectrum of **7c-e**.

Figure S30 ^{29}Si NMR (79.5 MHz, CDCl$_3$) spectrum of **7c-e**.

7c-f
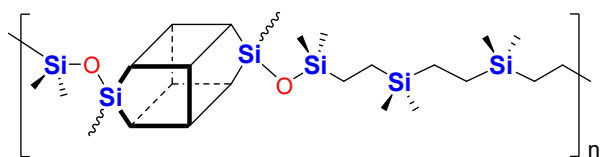
White viscous solid.

¹H NMR (300 MHz, CDCl₃, ppm): δ = -0.23 (s, SiCH₃), -0.22 (s, SiCH₃), 0.29 (s, SiCH₃), -0.07- -0.19 (m, -CH₂-CH₂-), 0.37-0.56 (m, -CH₂-CH₂-), 5.92-6.26 (m, -CH=CH₂-, terminal bond), 7.15-7.57 (m, Ph).

¹³C NMR (101 MHz, CDCl₃, ppm): δ = -4.56 (SiCH₃), -1.53 (SiCH₃), -1.01 (SiCH₃), 5.58 (Si-CH₂-), 6.53 (Si-CH₂-), 8.94 (Si-CH₂-), 9.84 (Si-CH₂-), 127.70-128.87 (Ph), 130.42 (Ph), 132.30 (Ph), 134.05-134.17(Ph).

²⁹Si NMR (79.5 MHz, CDCl₃, ppm): δ = 10.74 (Si(CH₃)₂), 5.76 (Si(CH₃)₂), 0.17 (Si(CH₃)₂), -64.26 (SiCH₃), -79.27, -79.55, -79.35, -79.27 (-Si-Ph).

IR (ATR, cm⁻¹): 3072.77, 3051.46 (C-H phenyl), 2953.65, 2905.53 (C-H), 1593.98, 1429.93 (C=C phenyl), 1257.98 (Si-C), 1079.78, 1027.88 (Si-O-Si), 997.58 (C-H phenyl).

Figure S31 ¹H NMR (300 MHz, CDCl₃) spectrum of **7c-f**.
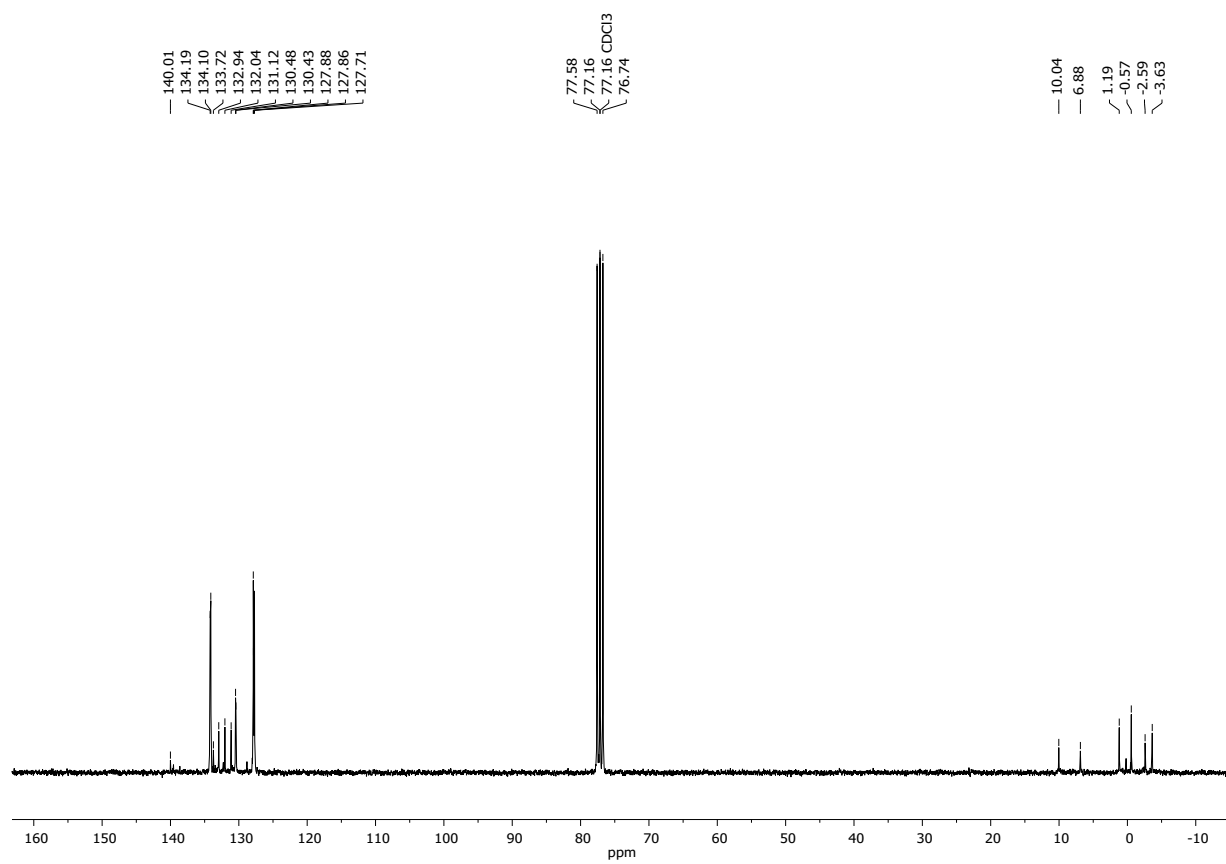
Figure S32 ^{13}C NMR (101 MHz, CDCl$_3$) spectrum of **7c-f**.

Figure S33 ^{29}Si NMR (79.5 MHz, CDCl$_3$) spectrum of **7c-f**.

7c-g
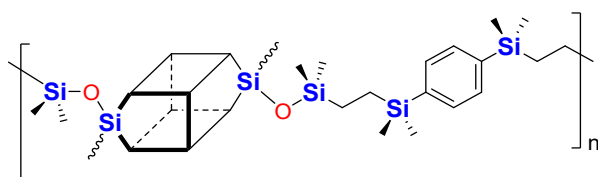
White viscous solid.

¹H NMR (300 MHz, CDCl₃, ppm): δ = 0.02 (s, SiCH₃), 0.11 (s, SiCH₃), 0.12 (s, SiCH₃), 0.29 (s, SiCH₃), 0.41-0.47 (m, -Si-CH₂-), 0.53-0.63 (m, -Si-CH₂-), 5.68 (dd, J_{H-H} = 20.2, 3.9 Hz, terminal bond), 5.77 (dd, J_{H-H} = 15.0, 3.9 Hz, terminal bond), 6.07 (dd, J_{H-H} = 20.1, 15.0 Hz, terminal bond), 7.15-7.46 (m, Ph), 7.57-7.60 (d, Ph).

¹³C NMR (101 MHz, CDCl₃, ppm): δ = -3.63 (SiCH₃), -2.59 (SiCH₃), -0.57 (SiCH₃), 1.19 (SiCH₃), 6.88 (Si-CH₂-), 10.04 (Si-CH₂-), 127.71-128.88 (Ph), 130.43-130.48 (Ph), 131.12 (Ph), 132.04 (Ph), 132.94 (Ph), 134.10-134.19 (Ph), 140.01 (Ph).

²⁹Si NMR (79.5 MHz, CDCl₃, ppm): δ = 10.72 (Si(CH₃)), -1.38 (Si(CH₃)), -1.61 (Si(CH₃)), -64.21 (SiCH₃), -79.26, -79.55 (-Si-Ph).

IR (ATR, cm⁻¹): 3072.70, 3050.43 (C-H phenyl), 2957.92, 2906.39 (C-H), 1594.22, 1430.02 (C=C phenyl), 1252.50 (Si-C), 1100.03, 1042.26 (Si-O-Si), 997.78 (C-H phenyl).
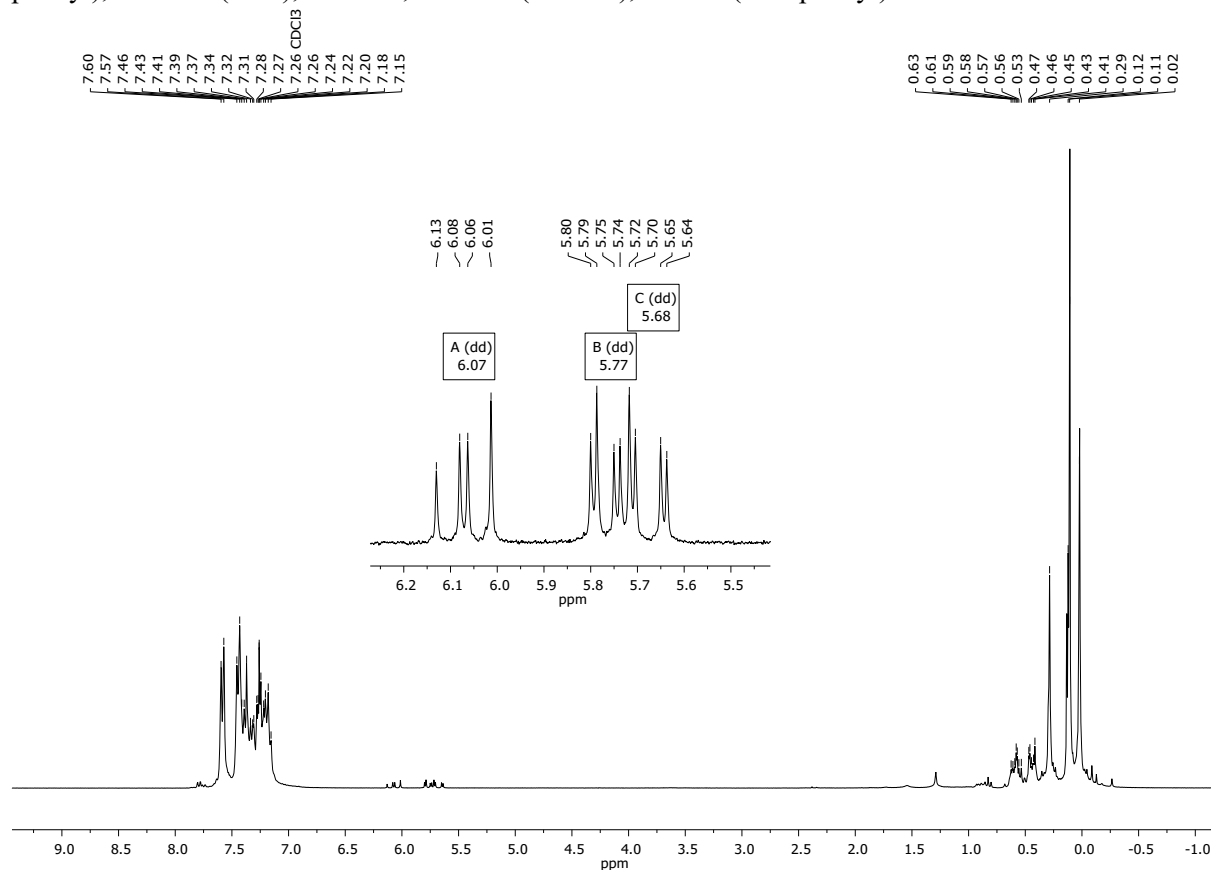
Figure S34 ¹H NMR (300 MHz, CDCl₃) spectrum of **7c-g**.

Figure S35 ^{13}C NMR (101 MHz, CDCl$_3$) spectrum of **7c-g**.
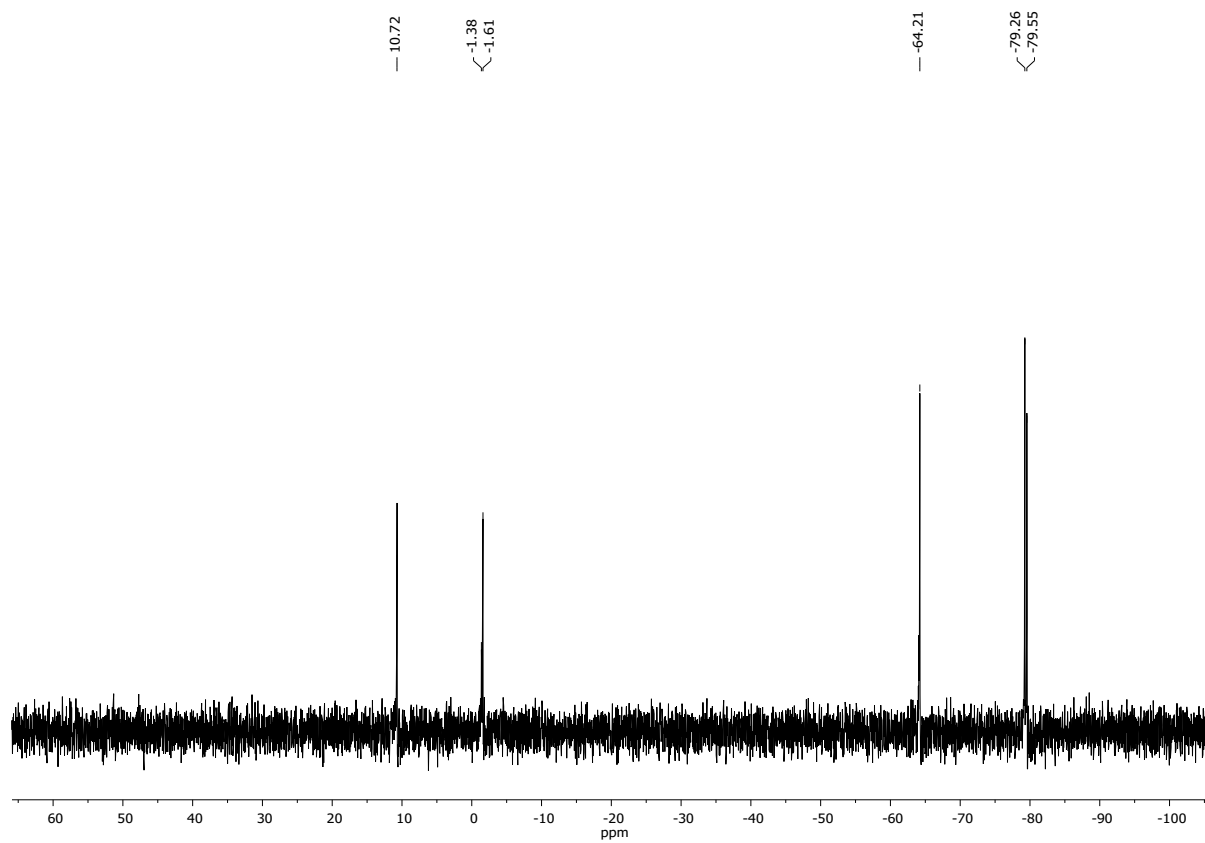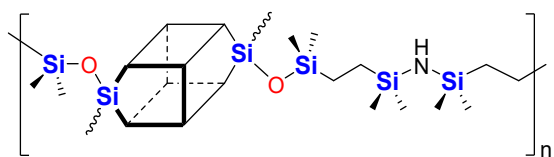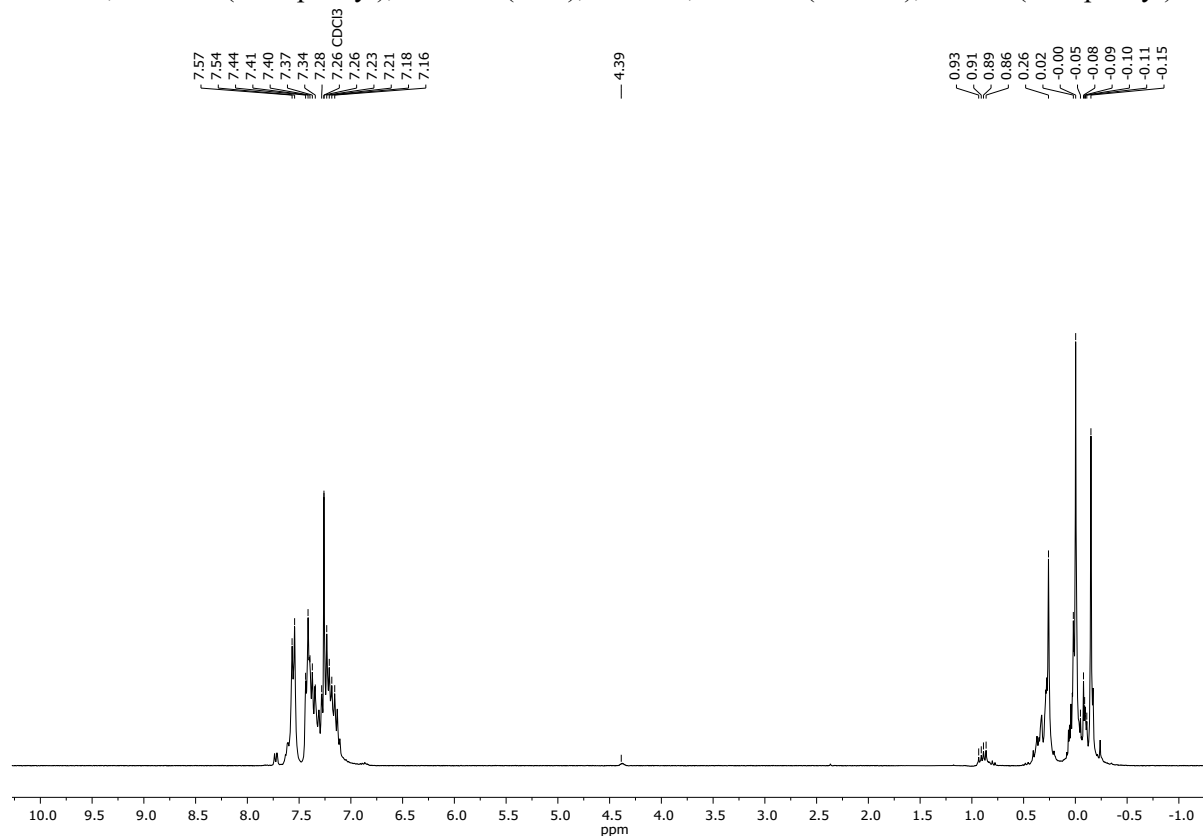
Figure S36 ^{29}Si NMR (79.5 MHz, CDCl$_3$) spectrum of **7c-g**.

7c-h

White viscous solid.

¹H NMR (300 MHz, CDCl₃, ppm): δ = -0.15 (s, SiCH₃), -0.11- -0.05 (m, -Si-CH₂-), 0.00 (s, SiCH₃), 0.02 (s, SiCH₃), 0.26 (s, SiCH₃), 0.86-0.93 (m, -Si-CH₂-), 4.39 (s, N-H terminal bond), 7.15-7.46 (m, Ph), 7.57-7.60 (d, Ph).

¹³C NMR (101 MHz, CDCl₃, ppm): δ = -2.56 (SiCH₃), -0.55 (SiCH₃), 0.08 (SiCH₃), 1.08 (SiCH₃), 9.98 (Si-CH₂-), 10.16 (Si-CH₂-), 127.62-127.88 (Ph), 130.35-130.57 (Ph), 131.18 (Ph), 132.11 (Ph), 134.14-134.28 (Ph).

²⁹Si NMR (79.5 MHz, CDCl₃, ppm): δ = 10.94 (Si(CH₃)₂), 4.61 (Si(CH₃)₂), 4.31 (Si(CH₃)₂), -64.25 (SiCH₃), -64.62 (SiCH₃, terminal bond), -79.26, -79.34, -79.76 (-Si-Ph).

IR (ATR, cm⁻¹): 3636.34, 3366.30 (N-H), 3072.99, 3051.54 (C-H phenyl), 2954.91, 2905.21 (C-H), 1594.28, 1430.10 (C=C phenyl), 1251.84 (Si-C), 1099.02, 1042.86 (Si-O-Si), 997.57 (C-H phenyl).

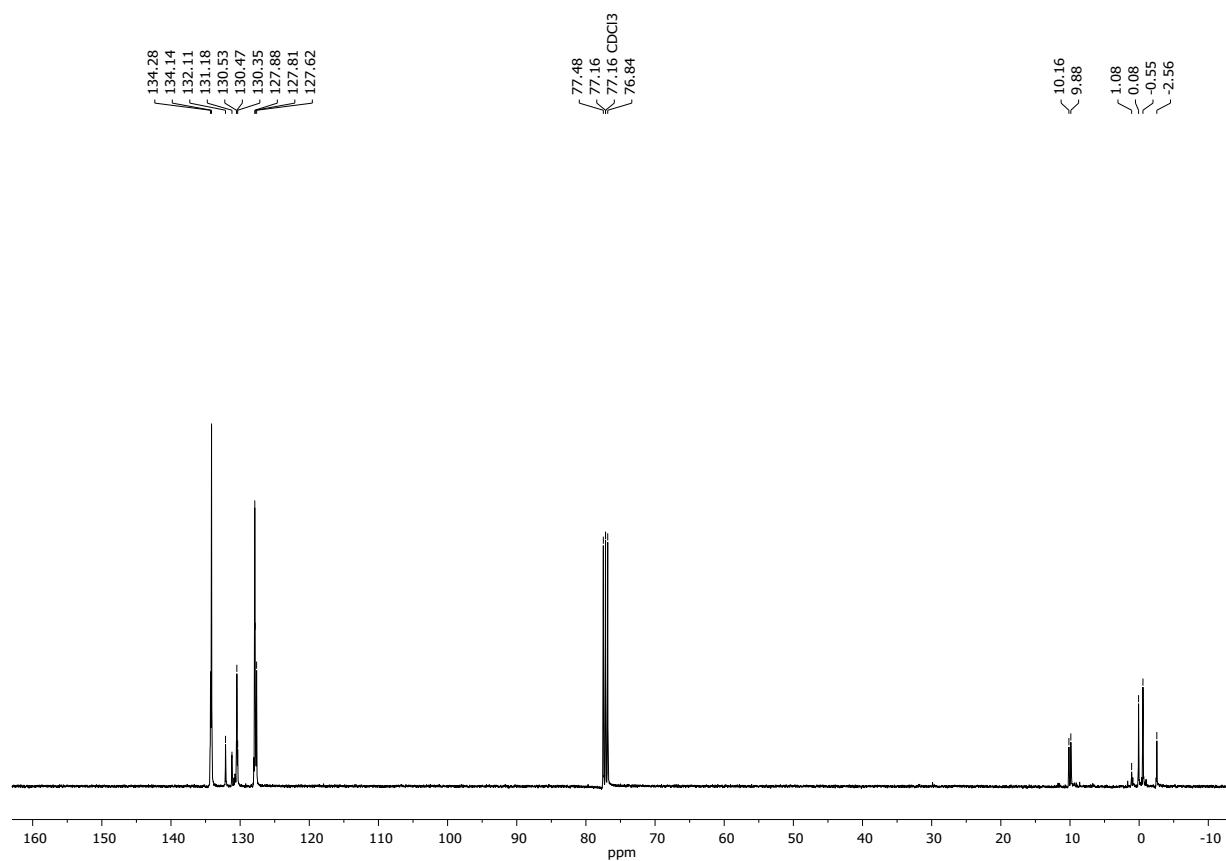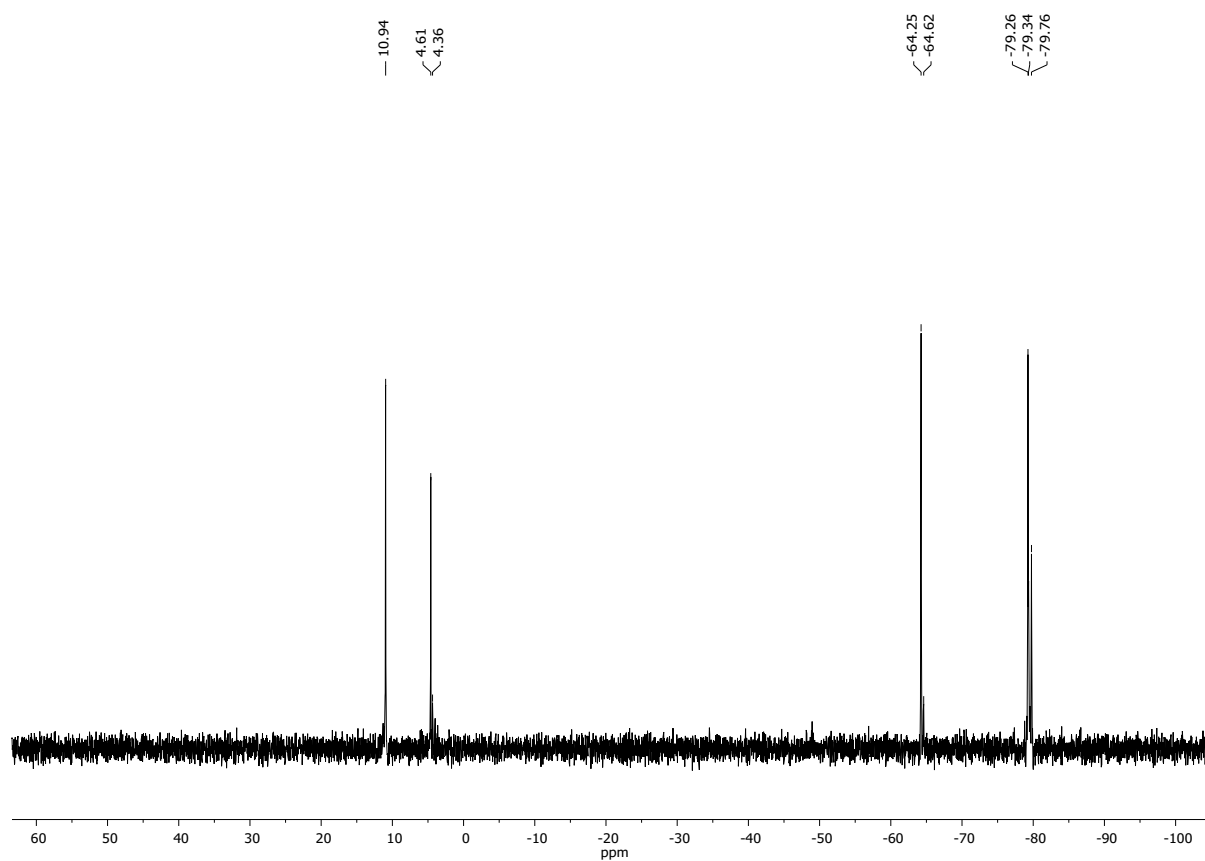**Figure S37** ¹H NMR (300 MHz, CDCl₃) spectrum of **7c-h**.

134.28
134.14
132.11
131.18
130.53
130.47
130.35
127.88
127.81
127.62

77.48
77.16 CDCl3
77.16
76.84

10.16
9.88

1.08
0.08
-0.55
-2.56

160   150   140   130   120   110   100   90   80   70   60   50   40   30   20   10   0   -10
ppm

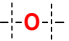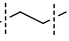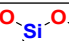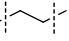**Figure S38** ^{13}C NMR (101 MHz, CDCl$_3$) spectrum of **7c-h**.
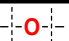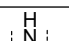
Figure S39 ^{29}Si NMR (79.5 MHz, CDCl$_3$) spectrum of **7c-h**.

5. GPC analysis of obtained products

Table S2. Molecular weights of co-polymers obtained *via* hydrosilylation of divinylsubstituted organosilicon derivatives (**4d**, **4f,** and **4g**) with dihydro-substituted DDSQ (**1a**) and divinylsubstituted DDSQs (**1b**, **1c**) with of dihydro-substituted organosilicon derivatives (**5d-h**) concerning the main fractions and the highest molecular weights fractions contents.

Entry	Sample	DDSQ		Main Fraction					Highest Fraction				
				M_w	M_n	Đ	Content [%]	DP_n	M_w	M_n	Đ	Content [%]	DP_n
1	6a-d-24h	1a	-O- (d)	8500	7100	1.2	63.4	5	8500	7100	1.2	63.4	5
2	6a-d-72h			9200	7300	1.3	68.3	6	9200	7300	1.3	68.3	6
3	6a-d-24h PtO2			8300	6900	1.2	59.3	5	8300	6900	1.2	59.3	5
4	6a-f-24h		(f)	9900	7800	1.3	67.1	6	9900	7800	1.3	67.1	6
5	6a-f-72h			12400	6900	1.8	100.0	5	12400	6900	1.8	100.0	5
6	6a-f-24h PtO2			8700	7400	1.2	58.3	5	8700	7400	1.2	58.3	5
7	6a-g-24h		(g)	22800	9500	2.4	100.0	7	22800	9500	2.4	100.0	7
8	6a-g-72h			26300	10000	2.6	100.0	7	26300	10000	2.6	100.0	7
9	6a-g-24h PtO2			16800	10500	1.6	77.5	8	16700	10500	1.6	77.5	8
10	7b-d-24h	1b	-O- (d)	41500	27700	1.5	46.3	21	41500	27700	1.5	46.3	21
11	7b-d-72h			16600	9100	1.8	75.4	7	119800	90800	1.3	24.6	68
12	7b-d-24h PtO2			12500	9700	1.3	59.6	7	12500	9700	1.3	59.6	7
13	7b-e-24h		Si (e)	18600	9800	1.9	40.0	7	2455800	1531900	1.6	21.1	1083
14	7b-e-72h			261500	152400	1.7	38.8	108	2837300	1593700	1.8	23.2	1127
15	7b-f-24h		(f)	5500	4900	1.1	68.1	4	5500	4900	1.1	68.1	4
16	7b-f-72h			10100	8000	1.3	66.3	6	10100	8000	1.3	66.3	6
17	7b-g-24h		(g)	13900	9200	1.5	68.8	7	13900	9200	1.5	68.8	7
18	7b-g-72h			17700	9100	1.9	100.0	7	17800	9100	1.9	100.0	7
19	7b-g-24h PtO2			13700	9100	1.5	67.5	7	13600	9100	1.5	67.5	7
20	7b-h-24h		H N (h)	2400	1600	1.5	100.0	1	2400	1600	1.5	100.0	1
21	7b-h-72h			13100	8100	1.6	41.8	6	13100	8100	1.6	41.8	6
22	7b-h-24h PtO2			1200	1000	1.2	88.8	1	2900	2800	1.0	11.2	2

#		1c		Mw	Mn	Đ	%	DPn	Mw	Mn	Đ	%	DPn
23	7c-d-24h	1c	(d)	18300	8400	2.2	100.0	6	18300	8400	2.2	100.0	6
24	7c-d-72h			67000	15100	4.4	100.0	10	67000	15100	4.4	100.0	10
25	7c-e-24h		(e)	23800	15800	1.5	40.5	10	3927400	2205800	1.8	10.0	1412
26	7c-e-72h			213500	122900	1.7	39.7	79	3752700	1639900	2.3	22.9	1049
27	7c-f-24h		(f)	6100	5500	1.1	62.9	4	6100	5500	1.1	62.9	4
28	7c-f-72h			127878	51600	2.5	81.3	34	127878	51600	2.5	81.3	34
29	7c-g-24h		(g)	16711	11000	1.5	56.2	7	16711	11000	1.5	56.2	7
30	7c-g-72h			43095	30991	1.4	38.7	20	43095	31000	1.4	38.7	20
31	7c-h-24h		(h)	4474	3107	1.4	100.0	2	4474	3100	1.4	100.0	2
32	7c-h-72h			46545	13142	3.5	97.7	9	46545	13100	3.5	97.7	9
33	7c-h-24h PtO2			1601	1527	1.0	80.4	1	3693	3500	1.1	19.6	2

Reaction conditions: $[Pt_2(dvds)_3]$ and PtO_2 – 10^{-3} per 1 mol of Si-H, equimolar stoichiometry of Si-H and Si-HC=CH$_2$ reagents, e.g. [**1a**]:[**4d**] = 1:1, toluene (m_{DDSQ}/V_{tol}=33mg/mL), 95 °C. DP$_{n=}$ degree of polymerization.
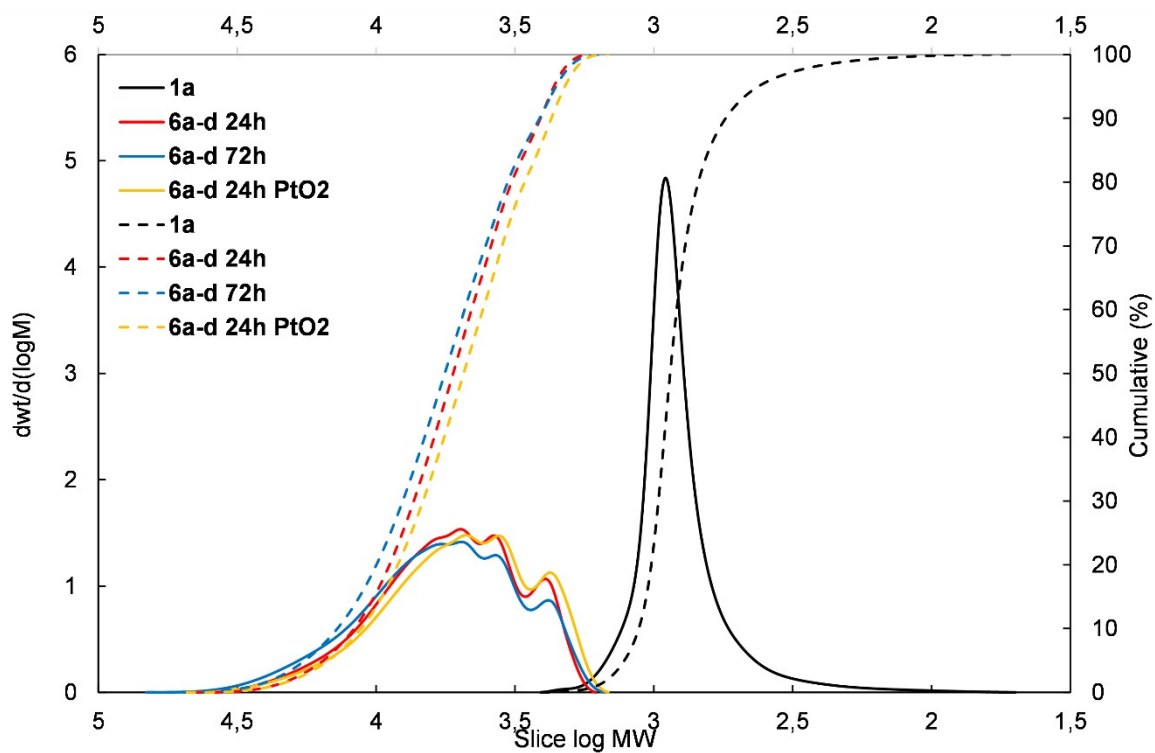
Figure S40 Molecular weight distribution plot of **6a-d**.
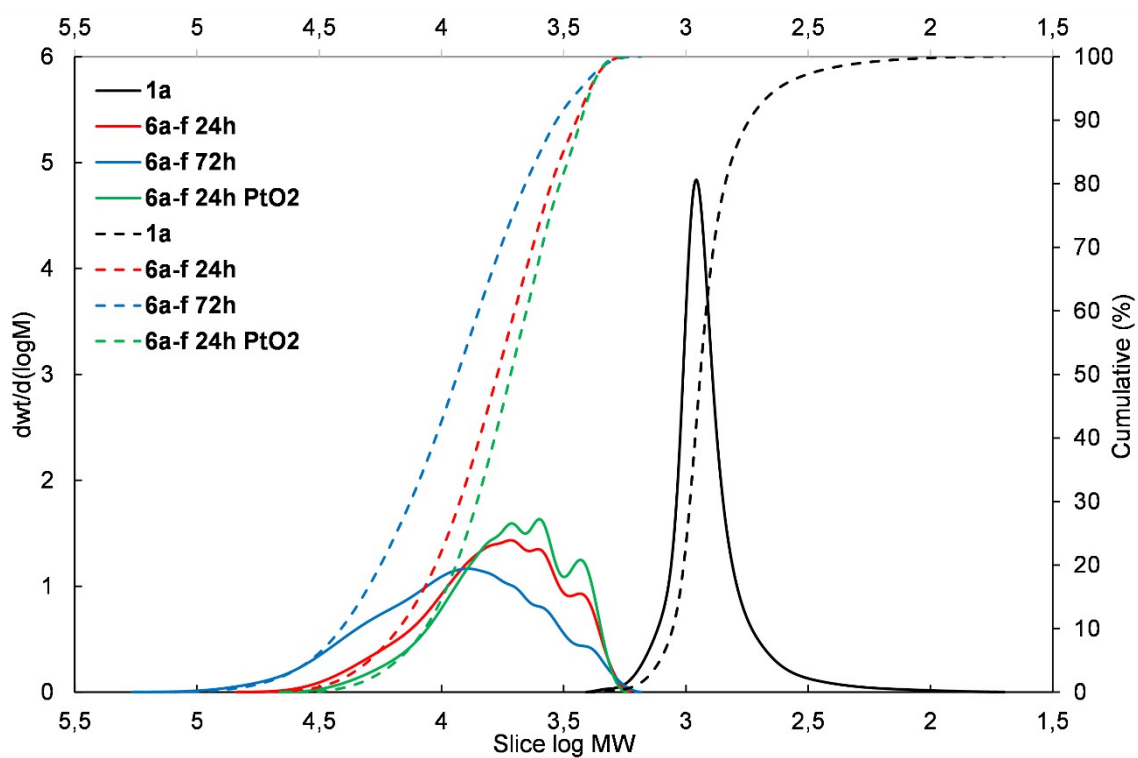
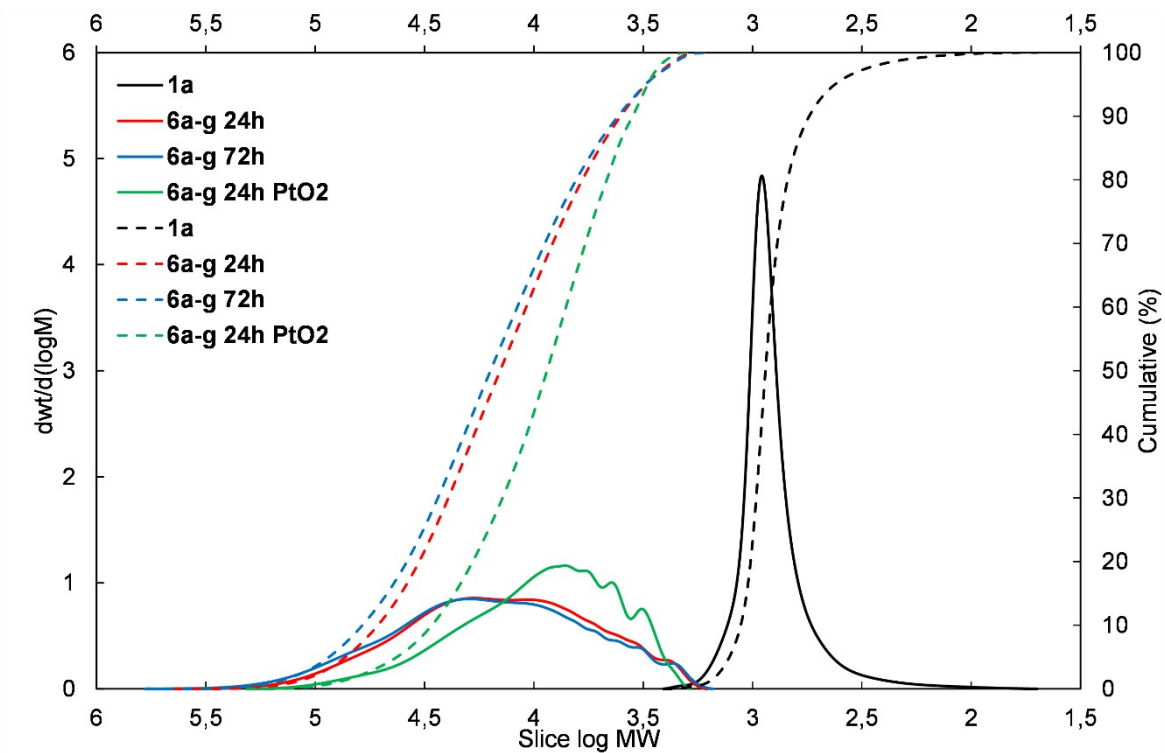**Figure S41** Molecular weight distribution plot of **6a-f**.

Figure S42 Molecular weight distribution plot of **6a-g**.
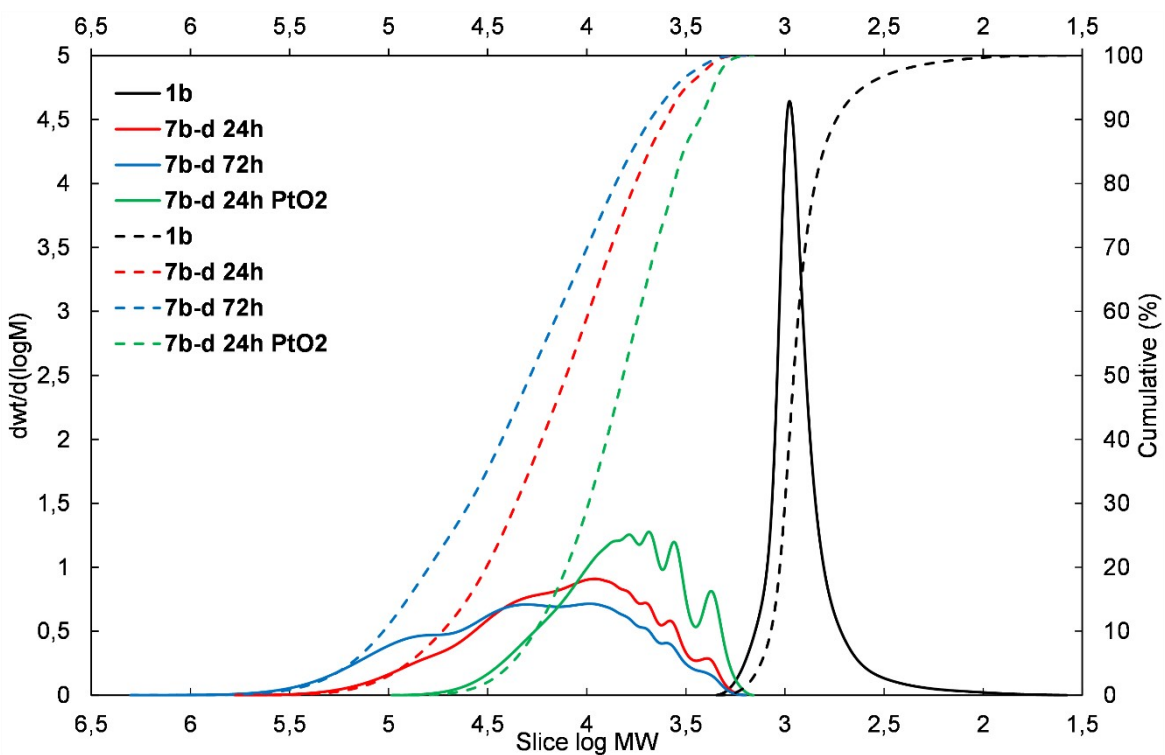

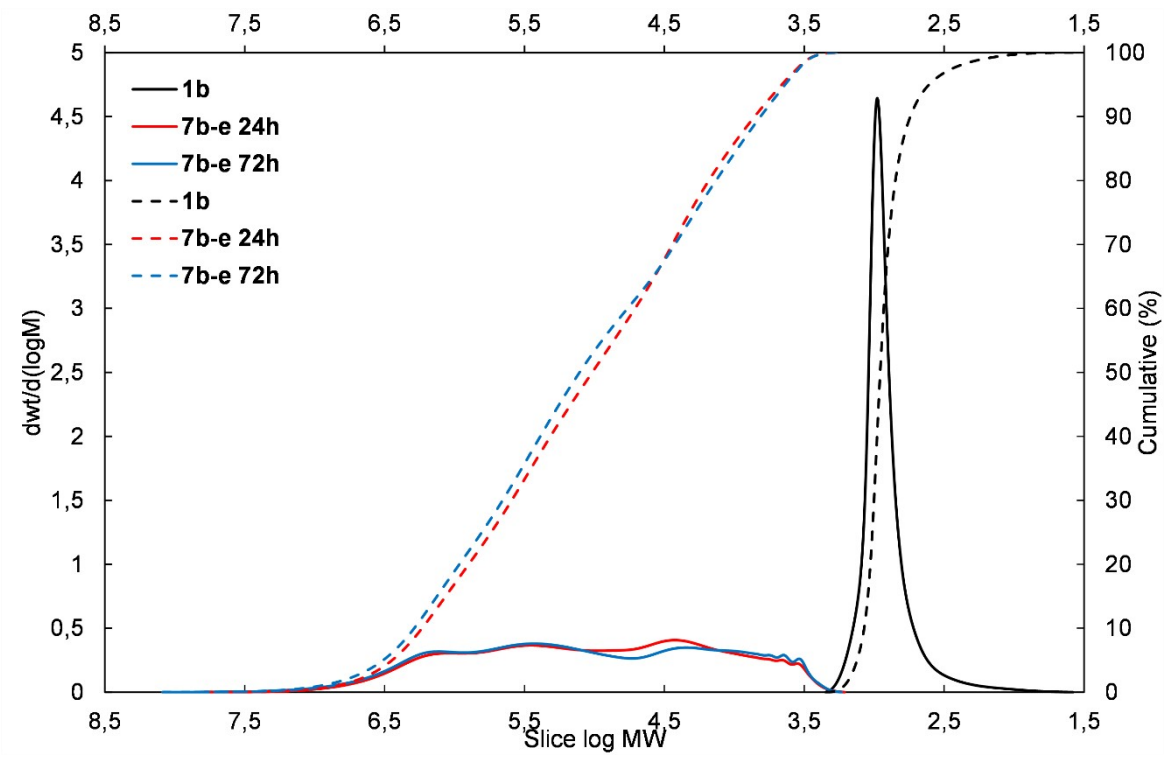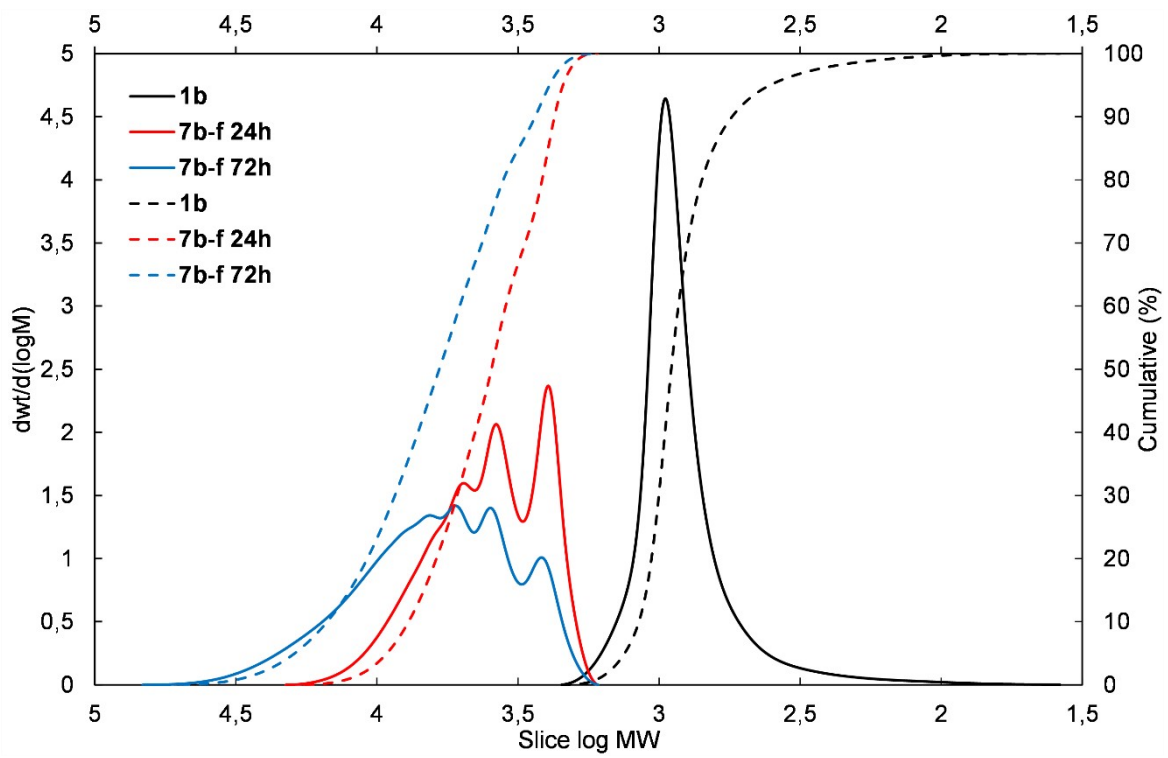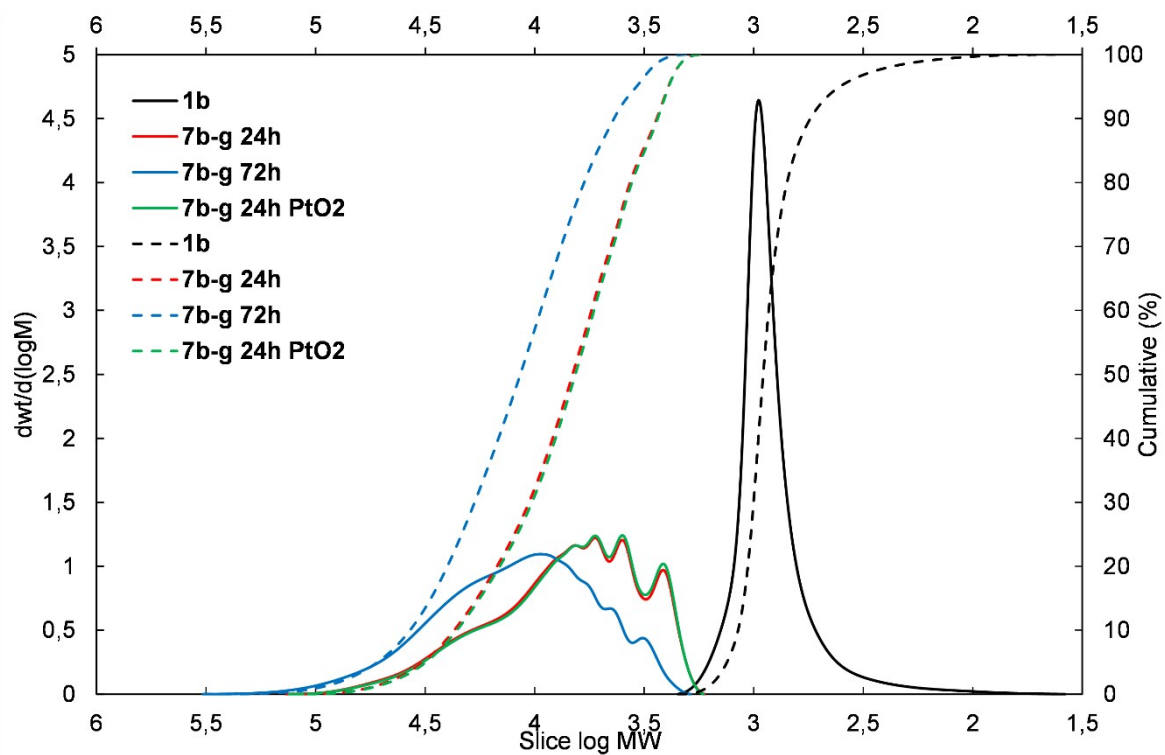**Figure S43** Molecular weight distribution plot of **7b-d**.

Figure S44 Molecular weight distribution plot of **7b-e**.

Figure S45 Molecular weight distribution plot of **7b-f**.
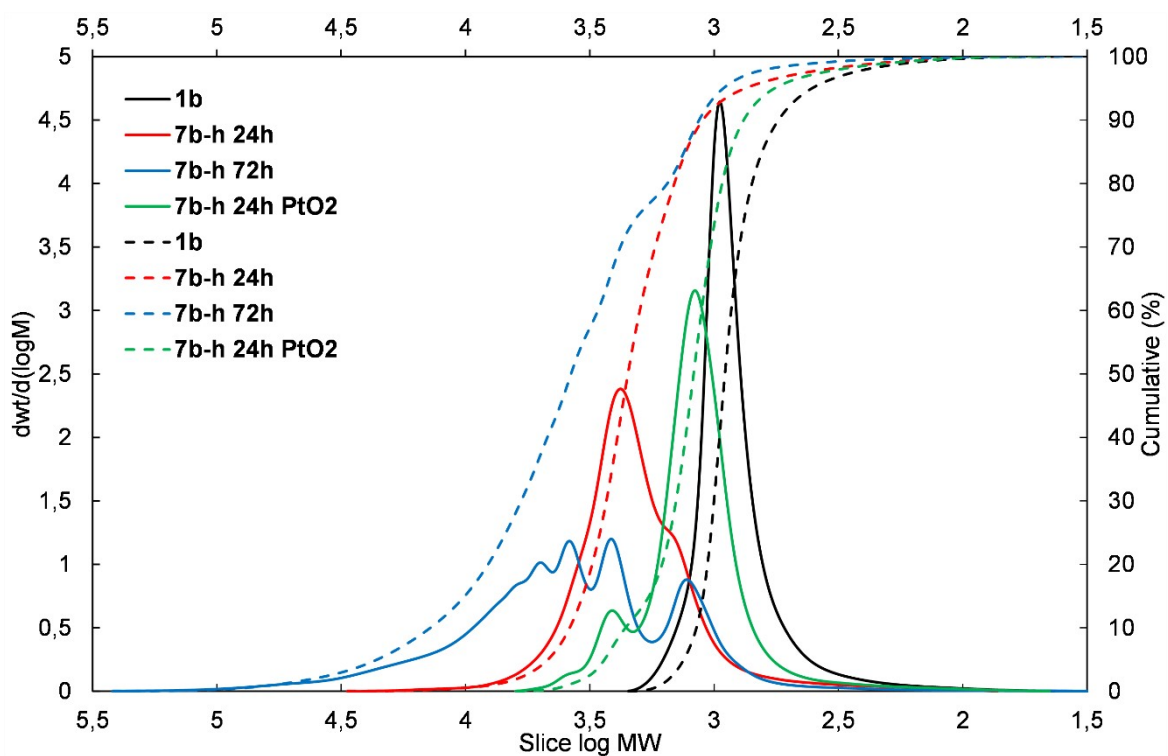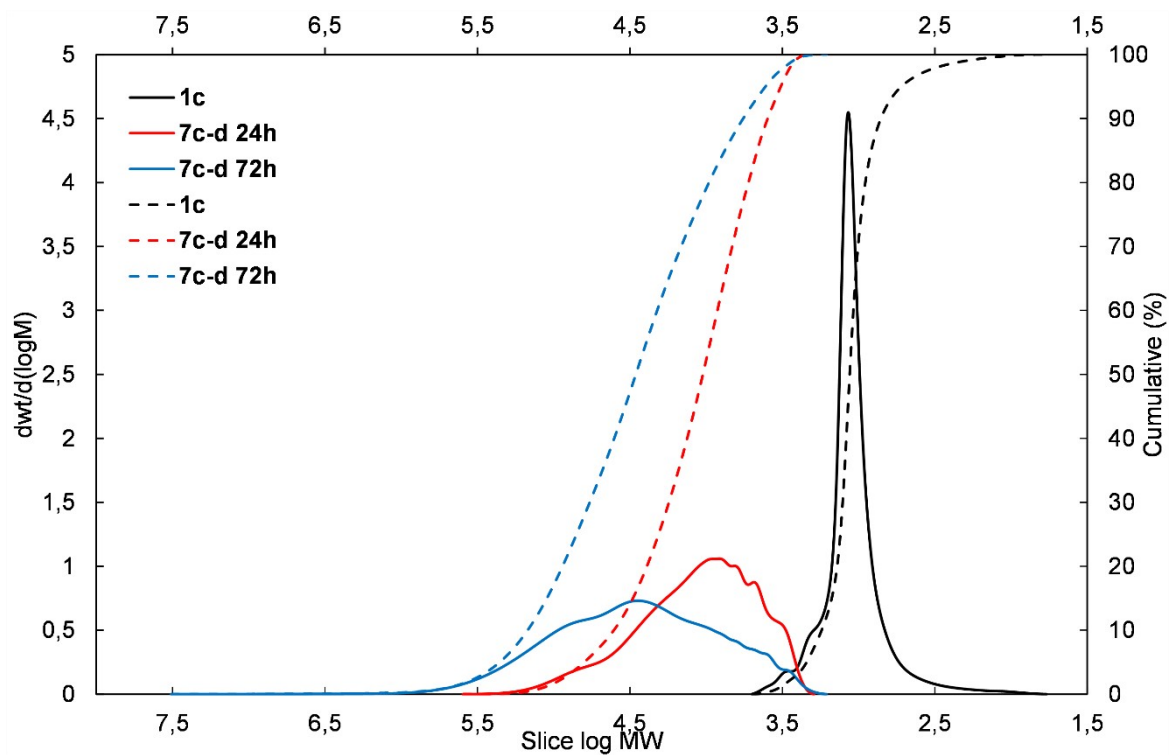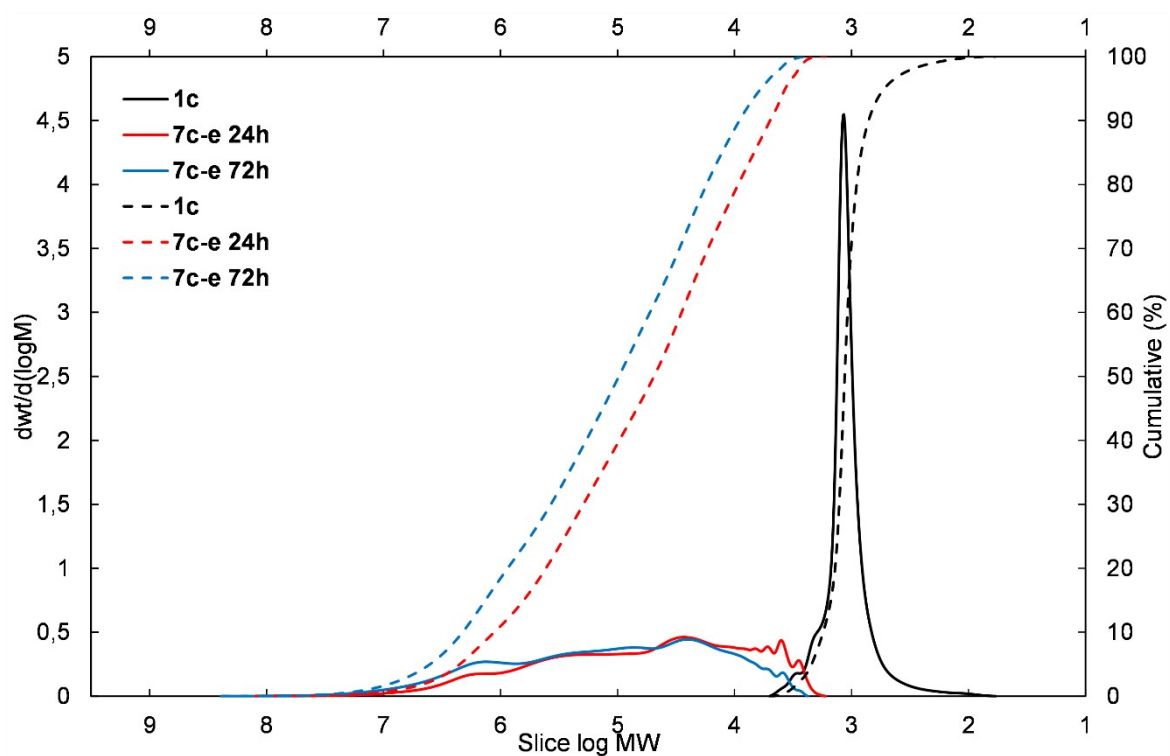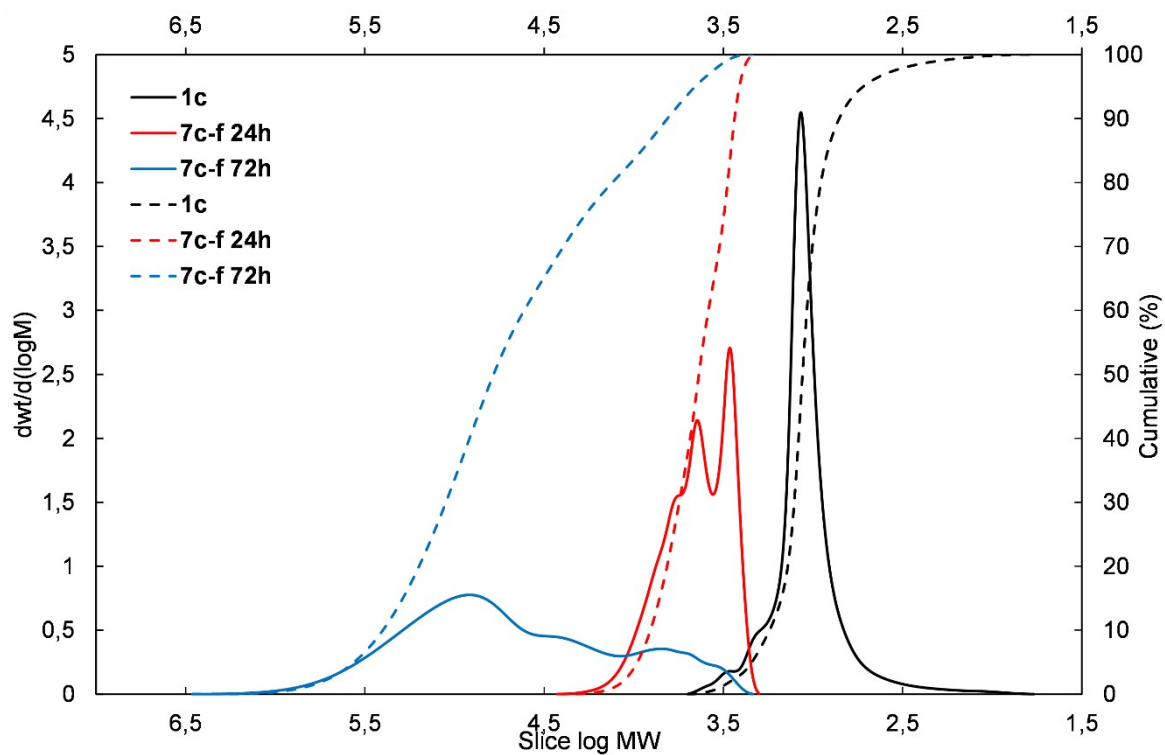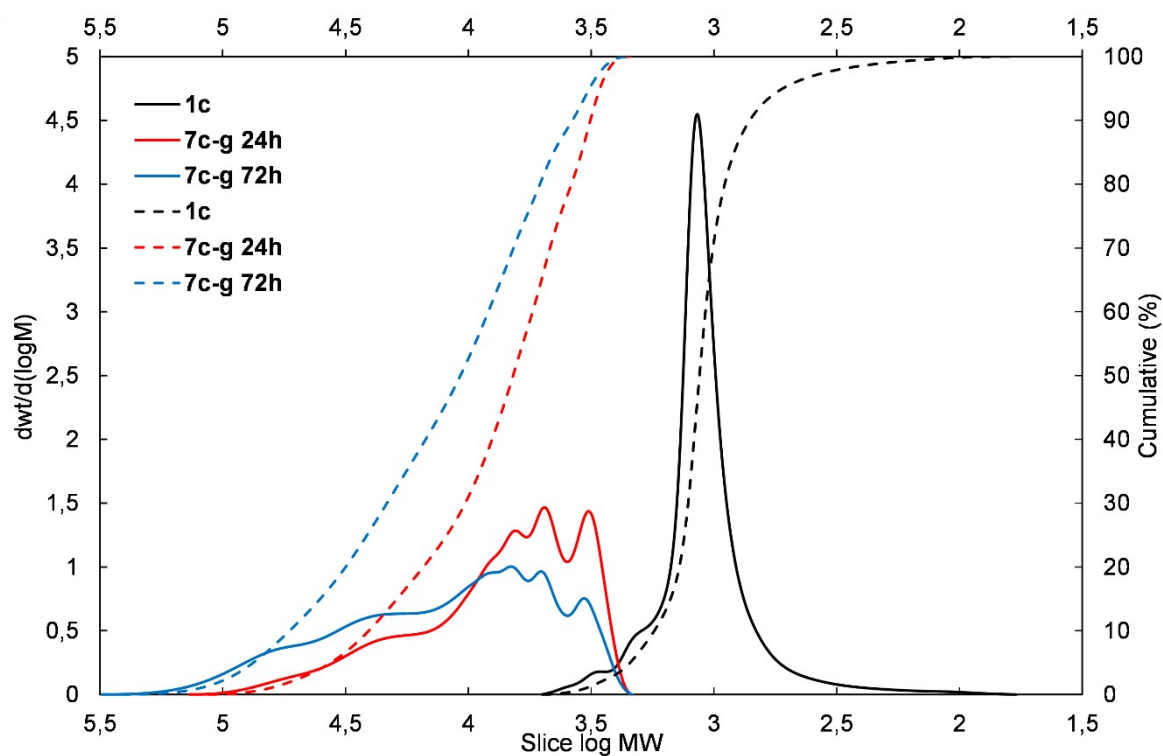
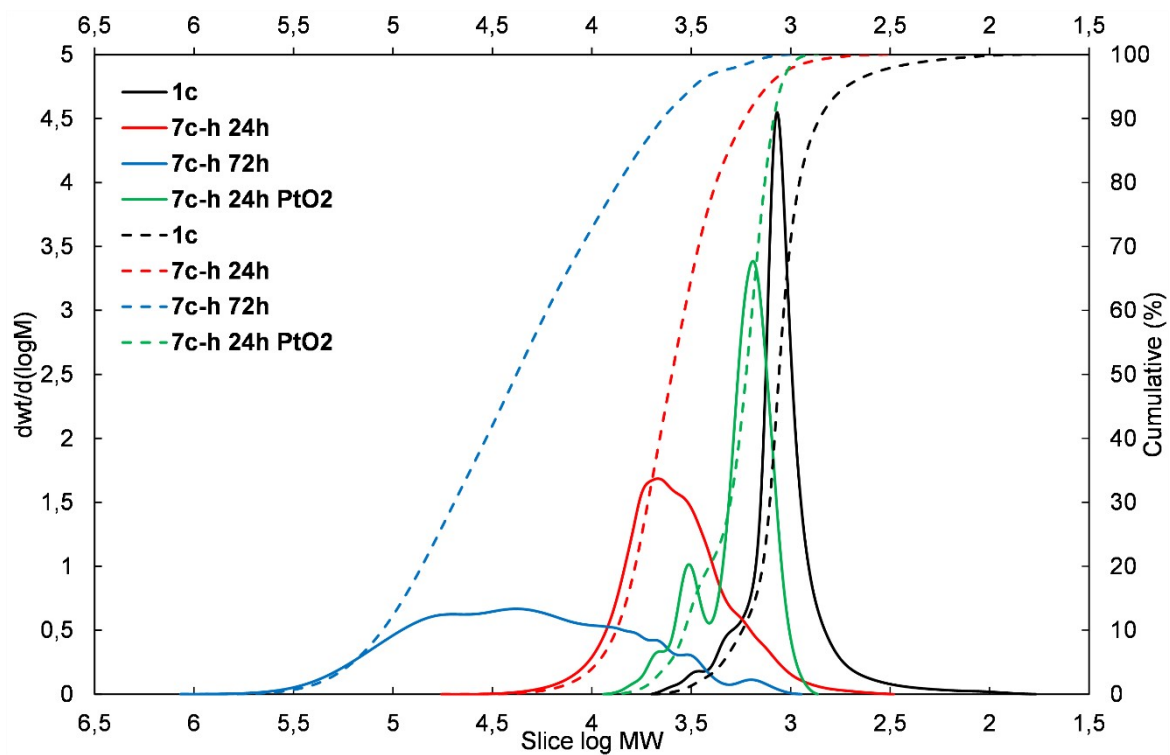**Figure S46** Molecular weight distribution plot of **7b-g**.

Figure S47 Molecular weight distribution plot of **7b-h**.

Figure S48 Molecular weight distribution plot of **7c-d**.

Figure S49 Molecular weight distribution plot of **7c-e**.

Figure S50 Molecular weight distribution plot of **7c-f**.

Figure S51 Molecular weight distribution plot of **7c-g**.
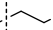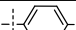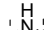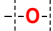
Figure S52 Molecular weight distribution plot of **7c-h**.

6. TGA analysis of obtained products

Table S3. Thermal properties of DDSQ substrates (**1a-c**) and respective copolymeric products **7b-(d-h)** and **7c-(d-h)**.

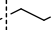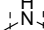| Entry	Product	DDSQ		Mass loss temperature [°C]		Residue at 1000˚C [%]
				$T_d{}^{5\%}$	$T_d{}^{10\%}$	
1	-	**1a**	-	373	400	41
2	-	**1b**	-	541	569	49
3	-	**1c**	-	490	534	48
4	**7b-d 24h**		(d)	151	183	46
5	**7b-d 72h**		(d)	139	173	45
6	**7b-e 24h**		(e)	366	481	50
7	**7b-e 72h**		(e)	159	210	48
8	**7b-f 24h**	**1b**	(f)	258	451	46
9	**7b-f 72h**		(f)	363	465	46
10	**7b-g 24h**		(g)	493	541	56
11	**7b-g 72h**		(g)	170	278	44
12	**7b-h 24h**		(h)	437	489	54
13	**7b-h 72h**		(h)	498	541	54
14	**7c-d 24h**		(d)	397	443	43
15	**7c-d 72h**		(d)	253	355	41
16	**7c-e 24h**		(e)	325	404	53
17	**7c-e 72h**		(e)	132	152	33
18	**7c-f 24h**	**1c**	(f)	233	471	49
19	**7c-f 72h**		(f)	400	457	50
20	**7c-g 24h**		(g)	303	390	43
21	**7c-g 72h**		(g)	229	285	35
22	**7c-h 24h**		(h)	375	456	53
23	**7c-h 72h**		(h)	462	511	55

7. Solubility tests of selected products
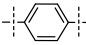
Table S4. Solubility of **7b-g-24h** and **7c-g 24h** compounds with different DDSQ core varying in additional -OSi(Me$_2$)- linkage.

Sample	7b-g-24h	7c-g-24h
Solvent	**Amount of solvent used [μL]**	
DCM	60	100-150
Acetone	70	1000 (+)
THF	70	1000
Hexane	1000 (-)	1000 (-)
Methanol	1000 (-)	1000 (-)
Acetonitrile	1000 (-)	1000 (-)

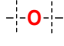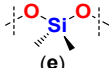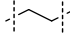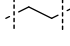Solubility at room temperature for 0.021g sample to obtain a transparent solution. (+) soluble after sonication, (-) insoluble even after sonication.

8. Young's Modulus and Hardness

Table S5. A list of Young's Modulus and Hardness values for measured samples

Entry	Sample	DDSQ		Young's modulus [GPa]	Hardness [GPa]
1	**6a-g**	**1a**	(g)	4.48±0.74	0.137±0.005
2	**7b-d**	**1b**	(d)	2.81±0.49	0.098±0.003
3	**7b-e**	**1b**	(e)	2.18±0.02	0.078±0.001
4	**7b-f**	**1b**	(f)	3.56±0.10	0.121±0.002
5	**7c-f**	**1c**	(f)	2.24±0.05	0.071±0.003

Samples were prepared on glass plates deposited from 5% DCM solution.

9. References

[1]   P. Żak, B. Dudziec, M. Kubicki, B. Marciniec, Silylative Coupling versus Metathesis-Efficient Methods for the Synthesis of Difunctionalized Double-Decker Silsesquioxane Derivatives, *Chem. - A Eur. J.*, 2014, **20**, 9387–9393.

[2]   M. Walczak, R. Januszewski, M. Majchrzak, M. Kubicki, B. Dudziec, B. Marciniec, Unusual cis and transfile architecture of dihydrofunctional double-decker shaped silsesquioxane and synthesis of its ethyl bridged π-conjugated arene derivatives, *New J. Chem.* 2017, **41**, 3290–3296.

[3]   D. Brząkalski, M. Walczak, J. Duszczak, B. Dudziec, B. Marciniec, Chlorine-Free Catalytic Formation of Silsesquioxanes with Si-OH and Si-OR Functional Groups, *Eur. J. Inorg. Chem.*, 2018, 4905–4910.

[4]   K. Cao, L. Yang, Y. Huang, G. Chang, J. Yang, High temperature thermosets derived from benzocyclobutene-containing main-chain oligomeric carbosilanes, *Polymer (Guildf)*., 2014, **55**, 5680–5688.

[5]   B. Marciniec, E. Małecka, M. Ścibiorek, Synthesis of silylene-alkylene-silylene-vinylene polymers via catalytic silylative coupling (SC) polycondensation, *Macromolecules*, 2003, **36**, 5545–5550.

[6]   H. Xie, J. Lu, Y. Gui, L. Gao, Z. Song, (HMe 2 SiCH 2) 2: A Useful Reagent for B(C 6 F 5) 3 - Catalyzed Reduction-Lactonization of Keto Acids: Concise Syntheses of (-)- cis -Whisky and (-)- cis -Cognac Lactones, *Synlett*, 2017, **28**, 2453–2459.

[7]   Agilent Technologies, CrysAlisPro (Version 1.171.33.36d), Agil. Technol. Ltd, UK. 2011.

[8]   G.M. Sheldrick, SHELXT - Integrated space-group and crystal-structure determination, *Acta Crystallogr. Sect. A Found. Crystallogr*. 71 (2015) 3–8. doi:10.1107/S2053273314026370.

[9]   G.M. Sheldrick, Crystal structure refinement with SHELXL, *Acta Crystallogr. Sect. C Struct. Chem.*, 2015, **71**, 3–8. doi:10.1107/S2053229614024218.

[10]   M.R. Vanlandingham, J.S. Villarrubia, W.F. Guthrie, G.F. Meyers, Nanoindentation of Polymers : A review, *Macromol. Symp.*, 2001, **167**, 15–43.

[11]   P.L. Larsson, S. Carlsson, On Microindentation of Viscoelastic Polymers, *Polym. Test.*, 1998, 17, 49–75.

[12]   W.C. Oliver, G.M. Pharr, An improved technique for determining hardness and elastic modulus using load and displacement sensing indentation experiments, *J. Mater. Res.*, 1992, 7, 1564–1583.